THE ELECTROCHEMICAL PHOTOEFFECT

Michael Heyrovský

Dissertation
submitted for the
Degree of Doctor of Philosophy
at the
University of Cambridge
1966.

Preface

The experimental part of the work on this thesis was done in the years 1962, 1964 and in Lent Term 1965 at the Department of Physical Chemistry of Cambridge University under the supervision of Professor R.G.W.Norrish, F.R.S., and the writing was accomplished in the Institute of Polarography, Czechoslovak Academy of Sciences, Prague, in Spring 1966.

I am greatly indebted to Professor R.G.W.Norrish who suggested to me the theme of the dissertation, enabled me to carry out the research in his Department, and was giving me helpful advice and encouragement during the work.

To Dr.J.Agar, Cambridge University, Dr.G.C.Barker, AERE Harwell, Dr.H.Berg, Academy of Sciences, Jena, and Professor A.N.Frumkin, Moscow University, I am obliged for inspiring discussions on some problems of the interpretation of results, and to Dr.L.Němec of Polarographic Institute, for critical remarks to the manuscript.

The work on the thesis could not be brought to end without the rare understanding from the side of the authorities of the Polarographic Institute which I thankfully acknowledge.

My sincere thanks are due to the Imperial Chemical Industries Ltd., to the British Petroleum Company and to Pembroke College, Cambridge, for financial support in the course of research.

Prague, April 1966.

Introduction

The effects observed when an electrode in solution is exposed to light have been a subject of research since Edmond Becquerel's discovery [1] in 1839. Most of the papers published in this field were reviewed by Copeland, Black and Garret [2]; more recent ones are quoted in articles by Paszyc [3] and by Mauser and Sproesser [4].

A study of these effects must consider both electrochemical and photochemical properties of the system electrode--solution. From the electrochemical point of view most of the systems studied have a common basic scheme : a polarizable electrode indicates the effects of light in reference to an unpolarizable electrode kept in dark. From the photochemical point of view there are three main types of systems according to different primary photoreactions initiating the photoeffect.

If the light is absorbed by the solution and a homogeneous photochemical process is started, the electrode only reacts upon resulting concentration changes of electroactive species in the solution without taking appreciable part in the photoprocess. Trümpler [5] was the first who proved this decisively; he has shown that the cause of the Becquerel effect in solutions of uranyl- and uranium sulphate must be sought in photochemistry of uranium. In such cases photolytic reactions in solutions can be conveniently studied by electrochemical methods from the effect of light on the course of potential (under the galvanostatic regime)

or current (in a potentiostatic arrangement). Rideal and Norrish [6] followed potentiometrically the photodecomposition of potassium permanganate. Rabinowitch [7] who later applied the same technique for investigation of photochemical reaction of thionine with ferrous ion, suggested the name "photogalvanic effect" for this "special case of the so-called Becquerel effect in which the influence of light .... is due to a photochemical process in the body of the electrolyte (as distinct from photochemical or photoelectric processes in the surface layer of the electrode, which are the basis of the original Becquerel effect)". Surash and Hercules [8] showed that the changes of potential on illumination of a platinum electrode in ethanolic solutions of organic compounds are due to free radicals formed by photochemical reactions between the solute and the solvent independently of the electrode and demonstrated a parallelism between the absorption spectrum of the solution and the photopotential. Mauser and Sproesser [4] examined some 120 solutions of organic compounds in non-aqueous solvents and concluded that photochemically inactive systems are also Becquerel-inactive. The polarographic method has been utilized for the study of photochemical reactions by Berg [9] and coworkers [10]; the "photoreaction-controlled diffusion currents" and "photokinetic currents" which they observed on illumination of solutions of organic compounds surrounding the dropping mercury electrode correspond to "photopotentials" followed potentiometrically by other authors with solid electrodes.

A different process occurs in the system : nonabsorbing solution - photosensitive electrode. A correct interpretation of this kind of Becquerel effect was first given by Volmer and Moll [11] on basis of their experiments with selenium electrode : the primary reaction after absorption of light by the electrode is the setting free of inner electrons in the electrode followed by chemical reactions in which both the electrode and the solution take part. A more concise formulation - internal photoeffect followed by chemical reactions - was used by Athanasiu [12] who studied the effect of light on silver, mercury and copper electrodes covered by layers of halides, sulphides or oxides. Later Veselovsky [13] in a paper on the photoelectrochemical process at zinc electrode covered with zinc oxide defined precisely that the absorption of light by the electrode surface leads to formation of electrons and holes of high energy which migrate to the interfaces metal-semiconductor and semiconductor-solution respectively where they are electrochemically discharged.

For many years the general distinction between these two basically different processes was obscured by the search for some common principle that would apply universally to all modifications of the Becquerel effect. In the early years of research on that field it was difficult to judge the problems correctly, because most of the systems, usually very complex, were studied without knowledge of their optical and photochemical properties, the measurements were carried out in presence of air and experimental condi-

tions were not always properly controlled. As late as in 1927 Winther [14] unambiguously distinguished between the "volume photoeffect" and the effect for which an illumination of the electrode is essential; only for the latter he suggested to keep the name "Becquerel effect".

The majority of experimental results reported in literature can be ascribed to either of the two effects or to their combination. However, a difficulty arises with the system of pure metallic electrode in transparent solution where neither part is "photosensitive" in the current sense of the word, but which, nevertheless, can yield a reproducible response to illumination. The offhand explanation by an outer photoeffect, i.e. by emission of electrons from the electrode was usually discarded by the authors as it was thought inconsistent with their experimental results.

Swensson [15] followed the potential changes of platinum electrode in solutions of various electrolytes on illumination by a mercury lamp, and found marked effects with compounds usually not considered as photochemically active, like H_2SO_4 or KCl. His results were confirmed by Lifschitz and Hooghoudt [16]. Audubert [17] studied the effect of visible light on polarized platinum and gold electrodes in various solutions and expressed the view that photolysis of water could be responsible for the observed phenomena. Unfortunately neither of these authors took into due consideration the absorption of light by the solution and consequently it cannot be decided to what extent their effects

should be ascribed to homogeneous photoreactions.

An important discovery was made by Bowden [18] who found that the electrodepositions of hydrogen on mercury electrode and of oxygen on platinum electrode are accelerated by UV light. The increment of current produced by illumination, or photocurrent, increases with increasing negative potential and with light of shorter wavelengths. Bowden's effect was further studied by Price [19] on various electrodes (bismuth, cobalt, antimony, mercury, lead, aluminium, graphite). Price showed that the photocurrent is directly proportional to the intensity of light, and that the quantum yield of photocurrent is an exponential function both of potential of electrode and of frequency of light. Hillson and Rideal [20] confirmed the results of Price. They studied the electrodeposition of hydrogen from 0,1N sulphuric acid under illumination on mercury, copper, nickel and silver electrodes and obtained a measurable photocurrent with light of wavelength as long as 4200 Å. The photoeffect in electrodeposition of oxygen on platinum, palladium, gold, silver and nickel was found to be of the same magnitude as in the case of hydrogen, and to follow the same laws. Hillson and Rideal conceived the photoeffect as influence of light on the kinetics of electrodeposition; this idea was disproved by later experimental results in this field.

Barker and Gardner [21] were the first who applied polarographic technique to investigation of photocurrents. They illuminated the electrode by a square-wave modulated

light from a mercury are and recorded the photocurrent with a square-wave polarograph. In this way they obtained appreciable photocurrents in solutions of acids and in neutral solutions containing hydrogen peroxide or anions NO_2^-, NO_3^- and BrO_3^-. Unfortunately all the 4 latter species are photolytically decomposed by light of the wavelengths used which complicates the interpretation of results. Barker and Gardner assume on the basis of outer photoelectric effect, that under illumination electrons are emitted from the electrode into a distance of 50 - 100 Å where their solvation occurs, and from where their subsequent diffusion back to the electrode takes place. The photocurrent appears only if some of the electrons are involved in a reaction in solution and fail to return to the electrode. For the photocurrent under these conditions the authors derived expression

$$i_p = F\, Ce \sqrt{k_A\, C_A\, D_e}$$

where F is the Faraday constant, C_e the concentration of solvated electrons in the average emission distance from the electrode, k_A the rate constant of the electron capture reaction, C_A the scavenger concentration and D_e the diffusion coefficient of the solvated electron. The experimentally measured photocurrents were found to agree with the equation only at low concentration of scavengers.

In their photopolarographic experiments with flash technique Berg and Schweiss [22] observed in pure solutions of supporting electrolytes a kind of photocurrent which

they called [23] the photoresidual current (Photoreststrom). This current is proportional to light intensity, increases with increasing negative potential and is especially high in acid solutions.

Heyrovský and Norrish [24] pointed to the relation between potentiometrically and polarographically studied photoeffects in solutions. They observed polarographic photocurrents in solutions of various acids and in presence of nitrous oxide, and suggested an interpretation based on photosensitized dissociation of water.

Recently Delahay and Srinivasan [25] used the coulostatic method to study the photocurrents produced by flash irradiation in acid solutions on a mercury pool electrode. They discussed their results on the ground of Barker's theory and pointed out that especially the effect of electrode potential and of the double layer on photocurrent needed further clarification.

The Becquerel effect on pure metallic electrodes in transparent solutions is particularly attractive from both the photochemical and electrochemical point of view. It intimately concerns the mechanism of the elementary process of transfer of charge across an interface. However, the review of work hitherto done on this problem shows that the essential points pertaining to the nature of the effect still remain obscure. In principle there are two different concepts at present : the "physical" concept of Barker who interprets the photoeffect in solution as a special case of

the classical photoelectric effect in vacuum, and a "chemical" concept formulated by Audubert who saw the origin of the photoeffect in a photochemical reaction in the interface electrode-solution. It is not impossible that both schemes are correct, each operating under different conditions.

The aim of the present thesis was to provide experimental data that would help to decide which concept is valid for the photoeffect in aqueous solutions. The name "electrochemical photoeffect" was introduced in order to specify the subject for which the term "Becquerel effect" is too general, and to underline its phenomenal analogy with the physical photoeffect.

Experimental

For a correct account of the electrochemical photoeffect a simultaneous control of optical factors - the intensity and energy of light - and of electrical factors - the current and the electrode potential - appears essential. The work of the previous authors has shown the importance of a complete elimination of photochemical processes in solution. In order to simplify the interpretation of results a simple experimental technique was used. Since the purity of electrode surface is the first condition for obtaining reproducible results, mercury was chosen as the electrode material.

Bidistilled mercury was used for the mercury pool and dropping mercury electrodes.

Solutions were prepared from chemicals of "Analar R" grade and water redistilled from permanganate. Ethanol was purified by treatment with sulphuric acid, potassium hydroxide and silver nitrate according to Leighton and coworkers [26], and its purity was controlled spectrophotometrically. Acetone was redistilled from permanganate.

The potentiometric measurements were carried out in parallel with two large quartz test-tubes connected by an electrolytic bridge to a common reference electrode. Mercury pool electrodes in the test-tubes were illuminated by a parallel beam of light from the mercury lamp. A stream of inert gas was constantly passed through or above the solution in the test-tubes.

The cell for polarographic measurements (Fig.1a), of circular cross-section with two planparallel walls and of about 50 ml volume, was made of quartz, with ground joints on four necks parallel for inlet and outlet of gas, inlet of solution, dropping electrode, thermometer and contact to the mercury pool (glass tube with sealed-in platinum wire and filled with mercury). To avoid liquid junction potentials and contamination of the solution by electrolyte from an electrolytic bridge, no separate reference electrode was used; a layer of mercury on the bottom of the cell served as counterelectrode. The cell was fixed by means of a special holder in a large water tank kept at 25.0 ± 0.5°C.

Throughout each experiment the solution was under a stream of nitrogen which had been purified from traces of oxygen by passing through two columns (35 cm long, 4 cm in diameter) containing amalgamated metallic zinc in alkaline solution (about 2M KOH) saturated with anthraquinone-β-sodium sulphonate and one column of amalgamated zinc in acid solution (about 0.1M HCl) of chromous chloride. After the last column a washing bottle with suspension of silver oxide in 2M KOH was placed to eliminate possible traces of HCl from the gas. Before entering the cell the nitrogen passed through a washing bottle containing the same solution as that in the cell. All parts of the glass apparatus were connected together by ground joints.

Nitrogen was bubbled through the solution first in the separate compartment (Fig.1b), with stopcocks 1 and 2 opened

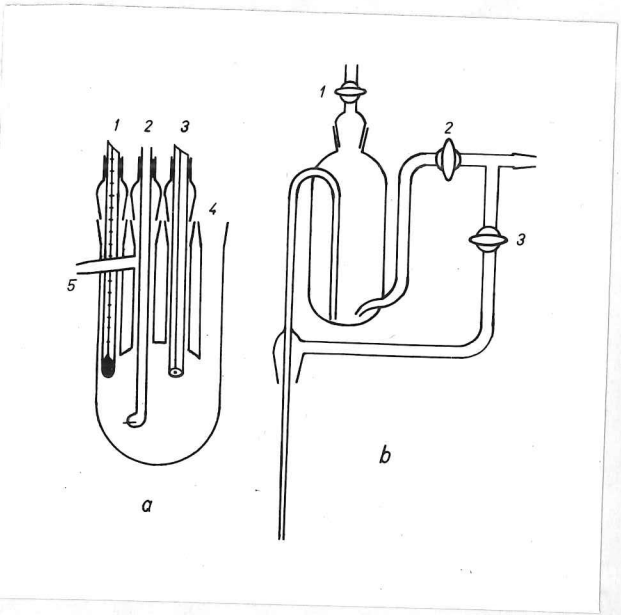

Fig.1. Cell for polarographic measurements. a - cell proper: 1 - thermometer, 2 - contact to the mercury pool, 3 - dropping mercury electrode, 4 - socket for part b - - inlet of gas and solution, 5 - outlet of gas; b - compartment for deaeration of solution; function of stopcocks 1, 2,3 described in text.

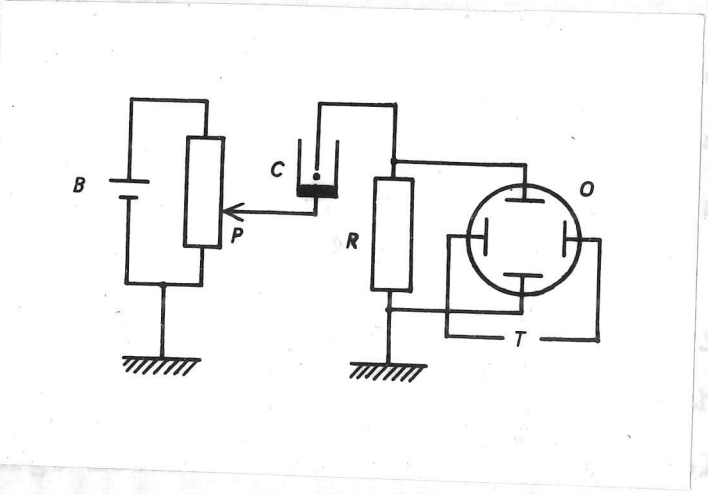

Fig.2. Circuit for polarographic current-time curves.
B - battery, P - potentiometer, C - cell; R - measuring resistance, O - oscilloscope, T - time base (internal).

and 3 half closed at a high rate for at least 1 hour before the solution was pressed over, by closing stopcocks 1 and 3, into the nitrogen-filled cell with mercury on the bottom. During the actual measurements nitrogen was passed above the solution (stopcock 3 opened). The cell was designed expressedly to exclude passage of solution through any stopcock.

The capillary used for the dropping electrode was of the type introduced by Smoler [27] for elimination of the transfer of electrolytic products on successive drops, with the lower end bent and cut at 45°. Its length was 20 cm, inner diameter 60 μ, the rate of flow of mercury under constant height of mercury column 39 cm was m = 0.529 g/sec and drop-time in 0.1M KCl at potential of zero charge t_1 = = 5.55 sec.

Light from a 1 kW high pressure mercury lamp type ME/D was focused by means of a quartz lens through a quartz window in the side of the water tank and through a 8 cm layer of water to the cell on the tip of the capillary, so that when exposed each drop of mercury was growing in a strong field of light. The lamp and the tank were kept in a large metallic box with a fan for cooling on the top and with removable front side.

The emission of the lamp covered nearly homogeneously the range of wavelengths from 2350 to 5400 Å with a gap between 2540 and 2640 Å and with two groups of lines at 5800 and 6100 Å. A continuous control of constancy of the inten-

sity of emission was provided by means of a cadmium photocell in circuit with a voltmeter. The drop of the voltmeter deflection was an indication that the lamp had to be changed for a new one.

For cutting off various portions of the spectrum from the short-wave side filter solutions were used in a quartz cell 2.5 cm thick. The filters and their absorption "edges" were following :

acetic acid 1:10	2460 Å	copper sulphate 15%	3360 Å
lead acetate 0.5%	2600	copper chloride conc.	3580
5 %	2800	copper nitrate conc.	3900
copper sulphate 1.5%	2980	sodium nitrite conc.	4150
pyrex plate 2 mm thick	3030	potassium chromate 2%	5000
4 mm thick	3130	potassium dichromate sat.	6000
6 mm thick	3200		

The emission of the lamp as well as the transmittance of the filters were measured and regularly checked by means of a small Hilger quartz spectrograph.

Of each solution examined an absorption spectrum was recorded before the experiment on the Perkin-Elmer Model 137 or on Unicam S.P.800 UV Spectrophotometers. According to the absorbance suitable filters were chosen to ensure that the light illuminating the electrode was not absorbed by the solution. For reducing the intensity of light wire gauzes of various thickness were used the transmittance of which

had been measured on the spectrophotometer.

In potentiometric measurements a slide resistance potentiometer and a spot galvanometer both made by Cambridge Instruments Co. were used. Polarographic curves were recorded by means of the Radiometer PO 4 Polariter.

In order to minimize the effect of stray fields on the measured currents, the reservoir of mercury and the tubing joining it with the capillary were provided by metallic screening, for electric connections coaxial cables were used, and all metallic parts of the whole apparatus were joined to a common earth.

For measuring the instantaneous current on single drops at constant applied voltage a simple circuit was built (Fig. 2) : from a 20 Ω Beckman Helipot precision potentiometer joined to a 4V lead battery with its negative terminal earthed the slider was connected to the mercury pool electrode and the dropping mercury electrode was joined to the earth across a 100 kΩ resistance. The voltage drop on the resistance as a measure of the current in the cell was followed on the screen of a Tektronix Type 531 A oscilloscope with maximal vertical sensitivity 1 mV d.c. per cm. Since the currents observed never exceeded 0.3 μA, the maximal error in the applied voltage in this circuit was 30 mV which represented the limits of precision in determining the red-limit potential of photocurrent (see Results). For exact evaluation the i-t curves were photographed and the photographs magnified.

The values of potentials were referred to the potential of zero charge in each solution. This potential can be easily found on the polarographic curve recorded at high sensitivity with minimal damping and especially when following the i-t curves : while potential of the dropping mercury electrode changes from positive to negative values, the amplitudes of oscillations due to the charging current decrease to zero when the potential of zero charge is reached and then start increasing in the opposite direction. The precision in determining the potential of zero charge from instantaneous currents is higher than from mean currents, since the former show the initial part, characteristic for charging current, unaffected by electrolytic current of impurities which prevails in later phase of the drop-time; with i-t curves the relative error of determination was less than $\pm$ 10 mV even in dilute solutions.

The determination of the potential of zero charge was repeated before and after each measurement of the red-limit potential. Values of the voltage applied to the electrodes and indicating the zero charge and red-limit potentials were measured on the screen of the oscilloscope calibrated with a Weston element. It was found that the mercury pool as counterelectrode held its potential in all solutions fairly constant - this was apparently due to the low current-density maintained throughout all experiments; exceptionally a small drift was observed which never exceeded 30 mV.

Since the dropping electrode was placed in the focus of

converging beams of light, the photocurrent was affected by every slight change of the position of the capillary. For this reason exact comparative measurements of photocurrent could be carried out only when the capillary did not have to be moved - that is, only in measurements in one solution, like following the effect of wavelength, of light intensity or of gaseous substances. This disadvantage was compensated by the high intensity of light on the electrode surface which produced high photocurrents.

Results

A. Potentiometric Measurements

Potentiometric measurements of the effect of UV light upon mercury pool electrodes in 0.1M aqueous solutions of K_2SO_4, KOH and H_2SO_4 have shown that in the atmosphere of hydrogen or nitrogen the potential of mercury begins to change towards negative values on illumination (Fig.3). In presence of oxygen the change of potential has positive direction (Fig.4). With full emission of the lamp the potential changes are of the order of millivolts per minute, whereas light of wavelengths above 3100 Å produces a shift of potential by several millivolts per hour only. Although the change of potential in the indicated direction was observed every time on illumination, its rate and its final limit were not sufficiently reproducible. In order to attain higher reproducibility instead of mercury pool the dropping mercury electrode was chosen which keeps its surface clean by constant renewing, and the effect was further studied by the polarographic method.

B. Polarographic Measurements

The dropping electrode was polarized in each solution within the limits of potentials where the electrolytic current does not exceed the magnitude of charging current. A current-voltage curve was recorded with a high sensitivity first in dark, then with electrode illuminated and then the

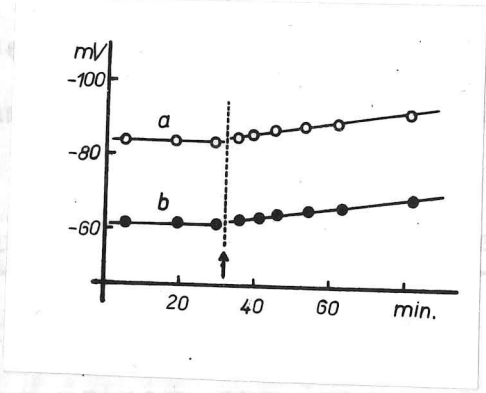

Fig.3. Change of potential of mercury pool electrodes in 0.1M H_2SO_4 on illumination. In parallel experiments solution in atmosphere of : a - nitrogen, b - hydrogen. Beginning of exposure of electrodes to light denoted by arrow; full emission of lamp; potentials versus 0.1M mercurous sulphate electrode.

Fig.4. Like in Fig.3 with the difference that under b the solution is in atmosphere of oxygen.

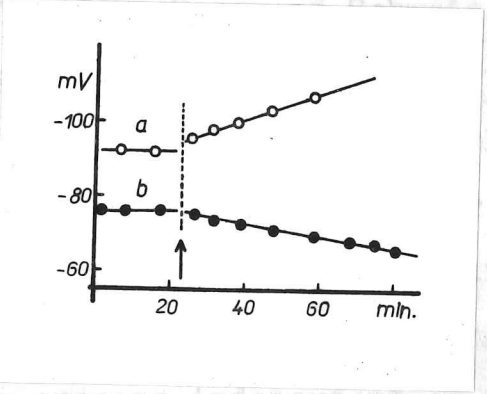

response of current to light passed through various filters was measured at constant potential.

Photocurrent, General Properties

It has been found that with sufficient light intensity in every solution there is a smaller or greater difference between the current on the dark and on the illuminated electrode. This difference, or the photocurrent, depends on the potential of the electrode, on the intensity and frequency of light, and on the composition of the solution. This is in general agreement with what was found under different conditions by Barker and Gardner [21] and by Berg and Schweiss [22].

The Bowden's effect of light on the electrolytic evolution of hydrogen in conditions of polarographic electrolysis is shown on Fig.5 for a 0.1M solution and on Fig 6 for a dilute solution of acid. From the polarographic curves it is evident that the Bowden's effect is not due to lowering of hydrogen overvoltage, but to a process independent of the electrode reaction of hydrogen ions. On Fig.6 the entire reduction wave of hydrogen ions has been recorded; otherwise in the present work the photocurrent was measured as a rule only in that part of the polarographic curve where the electrolytic reaction does not practically come into force, i.e. in the region of residual current before the foot of the wave.

The mean photocurrent is independent of the height of

Fig.5. Effect of illumination of dropping mercury electrode on polarographic curve of 0.1M H_2SO_4. a - dark curve, b - electrode illuminated by full light of lamp. Potentials versus mercury pool.

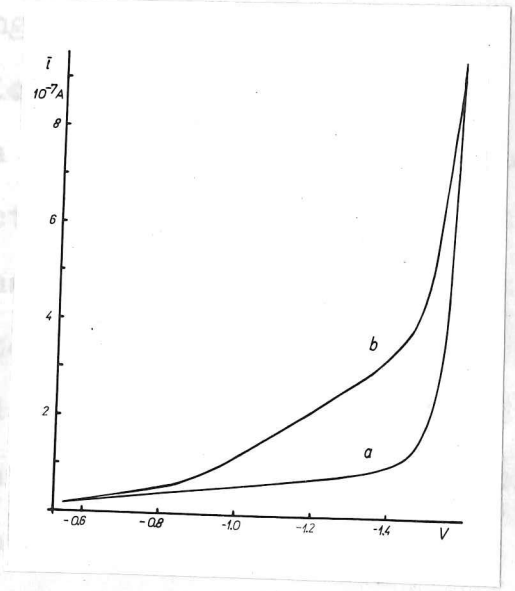

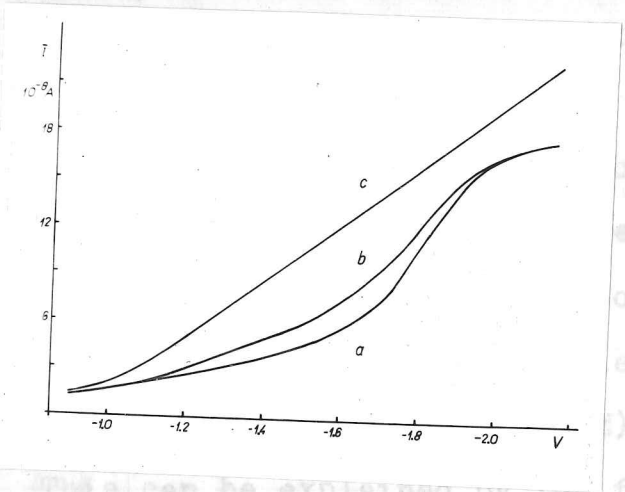

Fig.6. Effect of illumination of dropping electrode on polarographic curve of 10^{-5}M $HClO_4$. a - dark curve; electrode illuminated by light of wavelengths longer than: b - 3900 Å, c - 3030 Å. Potentials versus mercury pool.

mercury column above the tip of the capillary (Fig.7). This indicates that the determining step in the photoprocess is the rate of a chemical reaction in the vicinity of the electrode or on the electrode surface or of an electron--transfer process at the electrode. This conclusion has been confirmed in various solutions by measuring the instantaneous current at constant potential. The instantaneous photocurrent i_p (Fig.8) obtained by substraction of the "dark" current from the current under illumination is a parabolic function of time t with the exponent 2/3 :

$$i_p = k \cdot t^{2/3}$$

where k is a constant. This dependence proves also that the photocurrent is a faradaic current, and is not due to any eventual change of capacity of the electrode caused by illumination.

The time response of photocurrent at illumination, as could be observed on i-t curves, appeared to the eye and on the photographs as instantaneous, which is in agreement with Barker's and Gardner's experience [21]. Only in the very diluted solutions (10^{-5} - 10^{-6}M) a slower response was noticed. This can be explained by the fact that because of large resistance in the solution a sudden change of current Δi causes a change of potential of the polarisable electrode ΔE by the $\Delta i.R$ drop that can amount to some 0.1 V in our case. This change brings about an additional charging current Δi_c according to the formula [22]

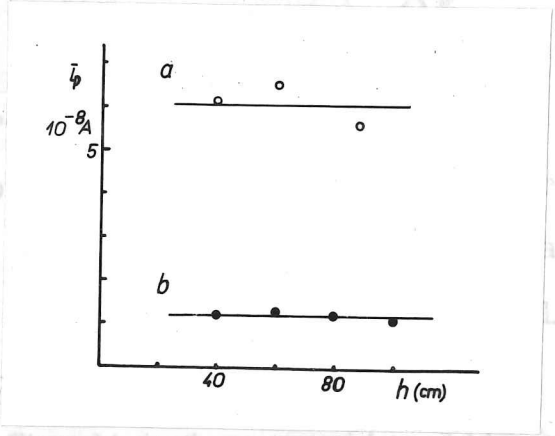

Fig.7. Dependence of mean photocurrent $\bar{i}_p$ on the height of mercury column h in solution of : a - 0.1M $NaHCO_3$ at -1.75 V versus mercury pool (see Fig.25); b - 0.1M H_2SO_4 at -1.0 V versus mercury pool (see Fig.5). Full light of the lamp.

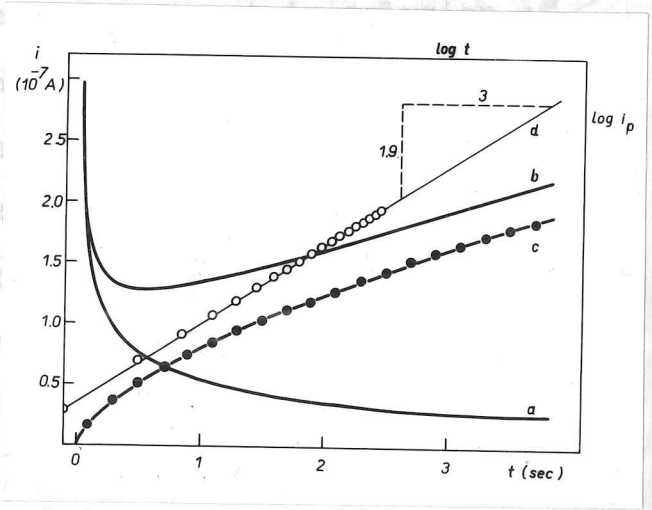

Fig.8. Effect of illumination of electrode on the instantaneous polarographic current. Solution of 0.1M $Na_2S_2O_3$, potential -0.14 V versus point of zero charge. a - dark curve, b - dropping electrode illuminated by light of wavelengths longer than 3360 Å, c - instantaneous photocurrent i_p obtained by substraction of a from b, d - dependence of log i_p on log t. Circles correspond to full points on curve c. Slope of the straight line is 1.9 : 3.

$$\Delta i_c = \frac{\Delta E}{R} \exp\left(-\frac{t}{Rc_D}\right)$$

where R is the total resistance in the circuit and c_D the double layer capacity (of the order of 10^{-6}F). This additional current which adds to the basic current is the cause of the slow response; in dilute solutions it can practically last as long as a second.

The direct proportionality between the photocurrent and intensity of light reported by Price [19], Hillson and Rideal [20] and Barker and Gardner [21] was found to hold in general (Fig.9).

Price [19] has measured the increase of photocurrent with increasing electrode potential in solution of sulphuric acid and obtained an exponential dependence. The graph showing the logarithm of polarographic photocurrent in solution of sulphuric acid as a function of potential is on Fig.10; it can be very nearly approximated by two straight lines. This type of dependence was ascertained with all solutions where sufficiently high photocurrent could be produced (Fig.11 and 12). The slopes and the proportions of the two linear parts of the dependence vary from one solution to another, and depend on the energy of the light used.

Dependence of Photocurrent on the Frequency of Light

According to Price [19] and Hillson and Rideal [20] the photocurrent in sulphuric acid is also an exponential funct-

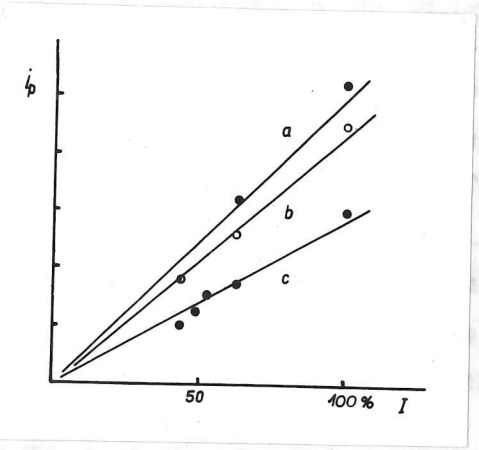

Fig.9. Dependence of photocurrent on light intensity. a - 0.1M LiCl saturated with CO, full light, -1.0 V versus potential of zero charge; b - 0.1M H_2SO_4, full light, -1.0 V versus potential of zero charge; c - 0.1M $Na_2S_2O_3$ + 0.1M KCl, light of wavelengths longer than 3360 Å, -0.27 V versus potential of zero charge. Values of current on arbitrary scale.

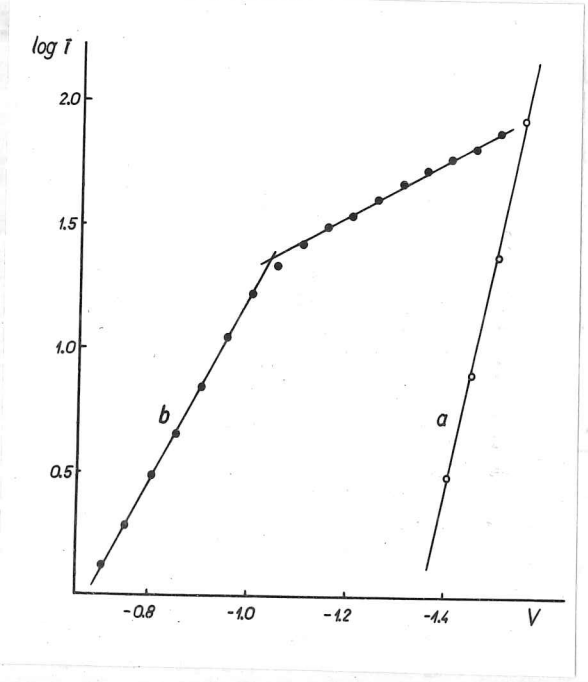

Fig.10. Dependence of logarithm of mean current on potential in 0.1M H_2SO_4 (see Fig. 5). a - current of electrolytic deposition of hydrogen, b - photocurrent. Unity of current scale 4.10^{-9}A; potentials versus mercury pool.

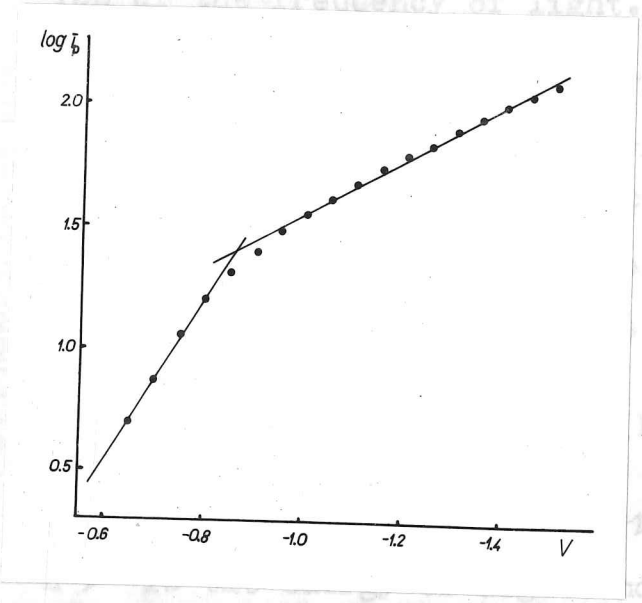

Fig.11. Dependence of logarithm of mean photocurrent on potential in 10^{-5}M KOH. Full light of the lamp; unity of current scale 8.10^{-10}A; potentials versus mercury pool.

Fig.12. Dependence of logarithm of mean photocurrent on potential in 0.1M $Na_2S_2O_3$. Light of wavelengths longer than 3030 Å; unity of current scale 8.10^{-10}A; potentials versus mercury pool.

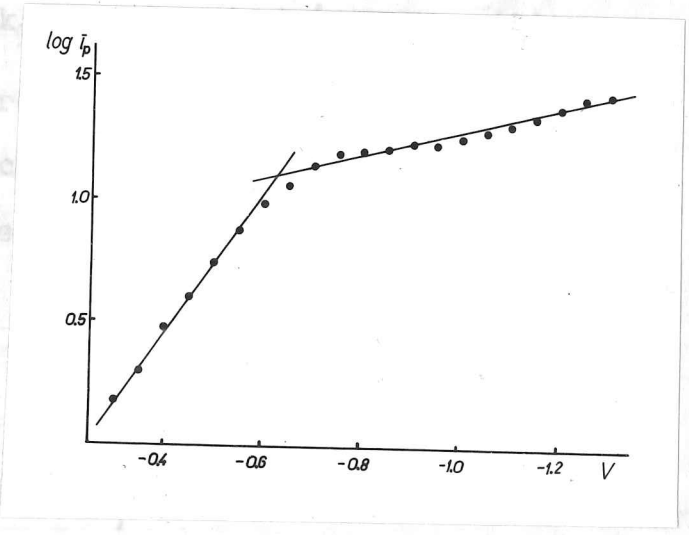

ion of the frequency of light. These authors were using monochromatic light for illumination of electrodes, and their result could not be verified in the present experimental arrangement with sufficient precision.

Let us accept that the photocurrent for monochromatic light at constant potential is given by the expression

$$di_p = \frac{I}{h\nu} \cdot k_1 \cdot \exp(k_2 \nu)\, d\nu \qquad (1)$$

where I is the intensity and ν the frequency of light, $h\nu$ is the energy of light and k_1 and k_2 are constants. Since

$$I = h\nu \cdot c \cdot \rho ,$$

where c is velocity of light and ρ the density of radiation, we can write

$$di_p = c \cdot \rho \cdot k_1 \exp(k_2 \nu)\, d\nu \qquad (2)$$

For light compased of frequencies changing continuously from a constant low frequency ν_c to a higher frequency ν the photocurrent will be given by the integral

$$i_p = \int_{\nu_c}^{\nu} c \cdot \rho \cdot k_1 \exp(k_2 \nu)\, d\nu . \qquad (3)$$

If the density of radiation ρ is constant, independent of frequency in the interval from ν_c to ν, it follows for the photocurrent

$$i_p = c \cdot \rho \cdot \frac{k_1}{k_2} \exp\left[k_2(\nu - \nu_c)\right] ,$$

or in another form

$$i_p = \frac{c \cdot \varphi \cdot k_1}{k_2 \exp(k_2 \nu_c)} \exp(k_2 \nu) \qquad (4)$$

where the first factor is a constant.

From the last formula it can be seen that with a light source emitting a continuous band the photocurrent is an exponential function of the short-wave limit, provided the number of photons per cm^3 is equal for each energy within the band.

We may try to apply equation (4) on results of our measurements since the experimental arrangement roughly fulfils its conditions. The spectrum of the high pressure mercury lamp between the wavelengths 2700 and 5500 Å can be considered as approximately continuous with uniform emission. The ratio of photocurrents recorded with electrode illuminated by various portions of spectrum of the lamp should be an exponential function of the difference of short-wave end frequencies, as requires equation (4). Fig.13 shows the current-voltage curves for 0.1M sulphuric acid with electrode illuminated through various filters. From the ratio of photocurrents and from the corresponding short-wave end frequencies the value of the constant

$$k_2 = \frac{\ln \frac{i_{p1}}{i_{p2}}}{\nu_1 - \nu_2}$$

has been calculated; for the cu
cm, for c and d, $k_2 c = 3.05 \times$
$= 3.15 \times 10^{-4}$ cm. This result p.
of equation (4) to the results obtai.
perimental arrangement is justified.

Potential - Red Limit Diagrams

The experimentally found dependence of photocurrent on frequency of light and on electrode potential can be put in an empirical equation :

$$i_p = k_a \cdot \exp(k_b \cdot h\nu) \cdot \exp\left[-k_c(E - E_R)\right] \qquad (5)$$

where E_R is a reference potential and k_a, k_b and k_c are constants provided the density of radiation is constant over the given range of wavelengths.

From this equation it is evident that a certain value of photocurrent can be reached either at a constant electrode potential by increasing the energy of light, or, with light of constant wavelength, by increasing the electrode potential. For a fixed value of photocurrent a linear relation results between the electrode potential and the energy of light producing the photocurrent :

$$h\nu = \frac{1}{k_b} \ln \frac{i_p}{k_a} + \frac{k_c}{k_b}(E - E_R) \qquad (6)$$

If the linear relation (6) holds for monochromatic light, it should be also applicable, in view of eq.(4), to continuous spectrum with short-wave limit energy $h\nu$. In order

has been calculated; for the curves b and c, $k_2 c = 3.10 \times 10^{-4}$ cm, for c and d, $k_2 c = 3.05 \times 10^{-4}$ cm and for b and d $k_2 = 3.15 \times 10^{-4}$ cm. This result proves that the application of equation (4) to the results obtained with the present experimental arrangement is justified.

Potential - Red Limit Diagrams

The experimentally found dependence of photocurrent on frequency of light and on electrode potential can be put in an empirical equation :

$$i_p = k_a \cdot \exp(k_b \cdot h\nu) \cdot \exp\left[-k_c(E - E_R)\right] \qquad (5)$$

where E_R is a reference potential and k_a, k_b and k_c are constants provided the density of radiation is constant over the given range of wavelengths.

From this equation it is evident that a certain value of photocurrent can be reached either at a constant electrode potential by increasing the energy of light, or, with light of constant wavelength, by increasing the electrode potential. For a fixed value of photocurrent a linear relation results between the electrode potential and the energy of light producing the photocurrent :

$$h\nu = \frac{1}{k_b} \ln \frac{i_p}{k_a} + \frac{k_c}{k_b}(E - E_R) \qquad (6)$$

If the linear relation (6) holds for monochromatic light, it should be also applicable, in view of eq.(4), to continuous spectrum with short-wave limit energy $h\nu$. In order

to verify this conclusion it is convenient to choose for the constant value of photocurrent its limit, i.e. its smallest measurable value, and to determine the "red-limit potentials" with light passed through various filters. By "red-limit potential" the potential is understood at which the photocurrent begins to appear under given illumination. Likewise, for a given potential light of a definite red-limit wavelength exists with which the photocurrent can just be observed.

The limit of photocurrent necessarily depends on the experimental arrangement used, on the intensity of light and on the sensitivity of the current-measuring instrument. Its value in our case was 10^{-9}A, corresponding to a deflection of 1 mm on the screen of the oscilloscope with full sensitivity. The potential of reference E_R was, for the mentioned practical reasons, in each solution the corresponding potential of zero charge. The "red-limit potentials" when plotted against the values of energy of the shortest wavelength transmitted by the filters showed a linear dependence in all solutions examined (Fig.14 and following).

The linear relation between the two variables determining the red-limit of photocurrent is a useful characterization of the electrochemical photoeffect. The intercept of the straight line on the energy axis at potential of zero charge gives the minimal quantum necessary for production of photocurrent in absence of electric field due to ionic double layer, whereas the slope of the line indicates to what extent the photoprocess depends on the potential of the electrode.

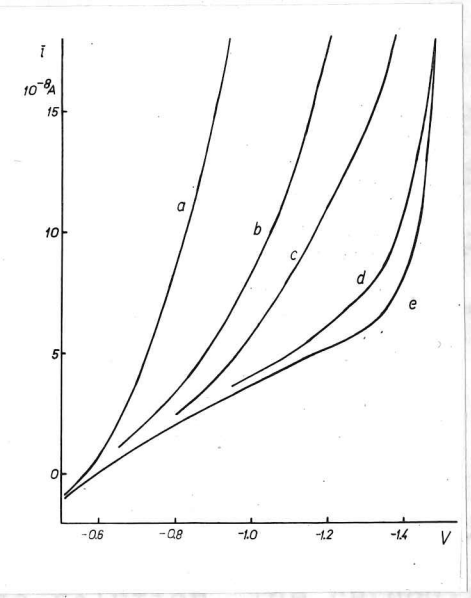

Fig.13. Current-voltage curves of 0.1M H_2SO_4 with electrode illuminated through various filters. a - full light of the lamp; b - light through Pyrex; c - through 15% $CuSO_4$ filter; d - light through $NaNO_2$; e - dark curve. Potentials versus mercury pool.

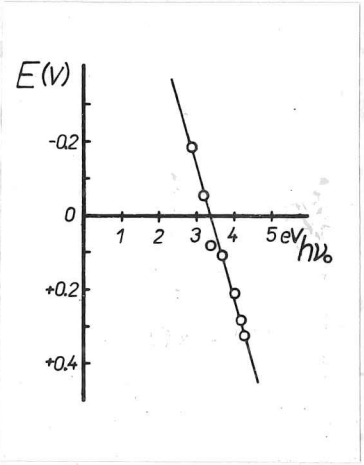

Fig.14. Potential-red limit diagram. Relation between potential of the electrode and energy of red limit of photocurrent. 0.1M $HClO_4$, potentials versus point of zero charge.

The straight line on the "potential-red limit diagrams" represents for each solution a border on the energy - potential plane under which no photocurrent can be obtained in the given experimental conditions. All the values of potential or energy of light exceeding this border line produce photocurrent, the further from the line, the higher.

Cathodic Photocurrent in Indifferent Electrolytes

The direction and magnitude of photocurrent varies according to the composition of the solution. The cathodic photocurrent, of the direction of electrons entering into the solution from the electrode, is in aqueous solutions a general phenomenon, and shall be dealt with first.

In neutral and alkaline aqueous 0.1M solutions containing cations of alkali or alkaline earth metals and anions like halides, hydroxide, chlorate, perchlorate, azide, cyanate, sulphite, sulphate, phosphate, acetate and benzoate the photocurrent is cathodic, approximately of equal magnitude - rather small, with the intercept on the potential - red limit diagram between 4.1 and 4.5 eV and the slopes of the straight lines between 0.9 and 1.4 eV/V (Fig.15). A finer distinction between the above solutions, as far as the effects of cations or anions on the photocurrent are concerned, has not been studied. The reproducibility in determination of the intercept with one solution, each time freshly prepared, was within $\pm$0.1 eV.

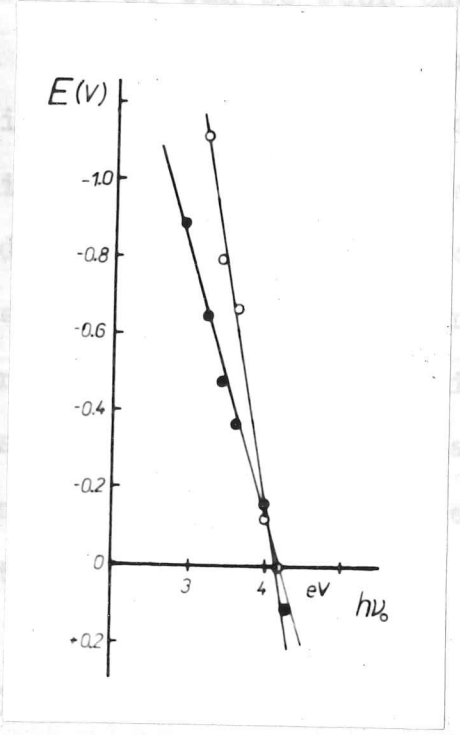

Fig.15. Potential-red limit diagrams of 0.1M solutions of sodium tetraborate (circles) and acetate (full points). Potentials versus point of zero charge.

Fig.16. Effect of dilution on the mean photocurrent. Solutions of: a - LiCl, b-$CaCl_2$; concentrations: 1 - 10^{-1}M, 2 - 10^{-3}M, 3 - 10^{-5}M. Full light of the lamp, potentials versus point of zero charge.

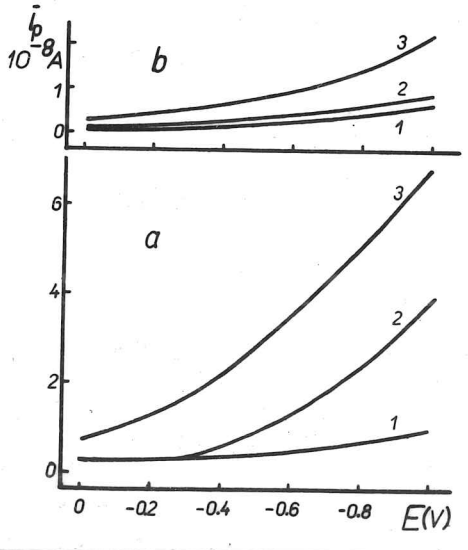

On Fig.6 it can be seen t
tration of acid the photocu
rographic reduction wave o
with this effect a marke
ved on dilution of electrolyti
16). The magnitude of photocurrent de
the charge of cations present in the solutio
of salts of alkaline earth metals have to be more t
red times more diluted than the solutions of salts of alka
metals to give photocurrent of the same magnitude. This difference is evident also on the potential-red limit diagrams (Fig.17): on dilution both the intercept and the slope of the straight line are changed. With monovalent cations on 10^4fold dilution the intercept decreases by about 0.5 eV whereas with divalent cations the decrease is only about 0.1 eV. Solution of lanthanum acetate did not give any increase of photocurrent even on 10^4fold dilution.

In purely ethanolic solutions the photocurrent is in general by more than one order less than in aqueous solutions. On Fig.18 are compared the potential-red limit diagrams of 0.1M and ethanolic solutions. It is evident that for producing photocurrent in ethanolic solutions more negative potentials must be applied to the electrode than in aqueous solutions. The effect of dilution on photocurrent appears in ethanol like in water with the difference that in water the slopes of the straight lines of the diluted and concentrated solutions with increasing negative potential diverge, where-

On Fig.6 it can be seen that in solution of low concentration of acid the photocurrent increases beyond the polarographic reduction wave of hydrogen ions. In accordance with this effect a marked increase of photocurrent was observed on dilution of electrolytic solutions in general (Fig. 16). The magnitude of photocurrent depends here strongly on the charge of cations present in the solution. The solutions of salts of alkaline earth metals have to be more than hundred times more diluted than the solutions of salts of alkali metals to give photocurrent of the same magnitude. This difference is evident also on the potential-red limit diagrams (Fig.17): on dilution both the intercept and the slope of the straight line are changed. With monovalent cations on 10^4fold dilution the intercept decreases by about 0.5 eV whereas with divalent cations the decrease is only about 0.1 eV. Solution of lanthanum acetate did not give any increase of photocurrent even on 10^4fold dilution.

In purely ethanolic solutions the photocurrent is in general by more than one order less than in aqueous solutions. On Fig.18 are compared the potential-red limit diagrams of 0.1M and ethanolic solutions. It is evident that for producing photocurrent in ethanolic solutions more negative potentials must be applied to the electrode than in aqueous solutions. The effect of dilution on photocurrent appears in ethanol like in water with the difference that in water the slopes of the straight lines of the diluted and concentrated solutions with increasing negative potential diverge, where-

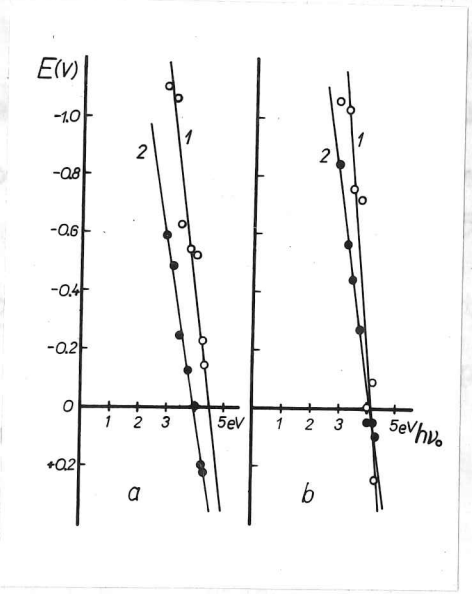

Fig.17. Effect of dilution on potential-red limit diagram. Solutions of: a - LiCl, b - $CaCl_2$; concentrations: 1 - 10^{-1}M, 2 - 10^{-5}M. Potentials versus point of zero charge.

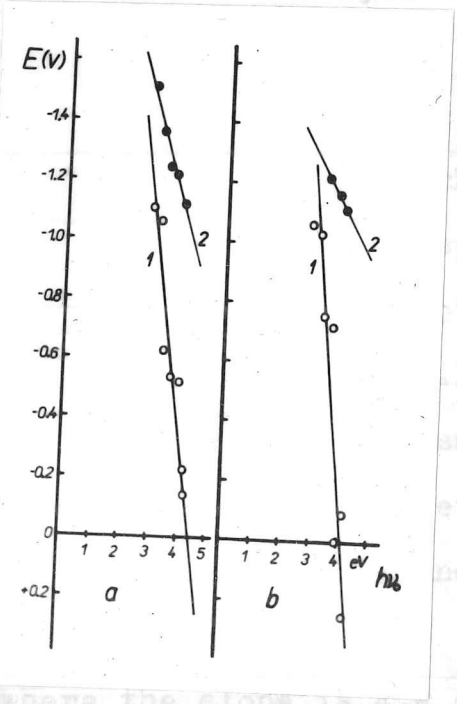

Fig.18. Comparison of potential-red limit diagrams of aqeuous and ethanolic solutions. 0.1M solutions of : a - LiCl; b - $CaCl_2$; 1 - aqueous, 2 - ethanolic. Potentials versus point of zero charge.

as in ethanol they converge (Fig.19). From Fig.19 it can be seen, for example, that on the electrode illuminated through filter of concentrated $NaNO_2$ (i.e. by wavelengths longer than 4200 Å) the photocurrent begins to appear in aqueous solution of KOH at potential -0.6 V at 10^{-5}M concentration, and at potential by 0.6 V more negative at 0.1M concentration. In ethanol, on the other hand, it appears in both the diluted and the concentrated solutions at the same potential of -1.6 V versus point of zero charge.

Cathodic Photocurrent in Specifically Active Solutions

Considerably higher photocurrents than in 0.1M neutral or alkaline solutions of the above mentioned compounds appear in solutions of acids, as has been known since the Bowden's discovery. Bowden [18], Price [19] and Hillson and Rideal [20] were studying the effect in sulphuric acid, Barker and Gardner [21] used also hydrochloric and perchloric acids, Berg and Schweiss [22] added phosphoric and Heyrovský and Norrish [24] acetic acids. The potential-red limit diagram of 0.1M perchloric acid is on Fig.14. The intercepts on the potential-red limit diagrams of sulphuric, hydrochloric, perchloric, oxalic, citric and acetic acids were all found to lie between 3.25 and 3.50 eV and the slopes of the straight lines between 2.4 and 2.8 eV/V (with the exception of oxalic acid where the slope is 4.2 eV/V) - see Tab.1.

T a b l e 1

Parameters of Straight Lines from Potential-Red Limit Diagrams for Cathodic Photocurrent

solution (0.1M unless stated otherwise)	aqueous		+0.1M KOH		ethanolic	
	slope (eV/V)	intercept (eV)	slope (eV/V)	intercept (eV)	slope (eV/V)	intercept (eV)
LiCl sat.with N_2O [a]	1.9	3.45	1.3	3.3	1.85	4.85
LiCl + acrylonitrile	1.6	3.45	1.6	3.45	2.3	4.65
LiCl sat.with CO [b]	2.5	4.4				
K_2SeO_3	2.1	3.85				
K_2TeO_4 [c]	2.3	2.9	1.1	3.1		
$NaNO_2$	2.7	2.4	1.9	3.40	2.3	5.15
KCNS	1.1	3.4	1.2	3.75		
KNO_3	1.5	3.3	1.8	3.45		
$KBrO_3$	2.0	2.15	0.9	3.1		
KJO_3	2.2	2.15	0.85	3.1		
$Na_2S_2O_3$	1.55	3.4	1.6	3.7		
$La(OCOCH_3)_3$	1.7	3.9				
NaH_2PO_4	1.2	3.65	0.75	4.05		
KCN	1.3	3.95	0.8	4.05		
$NaHCO_3$	2.2	3.45	0.9	4.3		
	8.4					
LiCl + CH_3COCH_3	7.6				3.6	
$(COOH)_2$	4.2	3.35			3.95	5.4
HCl	2.6	3.3				
$HClO_4$	2.8	3.35				
H_2SO_4	2.4	3.45				
HNO_3	1.7	3.1				
CH_3COOH	2.4	3.45				
citric acid	2.5	3.3				

[a] concentration of N_2O in aqueous solution about 2.5×10^{-2}M, in ethanolic about 8×10^{-2}M

[b] concentration of CO about 2×10^{-3}M

[c] ethanolic solution saturated about 4×10^{-2}M

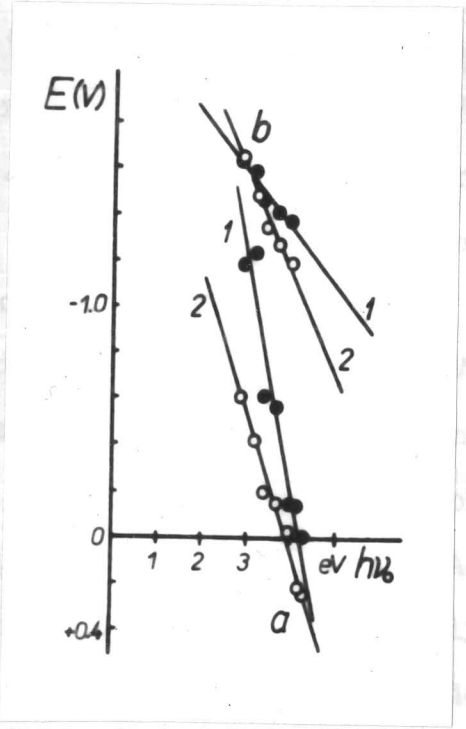

Fig.19. Comparison of the effect of dilution on photocurrent in aqueous and ethanolic solution. Solution of KOH : a - aqeuous, b - ethanolic; concentrations : 1 - 10^{-1}M; 2 - 10^{-5}M. Potentials versus point of zero charge.

Fig.20. Effect of illumination of dropping mercury electrode on polarographic curve of water saturated with CO_2 under atmospheric pressure. a - dark curve, b - electrode illuminated by light of wavelengths longer than 3030 Å. Potentials versus mercury pool. Exact copy of the original polarogram.

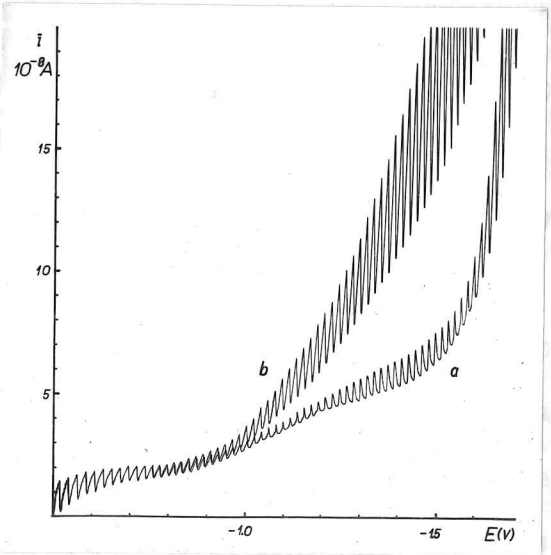

Weaker acids yield smaller photocurrents and higher intercepts on the potential - red limit diagrams; enhanced photocurrents were observed in solutions of acids with $pK < 10$. Considerable photocurrent appears in water saturated with CO_2 (Fig.20). A 0.1M solution of NaH_2PO_4 has an intercept of 3.65 eV and yields a high photocurrent, whereas Na_2HPO_4 with intercept of 4.05 eV does not differ on illumination from other neutral solutions (Fig.21). In 0.1M solutions of boric acid, glycine and phenol the photocurrent is several times higher than in 0.1M KCl. An increased photocurrent in 0.1M solution of KCN has probably to be ascribed to HCN formed by hydrolysis since after addition of KOH the photocurrent does not exceed that in KOH alone.

Besides acids there are other species yielding higher photocurrents when in neutral or alkaline solutions (Tab.1). Lanthanum acetate in 0.1M concentration has an intercept of 3.9 eV and displays a photocurrent noticeably higher than magnesium acetate with intercept of 4.4 eV (Fig.22); however, on 10 fold dlution the photocurrent due to lanthanum ions disappears and further dilution does not lead to its reappearance, as has been mentioned above. In solutions of zinc and manganese sulphates no specific photocurrents were observed. Other cations have not been examined as they either are reduced at potentials too positive or absorb visible light and so do not fit into the present conditions of measurement.

Barker and Gardner [21] reported a high photocurrent in presence of nitrate, nitrite and bromate ions in solution.

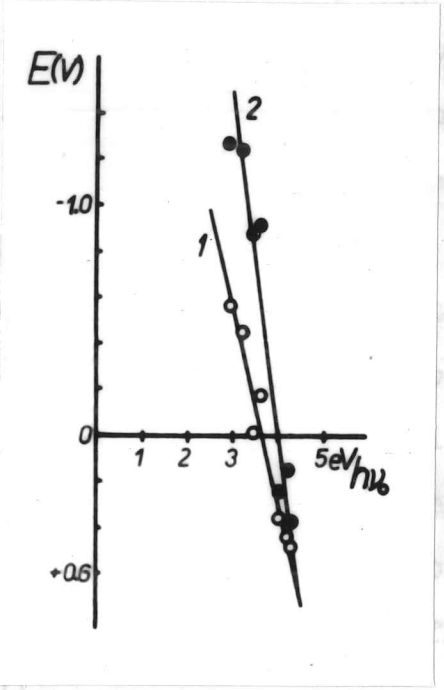

Fig.21. Comparison of potential-red limit diagrams of solutions of different acidity. 0.1M solution of 1 - NaH_2PO_4; 2 - Na_2HPO_4. Potentials versus point of zero charge.

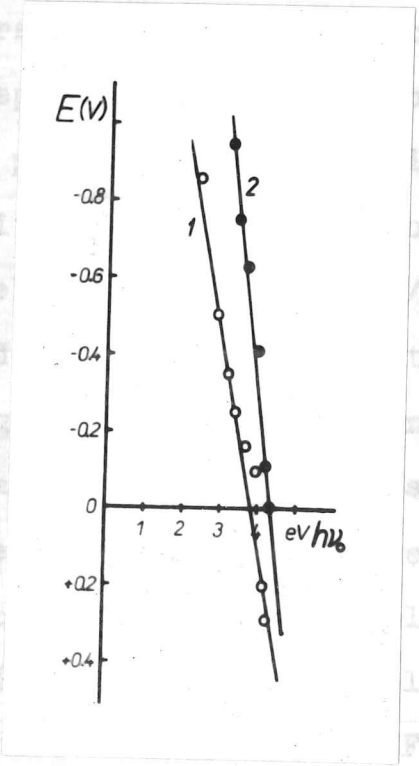

Fig.22. Potential-red limit diagrams of 0.1M acetates of: 1 - lanthanum, 2 - magnesium. Potentials versus point of zero charge.

This has been confirmed in present experiments, and few more active anions were found : iodate, thiocyanate, thiosulphate, selenite and tellurate. Heyrovský and Norrish [24] noticed a strong photoeffect in solutions of nitrous oxide N_2O; equally effective is acrylonitrile.

The photocurrent in aqueous solution of LiCl saturated with carbon monoxide under atmospheric pressure (about 10^{-3}M) increases notably with increasing negative potential; on the potential-red limit diagram there is hardly any change of the value of the intercept of LiCl solution noticeable, but the slope of the straight line changes to 2.5 eV/V from 1.4 eV/V in.pure 0.1M LiCl (Fig.23).

When the electrode is illuminated in aqueous solutions of bicarbonate or acetone, on the current-voltage curve there appears a shape of a polarographic "wave" (Fig.24) caused by a steep increase of photocurrent from zero at relatively negative potentials. The straight lines on the potential--red limit diagrams have in both cases an unusually high slope (7.6 eV/V acetone, 11.4 eV/V bicarbonate) which indicates a strong dependence of the photoprocess on electrode potential (Fig.25, 33). In bicarbonate solutions a cathodic photocurrent appears already at positive potentials, but disappears when the potential of zero charge is reached and does not reappear until at about -1 V versus potential of zero charge. The intercept extrapolated for the photocurrent on the positive side is 3.3 eV (Fig.25). The increase of photocurrent in solution of acetone occurs at potentials so nega-

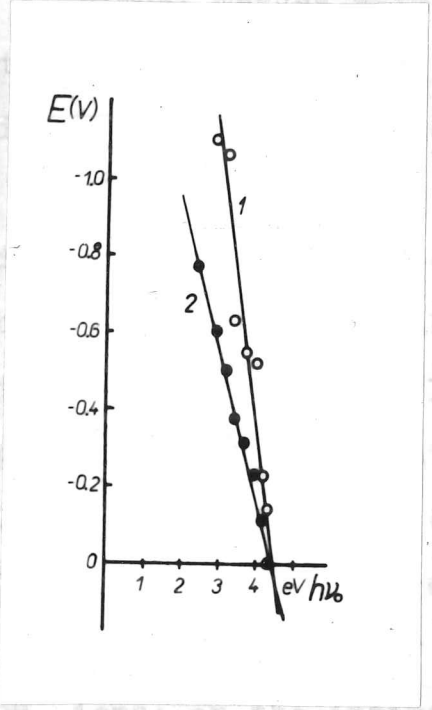

Fig.23. Potential-red limit diagram showing the effect of CO on photocurrent. 1 - 0.1M solution of LiCl, 2 - saturated with CO under atmospheric pressure. Potentials versus point of zero charge.

Fig.24. Effect of illumination of the dropping electrode on polarographic curve of bicarbonate solution. 0.1M $NaHCO_3$, potentials versus mercury pool. a - dark curve, b - electrode illuminated by full light of the lamp.

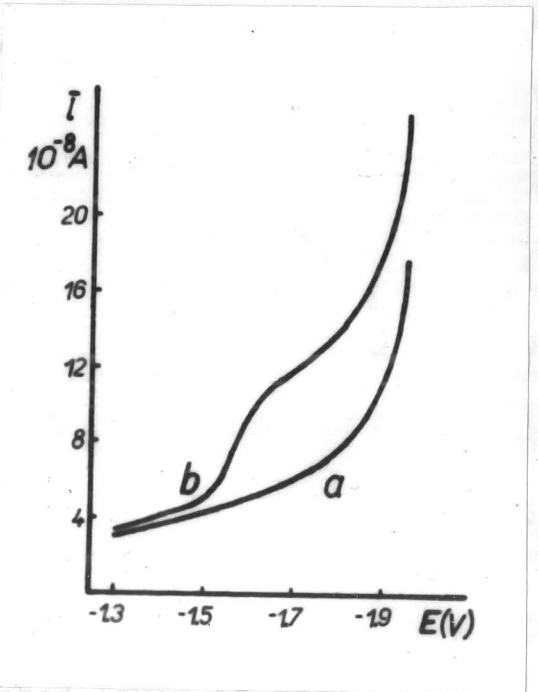

tive that it almost merges with the electrolytic current of supporting electrolyte.

Addition of alkali hydroxide to solutions of specifically active species increases, as a rule, the value of the intercept, i.e. reduces the photocurrent, but in different solutions to different extent (Tab.1). In presence of 0.1M KOH the strongest increase, by 1.0 eV, is observed with nitrite (Fig.26), then with bromate and iodate (0.9 eV), thiocyanate (0.4 eV), thiosulphate (0.3 eV) and tellurate and nitrate (0.2 eV). The photocurrent in solutions of nitrous oxide and acrylonitrile is very little affected by the presence of OH^- ions; on the intercept no change is observable (Fig.28, 31). The addition of an indifferent electrolyte to the specifically active solutions up to 0.1M concentration has no effect on the value of the intercept (Fig.27), and neither any effect of valency of the cation was observed (Fig.28).

In alkaline solutions of substances giving high photocurrent the effect of pyridine can be followed. Pyridine is known [28] to form in alkaline media at the surface of mercury an adsorbed layer which desorbs at negative potentials. It was found that pyridine suppresses the photocurrent to a certain extent in the whole potential range, but that the discontinuous increase of charging current resulting from a sudden disappearance of the adsorbed layer is accompanied by a simultaneous discontinuous increase of the photocurrent (Fig.29).

Fig.25. Potential-red limit diagrams of 0.1M solutions of $NaHCO_3$ (circles) and Na_2CO_3 (full points). Potentials versus point of zero charge.

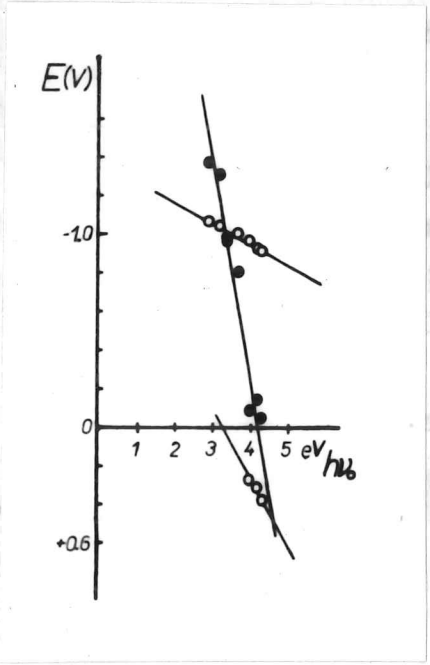

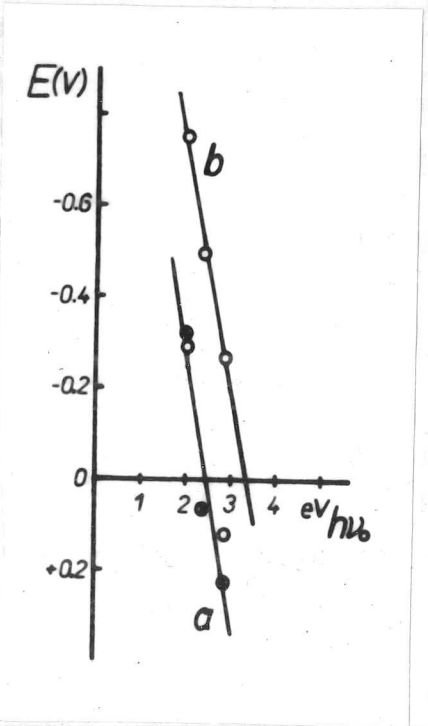

Fig.26. Effect of hydroxyl ions on potential-red limit diagram of $NaNO_2$ solution. a - circles - - 0.1M $NaNO_2$, full points - 0.1M $NaNO_2$ + + 0.1M KCl; b - 0.1M + + 0.1M KOH. Potentials versus point of zero charge.

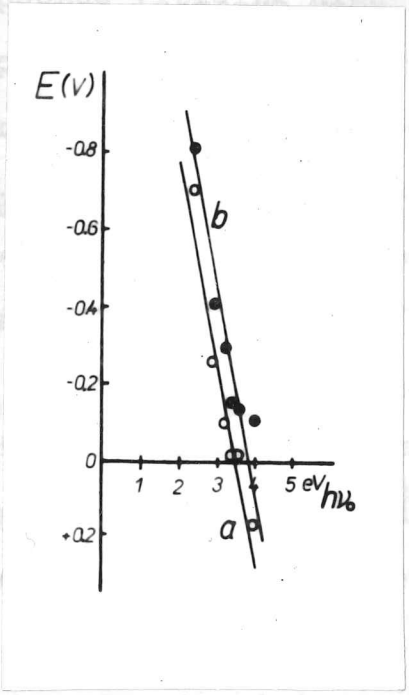

Fig.27. Effect of KCl and KOH on the potential--red limit diagram of $Na_2S_2O_3$ solution. a - 0.1M $Na_2S_2O_3$ + + 0.1M KCl; b - 0.1M $Na_2S_2O_3$ + 0.1M KOH. Potentials versus point of zero charge.

Fig.28. Potential-red limit diagram of nitrous oxide solutions. Circles - 0.1M $BaCl_2$, full points - 0.1M KOH, saturated with N_2O under atmospheric pressure. Potentials versus point of zero charge.

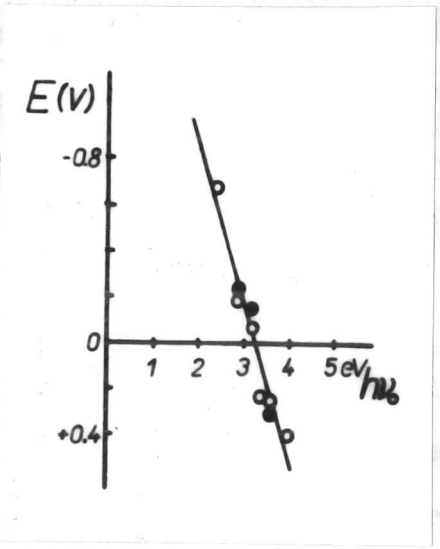

The compounds yielding high photocurrents in 0.1M solutions of supporting electrolytes cause an increase of photocurrent even in highly diluted solutions. Fig.30 shows the effect of N_2O on photocurrent in 10^{-6}M KCl; the effect of CO is smaller, but still pronounced.

In ethanol the specifically active species produce photocurrents by more than one order less than in water. The comparison of the effects of the two solvents is well demonstrated by the potential-red limit diagrams (Table 1). The smallest difference between the intercepts in water and in ethanol, 1.2 eV, was found in solutions of acrylonitrile (Fig. 31). Nitrous oxide with intercept in water of 3.45 eV, the same as acrylonitrile, has the intercept in ethanolic solution slightly higher, 4.85 eV (Fig.32). However, in both cases the straight lines in the two media remain nearly parallel. A considerable difference between the slopes in the two solvents can be observed in solutions of acetone (Fig.33).

Anodic Photocurrent

All the photocurrents described above were cathodic, i.e. of the direction of electrons going from the electrode into the solution. Anodic photocurrent, of the opposite direction, was found in acid, neutral or alkaline solutions of oxalate, dimethyloxalate, malate, tartrate, pyruvate, citrate, glycollate, lactate, chloro-acetate, glycine, diacetyl and glyoxal (Fig.34). It does not appear with any of the previously mentioned inorganic compounds, or with formate, acetate, fuma-

Fig.29. Mean photocurrent in presence of pyridine. a - 0.1M KCNS + 0.1M pyridine; b - 0.1M $Na_2S_2O_3$ + 0.1M pyridine. Potentials versus point of zero charge; light of wavelengths longer than 3030 Å.

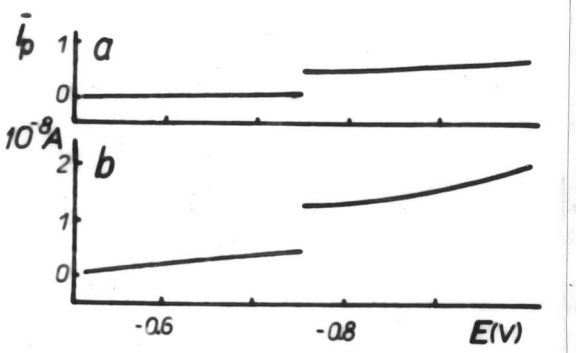

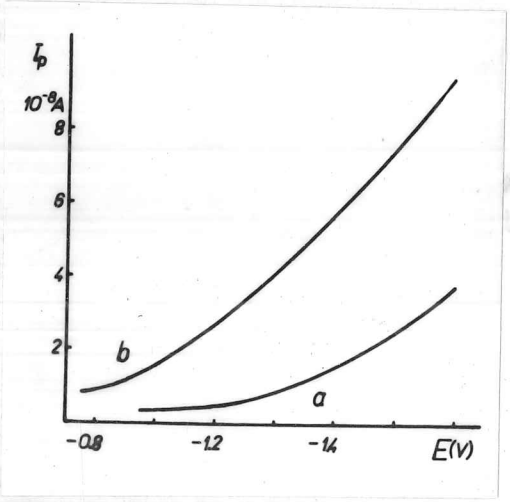

Fig.30. Effect of N_2O on mean photocurrent in dilute solution. a - 10^{-6}M KCl; b - 10^{-6}M KCl saturated with N_2O. Potentials versus mercury pool; light of wavelengths longer than 3030 Å.

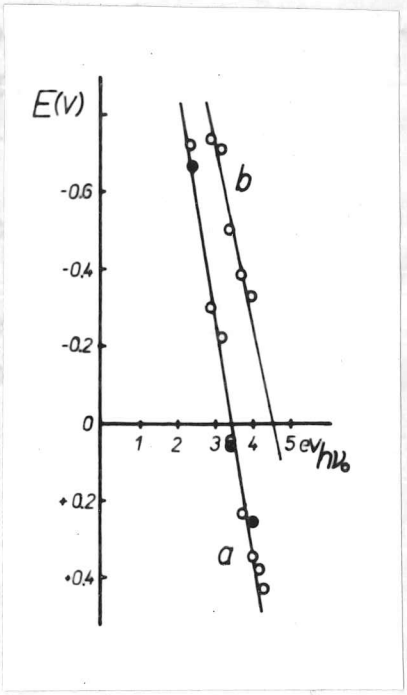

Fig.31. Potential-red limit diagram of 0.1M acrylonitrile in : a - 0.1M aqueous LiCl (circles) or KOH (full points); b - 0.1M ethanolic LiCl. Potentials versus point of zero charge,

Fig.32. Potential-red limit diagram of nitrous oxide in 0.1M LiCl in: a - water, b - ehtanol, Potentials versus point of zero charge.

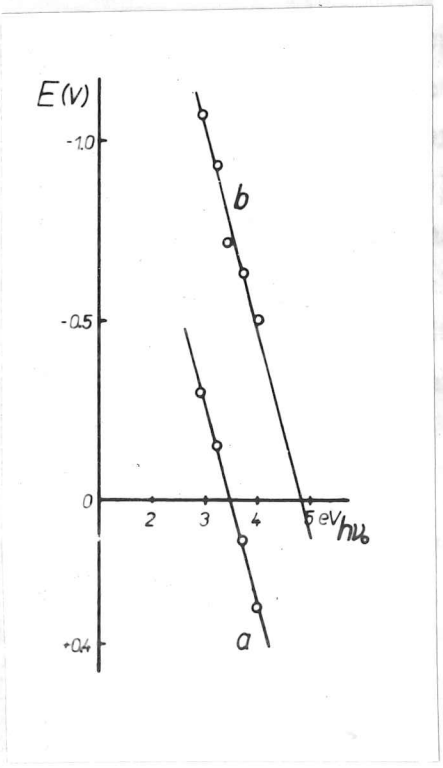

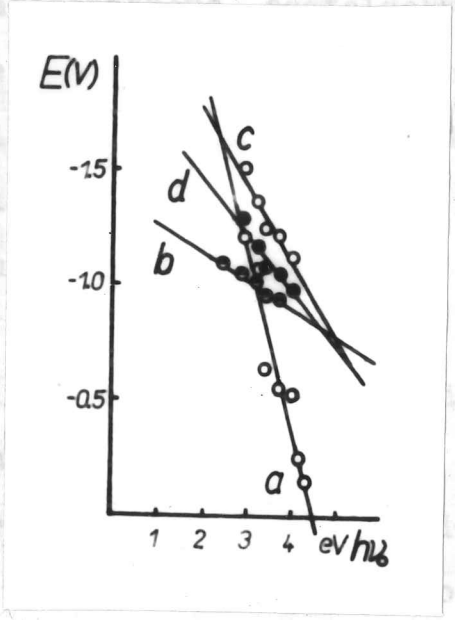

Fig.33. Potential-red limit diagram of acetone. 0.1M LiCl in: a - water, c - ethanol; + 0.1M acetone in b - water, d -ethanol. Potentials versus point of zero charge.

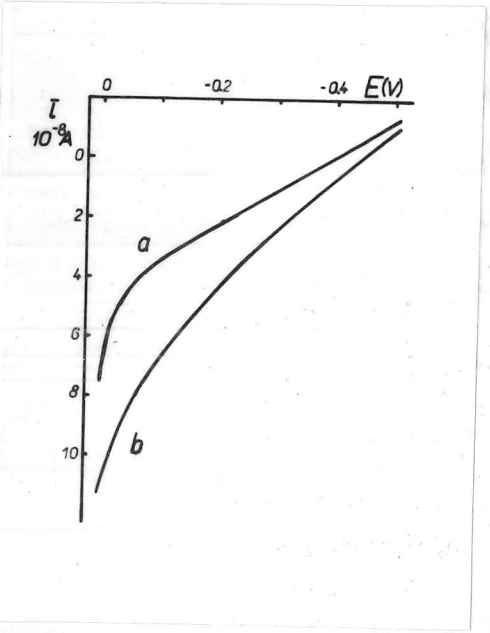

Fig.34. Anodic photocurrent. Polarographic curve of 0.1M Na-tartrate: a - in dark, b - electrode illuminated by light of wavelengths longer than 3030 Å. Potentials versus mercury pool.

rate or maleate, acrylonitrile, acetophenone, acetaldehyde or acetone. Non-occurrence of the anodic photocurrent in solutions of ethyleneglykole, ethylenediamine or ethylenediamine-tetraacetic acid is an indication that the effect is not connected with anodic dissolution of mercury.

The anodic photocurrent like the cathodic, but with opposite sign, increases exponentially with potential. The dependence of the logarithm of photocurrent on potential can also be approximated by two linear parts (Fig.35). The relation between the potential and energy of the red limit of anodic photocurrent is also linear (Fig.36, Table 2). Unlike the cathodic photocurrent the anodic photocurrent is of the same magnitude in aqueous and ethanolic solutions (Fig.37).

On the potential-red limit diagrams the intercepts of solutions of acids are higher than those of their salts (Table 2); an addition of alkaline hydroxide to the salts has no effect (Fig.38). The straight line on the diagram of oxalate ends at low potentials by a short section independent of light energy (Fig.36). A similar case was observed with malic, lactic and Cl-acetic acids (Fig.39) and in dilute solutions of oxalic acid (Fig.40).

T a b l e 2

Parameters of Straight Lines from Potential-Red Limit Diagrams for Anodic Photocurrent

solution (0.1M)	slope (eV/V)	intercept (eV)
oxalic acid aq.	3.2	4.9
ethan.	4.0	4.8
Na oxalate	3.8	3.9
dimethyloxalate	3.6	5.4
tartaric acid	3.2	5.0
Na tartrate	4.2	4.4
Cl-acetic acid	2.8	5.5
glycine	4.2	6.0
glycollic acid	2.2	4.5
lactic acid	2.2	4.5
malic acid	2.6	5.0
citric acid	2.5	5.0

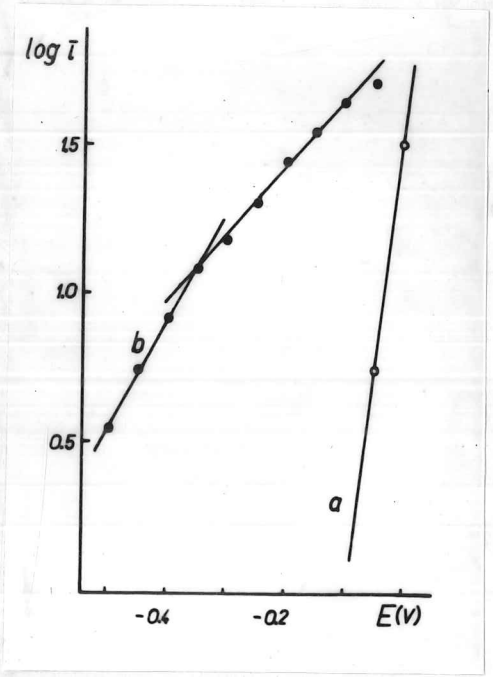

Fig.35. Dependence of logarithm of mean current on potential in 0.1M Na-Tartrate (see Fig.34). a - current of electrolytic dissolution of mercury, b - photocurrent. Unity of current scale 8.10^{-10}A; potentials versus mercury pool.

Fig.36. Potential-red limit diagrams of anodic photocurrents in some solutions: a - 0.1 M Na-tartrate, b - 0.1 M tartaric acid, c - - 0.1M dimethyl oxalate, d - 0.1M glycine. Potentials versus point of zero charge.

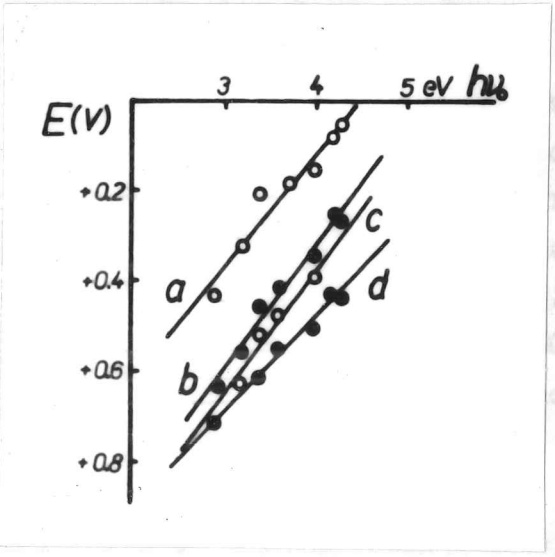

Fig.37. Potential-red limit diagram of anodic photocurrent in 0.1M solution of oxalic acid in : a - water, b - - ethanol. Potentials versus point of zero charge.

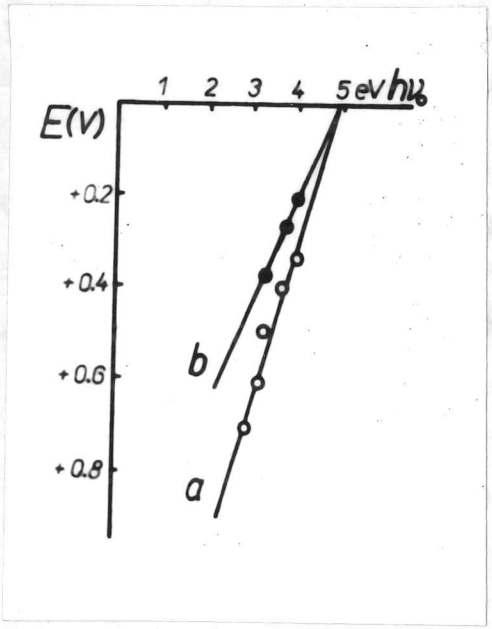

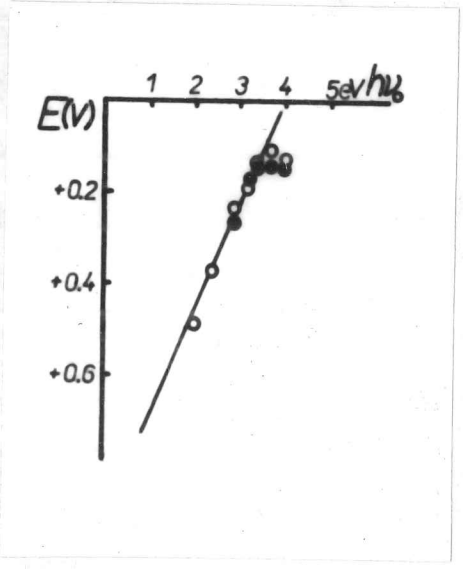

Fig.38. Effect of hydroxyl ions on potential-red limit diagram of anodic photocurrent. Circles - 0.1M Na-oxalate; full points - 0.1M Na-oxalate + 0.1M KOH. Potentials versus point of zero charge.

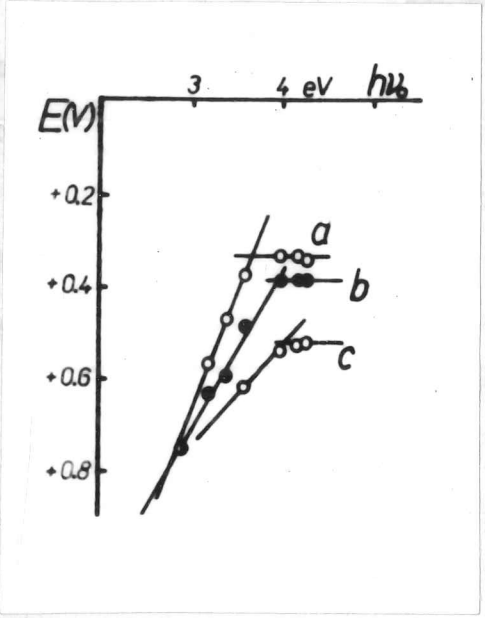

Fig.39. Potential-red limit diagrams of anodic photocurrents in: a - 0.1M lactic acid, b - 0.1M malic acid, c - 0.1M Cl-acetic acid. Potentials versus point of zero charge.

Fig.40. Potential-red limit diagrams of anodic photocurrent in dilute solutions of oxalic acid. a - 10^{-2}M; b - - 10^{-4}M. Potentials versus point of zero charge.

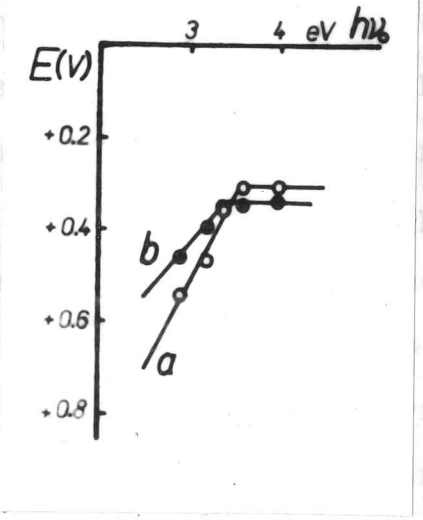

Discussion

In the discussion of results we shall concentrate upon photocurrents in aqueous solutions. The cathodic photocurrents in ethanolic solutions, much smaller than in water, were not well accessible to measurements and therefore little can be said about their character. However, from the comparison of potential-red limit diagrams for solutions in the two solvents important conclusions can be drawn concerning the nature of the photoeffect in water.

Arguments against the Theory of Photoemission of Electrons

The photocurrent, if initiated by emission of electrons according to the theory of Barker and Gardner [21], should be based on qualitatively the same mechanism in aqueous and ethanolic solutions. The supporting electrolyte, specifically the cations, have a suppressing effect on the cathodic photocurrent in water as in ethanol, since in both an increase of photocurrent is observed on dilution. This suppressing effect does not come into force in presence of the active species. There are apparently two opposing processes taking place in either solvent : one of the electrons returning back to the electrode, catalysed by cations, and the other, more rapid one, of the active species, helping to accomplish the transfer of the electrons into the solution. However, in dilute solutions appears the different nature of photoeffect in water and ethanol. The rate of a process in which electrons

return back to the electrode can be supposed to decrease with increasing negative potential; consequently the participation of cations in the mechanism of photocurrent will also decrease. Judging from the potential-red limit diagrams (Fig. 19), this is what happens in ethanolic solutions. In aqueous solutions, on the other hand, obviously a new reaction appears with dilution which accelerates the transfer of electrons from the electrode. This essential difference between the properties of photocurrent in the two solvents is incompatible with the idea of electron emission.

Another point where the difference of the cathodic photoeffect in water and ethanol stands out markedly is the intercept on the potential-red limit diagrams. The values of intercepts in ethanolic solutions are always higher than in aqueous solutions and have to be obtained by extrapolation : no photocurrent can be produced by light of wavelength 2800 Å or longer at potential of zero charge in ethanol. The smallest difference between intercepts in water and in ethanol, found in solutions of acrylonitrile, is 1.2 eV. There are two factors that must be taken into consideration when comparing the intercepts. One is the difference in zero charge potentials : the potential of zero charge of mercury in aqueous solutions is by about 0.2 V more negative than in ethanol when measured against a common reference electrode [29]. The other one is the difference in the interface potentials between mercury and water and mercury and ethanol. If the photocurrent were based on the same mechanism in both solvents and the differences

were due only to different physical properties of the two systems, the value 1.2 eV could be ascribed to the effect of differences in the interface and zero charge potentials. In that case the value 1.2 eV should figure as a constant difference between the aqueous and ethanolic solutions in general. However, this was not found to be the case, as can be seen from Tab.1.

The intercept on the potential-red limit diagram represents the minimal energy necessary for producing photocurrent in absence of electric field due to ionic double layer. For cathodic photocurrent, if there are no kinetic complications, the intercept corresponds to the work function referring to the escape of electron from the electrode into the solution. In case of a reaction opposing to the escape of electrons a higher value of intercept will be obtained, but under no conditions can the intercept be lower than the work function. Equation for the work function for escape of electron from metal into the solution was derived by Frumkin [30]. According to this equation after substitution of the known data for the potential of zero charge of mercury in aqueous solutions an approximate value of 2.5 eV is obtained. Frumkin considers this value by more than 0.5 eV, lower than should be expected. The fact that some of the intercepts were found still lower (2.15 eV in solutions of iodate and bromate, 2.4 eV in nitrate) proves that in these solutions the photocurrent cannot be caused by electron emission.

The strongest argument against the theory of electron

emission remains the existence of anodic photocurrent which has all the properties of cathodic photocurrent but for its sign.

In order to account for the experimental results speaking against the applicability of the "physical concept" on the photoeffect in aqueous solutions, we shall approach the problem from the chemical side.

Outline of the Charge-Transfer Theory

The system metal-solution differs from the metal in vacuum not only in the presence of a new phase, but also in the existence of an interface. In the interface metal-solution various kinds of forces and bonds exist between the metal and the components of the solution, and the interface layer can be regarded as a chemical individuality, different from the atoms or molecules in the bulk of either phase. When analysing the effect of light on a metal in a transparent solution we must take into account, besides the absorption and reflection by the metal and the outer photoeffect like for the metal in vacuum, also the absorption in the interface. This absorption in a monomolecular layer may hardly be measurable by physical means, but it can have detectable chemical consequences, like generation of a photocurrent.

Matsen, Makrides and Hackerman [31] have shown that adsorption on a metal from solution can be formulated as a charge-transfer - no-bond interaction between the metal and the

adsorbed species. For occurence of a charge-transfer-no-bond interaction the necessary condition [32] is an overlap between the highest occupied molecular orbital of the electron donor and the lowest unoccupied orbital of the acceptor. The occupation of orbitals of the electrode changes with its potential; according to the electrode potential and to the electronic structure of the partner from the solution the electrode can figure either as donor or as acceptor of electron in the surface charge-transfer complex. The bond between the donor and acceptor in the ground state of the complex may be, and usually is, very weak; however, the characteristic feature of charge-transfer interaction is the excited state : an absorption of light quantum leads to transfer of electron from the donor to the acceptor.

The typical absorption by a charge-transfer complex occurs as a rule in the visible or near UV region at wavelengths longer than absorption due to the individual components of the complex. For energy of charge-transfer absorption it follows from the theory [33] :

$$h\nu = I_D - E_A - G_1 - G_o + X_1 - X_o \qquad (7)$$

where I_D is the ionization energy of the donor, E_A the electron affinity of the acceptor, G_1 and G_o the energies of non-resonance interaction between the donor and acceptor in excited and ground states respectively, and X_1 and X_o the corresponding resonance energies of interaction between the no-bond and dative states.

When one of the partners of the complex is the electrode, the energy of both the ground and the excited states will depend on the electric field of the double layer. In case of electrode acting as electron acceptor the value of electron affinity E_A is given by its potential E :

$$E_A = E_{A,O} + (E - E_o) , \qquad (8)$$

where index O refers for convenience to the potential of zero charge. Each of the other terms in equation (7) can be a priori expected to depend on the double layer field. For this dependence a linear approximation may be used of the form

$$L = L_o + k (E - E_o) \qquad (9)$$

where L stands for any term of eq. (7) and the value k is specific for each donor, determined mainly by its polarizability. The expression for the energy of charge-transfer absorption of the complex between the electrode and an adsorbed substance can be thus written in the form

$$h\nu = M + N (E - E_o) \qquad (10)$$

where M is the sum of the constant terms L and the electron affinity $E_{A,O}$ referring to the potential of zero charge, and N is the sum of the constants k.

For the opposite case when electrode plays the role of electron donor in the complex, the electrode potential stands for the ionization energy of the donor

$$I_D = I_{D,O} + (E - E_o) \qquad (11)$$

and the above considerations and equations apply mutatis mutandis. Equation (10) shows that for a charge-transfer complex in which an electrode is involved a linear relation exists between the energy absorbed and the electrode potential.

Photocurrent in the Terms of Charge-Transfer Theory

Let us suppose that the light which passes the solution and illuminates the electrode in the present experiments is partly absorbed by the charge-transfer complex on the electrode surface according to formula (10). The transfer of electron from the donor to the acceptor in the excited state of the complex brought about by the absorption can cause an initiation of photocurrent if the return of the electron to the donor is in some way prevented. This can happen by means of a reaction sufficiently rapid to involve the complex within the lifetime of its excited state.

In the discussion of the mechanism and kinetics of photocurrent first the initial process must be considered, i.e. the formation of excited state of the complex. The rate of formation of excited state v_e, or the rate of absorption, is given by the number of photons absorbed by the surface charge-transfer complexes per unit area of the electrode in one second. For this number the following formula has been deduced [34]:

$$v_e = \alpha \cdot \frac{I}{h\nu} \cdot n = k_e \cdot n \qquad (12)$$

where α is the coefficient of absorption, n the surface concentration of the complex and k_e the rate constant of excitation. The absorption coefficient α is a function of frequency of light and therefore, in view of eq. (10), also of the potential of electrode.

Equation (12) would yield the expression for photocurrent if every absorbed light quantum led to an elementary photocurrent - a definite one-way transfer of electron either from the electrode into the solution or in the opposite direction. However, the experimental results show that this do not happen. The dependence of logarithm of photocurrent on potential suggests that at lower potentials a back reaction oposes the photocurrent and that only at higher potentials a one-way electron transfer prevails. This back reaction obviously corresponds to the deactivation of the excited state. The deactivation is a complex of processes consisting in return of electron to the donor, to the ground state, which can occur with emission of radiation, either spontaneously or under the effect of light, or in a radiationless transition brought about by interaction with components of the solution - in this respect the cations are particularly efficient in cathodic photocurrent. With increasing potential the rate of deactivation can be expected to decrease, in consequence the excited state becomes more stable.

In order to find out what are the charge-transfer complexes and what are the actual reactions producing photocurrent in competition for the excited complexes with deactivation,

we shall examine the experimental results.

a) Anodic Photocurrent

The anodic photocurrent is of the same magnitude in aqueous and ethanolic solutions which shows that the solvent does not enter into the primary photoreaction. Although absorption in the solution is excluded, the photocurrent is specific for organic compounds containing the structural group $-\overset{\overset{O}{\|}}{C}-\overset{\overset{X}{|}}{C}-$ in the molecule (X stands for a negative substituent). Absorption of light by the metallic surface of the electrode should give rise to cathodic photoemission of electrons rather than to the observed opposite anodic photocurrent. These facts lead to the conclusion that the light absorbing species responsible for the anodic photocurrent is a complex between the dissolved substance adsorbed at the electrode and the electrode surface.

In terms of the charge-transfer-no-bond theory applied to adsorption the electrode will act as electron acceptor and the adsorbed organic substance as electron donor. The adsorption occurs most probably through the lone electron pairs on oxygen and on the negative substituent, so that in the adsorbed state a five-membered ring with the metal surface is formed. The surface complex has a characteristic absorption at longer wavelengths than the organic molecules in the bulk, and the absorption shifts to longer wavelengths with potential of the electrode becoming more positive, i.e. with increasing electron affinity of the acceptor, in agreement with eq.(7).

On excitation by absorption of a light quantum an electron is transferred from the adsorbed donor to the electrode. If the electron returned back to the ground state, there would be no net direct current flowing across the interface and no photocurrent could be found polarographically. The existence of anodic photocurrent indicates that during the lifetime of the excited state some reaction takes place which prevents the return of the electron to the donor. The nature of this reaction can be inferred from photochemical behaviour of similar systems.

Bisikalova [35] found that the photoreaction of complex oxalates of mercury and some other metals in solution starts by a transfer of electron from the ligand to the central ion leading to formation of a reducing radical $C_2O_4^-$. The reducing properties of this radical have been also postulated in different other studies [36,37]. If the photoreaction of the oxalate anion adsorbed at the electrode is similar, i.e. if the oxalate anion-radical appears as dative form of the donor at the electrode surface it will be electrolytically oxidized to CO_2 by giving up the second electron.

~~On~~ The mechanism of the oxidation can be judged by analogy from homogeneous chemical reactions in solution. In complex oxalates the C-C bond is known to be weakened by coordination and to break easily [38,39]. The oxidation of pyruvic acid [40], α-OH acids [41,42] and α-diketones [43] is believed to proceed through formation with the oxidizing agent of intermediate cyclic complexes which after the transfer of the

first electron break up in the C-C link between the oxygen--bearing carbon atoms, yielding reducing radicals. The irreversible step in the combined photoelectrolytical oxidation of the present donors is probably in this breaking of the C-C bond between the carbon atoms carrying the oxygen and the negative substituent.

If the above conclusions are correct, in the case of anodic photocurrent the reaction which the charge-transfer-complex undergoes in its excited state is electrolytic oxidation. This mechanism of photocurrent can be represented by the following general scheme :

$$D \ldots\ldots A \underset{k_d}{\overset{k_e}{\rightleftharpoons}} D^+ \ldots\ldots A^-$$

$$D^+ \ldots\ldots A^- \pm z \cdot e \xrightarrow{k_1} P_1 .$$

Here D symbolizes electron donor, A acceptor, P_1 reaction products, z number of electrons in electrode reaction, k_e the rate constant of formation of excited state, k_d rate constant of deactivation and k_1 the rate constant of electrode reaction.

The expression for photocurrent according to this scheme will be obtained by application of the steady-state treatment :

$$k_e n = k_d [B] + k_1 [B]$$

where $[B]$ denotes the small equilibrium concentration of

the excited complex. From here it follows for $[B]$

$$[B] = \frac{k_e n}{k_d + k_1}$$

and for the photocurrent i_p

$$\frac{i_p}{z \cdot F \cdot q} = k_e \cdot n \frac{k_1}{k_d + k_1} \qquad (13)$$

where F is the charge of Faraday and q the surface of the electrode. Equation (13) shows that the photocurrent is directly proportional to the rate of excitation of the complex; the proportionality factor approaches unity with increasing potential, as k_1 increases and k_2 decreases. Consequently the photocurrent is proportional to light intensity and also its other properties are given by the reaction of excitation. As far as can be judged from the present experimental results, the anodic photocurrent is in agreement with equation (13).

Since according to our hypothesis the photocurrent is a direct consequence of absorption of light by the surface c charge-transfer complex, the experimentally found linear relation between the energy of red limit of photocurrent and the electrode potential is an approximate picture of equation (10), modified by kinetics of photocurrent, specifically by the deactivation reaction. The comparison of the values of intercepts shows the relative ease with which the donors lose an electron according to their ionization energy. The intercepts vary between 3.9 eV for oxalate anion and 6.0 eV

for glycine. The energy necessary for transferring electron from oxalic acid to the electrode is by 0.5 eV lower than from dimethyl oxalate, but by 1.0 eV higher than from oxalate anion. Similarly from tartrate anion the electron is by 0.6 eV more easily removed than from tartaric acid. Acids forming charge-transfer complexes of a near structure, like tartaric, malic and citric, or like lactic and glycollic, have the same value of intercept.

The potential region in which donor-acceptor complexes can be formed between the electrode and a partner from the solution is necessarily limited : with potential becoming more negative the electrode loses the ability of accepting electron in charge-transfer interaction. The partial deviations from linearity observed on some potential-red limit diagrams can be explained by these limiting conditions.

The formation of charge-transfer complexes with the electrode as acceptor probably occurs more generally; however, most of the donors in dative state are likely to be not electrolytically oxidizable but reducible which case cannot lead to production of photocurrent.

The anodic photocurrent described could be explained on ground of one common mechanism : electrooxidation of the excited state of the donor. The cathodic photocurrent in aqueous solutions, on the other hand, represents a complex of processes among which under suitable conditions the elementary mechanisms can be distinguished.

b) Cathodic Photocurrent in Solutions of Scavengers

Table 1 shows that from the species giving higher photocurrent 13 have a common intercept of 3.40 ± 0.1 eV which means that for production of photocurrent in solutions of compounds as different as acrylonitrile, sodium thiosulphate or hydrochloric acid at potential of zero charge of mercury the same amount of energy is needed. The only common component in all solutions giving this intercept is water. In ethanolic solutions the values of intercepts are higher and dispersed. The important rôle of water in photoeffect is confirmed by the experiment with pyridine (Fig.29) : the photocurrent increases discontinuously in the moment when the desorbed pyridine is replaced by water at the mercury surface.

Kemball [44] has found on mercury that the heat of adsorption of water is higher than of other polar solvents and that its entropy of adsorption is so large that it seems probable that the molecules are immobile on the surface forming a monolayer. In our concept of photocurrent we suppose that these molecules are in charge-transfer interaction with the metallic surface; this time the electrode functions as electron donor and water as electron acceptor. An absorption of light quantum brings about a photochemical transfer of electron from the electrode to the adsorbed molecule of water. In this way in the excited state there is on the electrode surface a molecule of water bearing a negative charge; it reminds of the hydrated electron [45] but differs from it in localization of the charge.

Before the electron returns to the ground state to the electrode it can be removed from the water molecule by a fast reaction with an active component of the solution. These active components causing high cathodic photocurrents according to Tab.1, are efficient scavengers of hydrated electrons with the exception of thiosulphate and thiocyanate ions [46]. Thiosulphate is known to react readily with atomic hydrogen [47] which suggests that the water molecule carrying a negative charge is in equilibrium with hydrogen atom and hydroxyl anion. The reaction can be schematically expressed :

$$\text{Me} \ldots H_2O \underset{k_d}{\overset{k_e}{\rightleftharpoons}} \text{Me} \ldots (H_2O)^- \rightleftharpoons \text{Me} \ldots (H + OH^-).$$

In alkaline solutions the ability of the negatively charged water molecule to react as H and OH^- is reduced. This can explain why addition of potassium hydroxide causes a shift of the intercept in solutions of thiocyanate and thiosulphate; their reaction rate with atomic hydrogen is apparently higher than with electron. The other scavengers having the common intercept - nitrous oxide, acrylonitrile and nitrate ion - react rapidly with electron in neutral and alkaline solutions, and an addition of alkaline hydroxide does not affect their intercept.

The variety of slopes of the straight lines on potential--red limit diagrams in aqueous solutions of electron and hydrogen atom scanvengers indicates that the absorption by the

charge transfer complex water-electrode and the kinetics of scavenging reactions are specifically affected by the field of the double layer. However, all the differences disappear at potential of zero charge in absence of the ionic double layer when the photocurrent is given only by the difference between the rate of the photochemical transfer of electron from the electrode to the water molecule and the rate of an elementary deactivation reaction which, judging from the dependence of photocurrent on potential, occurs even in the solutions of efficient scavengers. The energy necessary for this process corresponds to the common value of intercept, 3.4 eV.

The reaction of transfer of electron to water is well known in photochemistry of aqueous solutions. Dainton and James [48] found a linear relation between the energy of red limit of charge-transfer band in absorption spectra of a series of hydrated transition metal cations and their standard redox potentials. The energy of the long-wave limit of absorption in this series is separable into two terms [49], namely the ionization energy of the reduced form, and a constant term characteristic of water molecule and its ion and radical. The ionization energy of a noble metal electrode in solution changes according to its applied potential; at potential equal to the standard potential of a redox system it is equal to the ionization energy of the reduced form of the couple. At potential of its zero charge (-0,2 V versus normal hydrogen electrode) will mercury in aqueous solution have about the

same ionization energy as the hydrated vanadous ion. The energy of red limit of charge-transfer absorption of vanadous solution is, according to the above authors' results, 81 kcal, or 3.5 eV. The fact that this amount of energy necessary for the transfer of electron to water is near the minimum energy for production of photocurrent, 3.4 eV, is in agreement with our hypothesis about the nature of photocurrent.

The value of the energy of red limit of photocurrent at potential of zero charge of mercury, the 3.4 eV, obviously corresponds to the value of the work function referring to the escape of electron into aqueous solution, estimated by Frumkin [30] as higher than 3 eV.

A transfer of electron to adsorbed water molecule has been suggested as primary reaction in heterogeneous photoprocesses on surfaces of zinc oxide [50] and anthracene [51]. The concept of water as electron acceptor in charge-transfer interaction between water and aromatic hydrocarbons appeared in a paper by Bohon and Claussen [52].

Valnev [53] found that water vapour when adsorbed on cadmium or zinc is decomposed by light of energy by 2 eV lower than when in gas phase, with simultaneous evolution of hydrogen, in a mechanism independent of photoemission; it seems that this effect could be interpreted on ground of photoexcitation of a charge-transfer complex between the metal and adsorbed water, like in our case.

From the discussion of the cathodic photocurrent in aqueous solutions of scavengers we may conclude that here

the excited state is formed betweeh the electrode and a common acceptor, water molecule, and that from the acceptor the electron either returns to the donor or is removed by a chemical reaction with the scavenger. For this mechanism following scheme applies :

$$D \ldots A \underset{k_d}{\overset{k_e}{\rightleftharpoons}} D^+ \ldots A^-$$

$$D^+ \ldots A^- + S \xrightarrow{k_2} P_2$$

where S stands for scavenger, and other symbols have the same meaning as in the case before.

The steady state condition on illumination :

$$k_e\, n = k_d\, [B] + k_2\, [B] \cdot [S]$$

leads to the expression for intermediate concentration of excited complex

$$[B] = \frac{k_e\, n}{k_d + k_2\, [S]}$$

and for the photocurrent

$$\frac{i_p}{F \cdot q} = k_e \cdot n \, \frac{k_2\, [S]}{k_d + k_2\, [S]} \, . \qquad (14)$$

Here again the photocurrent is directly proportional to the rate of excitation of the complex; the proportionality factor approaches unity at high concentration of scavengers and with increasing potential, when k_d decreases. Like in case of anodic photocurrent, the cathodic photocurrent is directly proportional to the light intensity and on the light fre-

quency and electrode potential depends according to the excitation reaction. The dependence of the photocurrent on concentration of scavenger is nonlinear and tends to a limit. Experimental evidence is in favour of equation (14). The postulated dependence on scavenger concentration agrees with preliminary results of Heyrovský and Norrish [24] and with the data of Delahay and Srinivasan [25] who found that photocurrent becomes independent of concentration of acid at concentration about 1M, and that at still higher concentrations it decreases. The decrease is probably due to interference of acid with the charge-transfer interaction of water at the electrode surface.

The seemingly anomalous behaviour of the two efficient electron scavengers, bicarbonate ion and acetone, can be explained on basis of an electrolytic back reaction. Bicarbonate anion when adsorbed at positively charged electrode reacts with the excited state of the complex like an acid, as indicates the intercept 3.3 eV (Fig.25). On negatively charged electrode no bicarbonate anions are adsorbed, but as electron scavenger in the vicinity of the electrode will act the molecule of carbon dioxide [54] present in the solution in equilibrium. However, the molecule of CO_2 on accepting an electron turns into a reactive reducing radical CO_2^- ready to give up the electron to the electrode as long as its potential is sufficiently positive. Under these conditions the molecule of carbon dioxide functions as an efficient deactivator of excited charge-transfer complexes on the electrode

surface. It is only at potentials more negative than -1.0 V versus potential of zero charge that CO_2^- retains the electron and CO_2 behaves as electron scavenger producing a high photocurrent. Similarly with acetone in aqueous solution the radical [55] $(CH_3COCH_3)^-$ is evidently electrolytically oxidized at potentials less negative than -1.0 V and there suppresses the photocurrent until this potential is reached.

In solutions with values of intercepts higher than 3.4 eV the solutes also react at the electrode with the negatively charged water molecule or with atomic hydrogen, but their reaction is not sufficiently fast for a successful competition with deactivation processes; in accordance with equation (14) the photocurrent becomes smaller with decreasing k_2.

c) Cathodic Photocurrent in Indifferent Electrolytes

In the inert 0.1M aqueous solutions with intercepts between 4.0 and 4.5 eV the rate of deactivation k_d is high and the only thinkable scavenger is water itself [56] which, however with its very small value of k_2 would produce hardly any measurable current. It seems more probable that the photocurrent observed in absence of scavengers is due to a bimolecular reaction between two excited complexes. With water molecule as acceptor the product of such reaction will be hydrogen molecule and two OH^- ions like in the reaction between two hydrated electrons [57]. This mechanism could account for the above mentioned Valnev's experiment [53]. In our symbols the scheme is as follows :

$$D \ldots A \underset{k_d}{\overset{k_e}{\rightleftharpoons}} D^+ \ldots A$$

$$D^+ \ldots A^- + D^+ \ldots A^- \xrightarrow{k_3} P_3 .$$

From the steady-state condition

$$k_e \cdot n = k_d [B] + k_3 [B]^2$$

the concentration of excited complex is obtained

$$[B] = \frac{- k_d + \sqrt{k_d^2 + 4 k_3 k_e \cdot n}}{2 k_3}$$

by means of which after a small arrangement the expression for photocurrent is given

$$\frac{i_p}{Fq} = k_e \cdot n - \frac{k_d^2}{2k_3}\left(\sqrt{1 + \frac{4 k_3 k_e \cdot n}{k_d^2}} - 1\right). \quad (15)$$

The photocurrent according to equation (15) is always smaller than the rate of excitation, since, as we have seen, $k_d > 0$. Its magnitude depends above all on the rate of deactivation k_d.

Dilution brings about a decrease of concentration of cations favouring the deactivation and therefore an increase of photocurrent is to be expected. However, since the ionic concentration in the double layer, which is clearly most important in deactivation, is an exponential function of the ionic charge [58], the effect of dilution on the back reaction will depend strongly on the valency of cations. The photocurrent in diluted aqueous solutions in absence of scavengers demonstrates this dependence.

In solutions of efficient scavengers no effect of valency of cation of the supporting electrolyte on photocurrent was observed (Fig.28) - evidently because here the deactivation reaction is suppressed and plays but a small rôle besides the scavenging (eq.14), whereas in absence of scavengers its role becomes determining for the photocurrent (eq.15). An increase of photocurrent in 10^{-6}M KCl after introduction of electron scavengers into the solution (Fig.30) indicates that the deactivation reaction at this dilution is still considerable, as can be also judged from the intercept on potential-red limit diagram (Fig.17).

d) Cathodic Photocurrent-Special Cases

It has been shown that the value 3.4 eV of intercept of the straight lines on potential-red limit diagram is given by the energy of electron transfer to water molecule. The cases where the value of intercept is found lower than 3.4 eV cannot be explained by donor-acceptor interaction between electrode and water. The acceptors are here apparently either the anions of the dissolved compounds or species formed from them in solution. Tellurate, bromate and iodate are electrolytically reducible and it can be expected that if after the phototransfer of an electron a radical-anion is formed, it will be further reduced on the electrode. Such mechanism would be exactly analogous to the anodic photocurrent, and the photocurrent would follow equation (13). The shift of the intercept by potassium hydroxide might indicate that the

acceptor in neutral solution is not anion, but the corresponding acid formed in small concentration in solution by hydrolysis and adsorbed at the electrode surface, and that the anions appear in the charge-transfer complex only in alkaline solution. Nitric acid which is the only strong acid having the intercept lower than 3.4 eV, also probably enters directly into donor-acceptor complex with the electrode and is reduced in excited state. The nitrate anion, on the other hand, reacts as a scavenger of electrons yielding the intercept 3.4 eV.

Slightly different is the problem with solutions of nitrite. Nitrites in aqueous solutions are known to hydrolyse slightly forming nitric oxide NO [59]. From the polarographic behaviour of nitric oxide Rampazzo and Cardinali [60] concluded that the compound is adsorbed at the electrode in the inner part of the compact double layer. We have tried to ascertain the adsorption of NO on the dropping mercury electrode by means of electrocapillary curves. The curves obtained by measuring the time of 10 drops are shown on Fig.41 and 42. The surface tension on mercury in neutral solution of sodium nitrite increases after addition of alkali hydroxide and bubbling nitrogen through the solution - it is because in this way hydrolysis is suppressed and NO expelled from solution (Fig.41). A direct proof of adsorption of NO on the electrode is brought on Fig.42 where after dissolution of NO in alkaline solution the surface tension is lowered. Nitric oxide is therefore apparently the acceptor in surface charge-

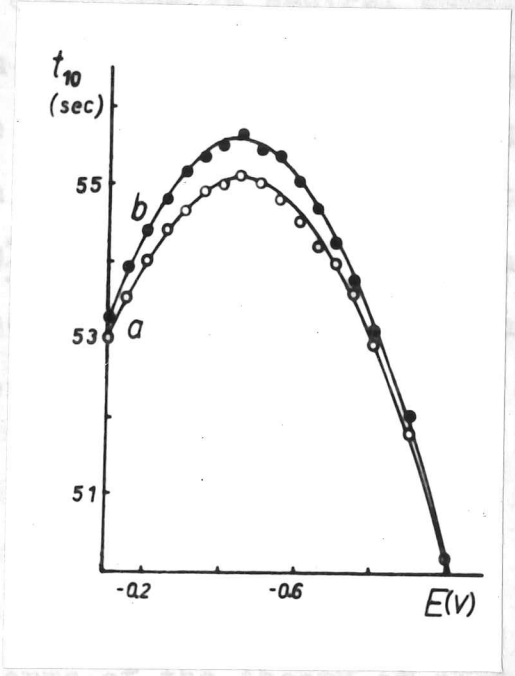

Fig.41. Effect of hydroxyl ions on the electrocapillary curve of nitrite solution. a - - 0.1M $NaNO_2$; b - - 0.1M $NaNO_2$ + 0.2M NaOH. Electrocapillary curves measured as time of 10 drops; in atmosphere of nitrogen; potentials versus silver chloride electrode.

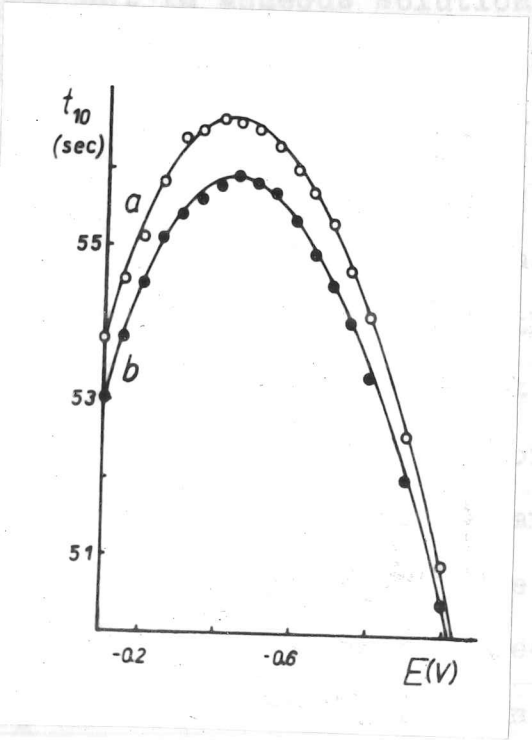

Fig.42. Effect of nitric oxide on electrocapillary curve of alkaline solution. a - 0.6M NaOH; b - 0.6M NaOH after bubbling of 10 ml of NO through the solution. Conditions like on Fig.41.

-transfer complex with the electrode in neutral solutions of nitrite. The photo~~oxidation~~ excitation of the complex is probably accompanied by an irreversible electroreduction, judging from polarographic results. In alkaline solutions of nitrites no NO is formed and the NO_2^- ion behaves like a strong electron scavenger in photoreaction between electrode and water, with intercept 3.4 eV on the potential-red limit diagram.

Potentiometric Effects

It remains to explain in terms of the theory of photochemical charge-transfer the shifts of potentials of mercury pool electrode on illumination. If the experiments are carried out in aqueous solutions of inert electrolytes, the charge-transfer complex with the electrode will be formed by water molecules. It is known [61] that atomic hydrogen causes a shift of potential of mercury electrode to negative values. Because the molecule of water as acceptor in excited state can react as atomic hydrogen, the illumination of electrode by constant light is equivalent to maintaining a certain very low constant concentration of hydrogen atoms at the surface. Besides that, on stationary electrodes all traces of impurities accumulated from the solution are subject on illumination to the reducing effect of electrons or hydrogen atoms, and their slow reduction will impart to the electrode a trend towards negative potentials. Oxygen will immedia-

tely react with negative water molecules under formation of oxidizing radicals O_2^- or HO_2 which will shift the potential in positive direction.

Conclusion

The "chemical" concept of the electrochemical photoeffect based on photochemical charge-transfer reactions between the electrode and components of the solution seems to suceed in explaining a variety of experimental facts. However, more thorough and, above all, quantitative investigation is necessary to prove how far the idea of charge-transfer complexes with the electrode is justified. Comparison of theoretical equations (12), (13) and (14) with the empirical formula (5) shows that the dependence of the absorption coefficient on the frequency of light and on the electrode potential ought to be exponential. This is the most essential conclusion which must be checked on ground of quantitative results before further work can be done on the photo-electrochemical charge-transfer.

Summary

On illumination of dropping mercury electrode in transparent solutions both cathodic and anodic photocurrent can be observed. The cathodic photocurrent appears in every solution, anodic photocurrent was observed only in presence of organic substances bearing a =C=O group and a negative substituent on the neighbouring carbon atom.

The cathodic photocurrent increases with dilution of supporting electrolyte; the increase depends on the charge of the cation being greatest in solutions of univalent and negligible in solutions of trivalent cations.

A particularly high cathodic photocurrent appears in solutions of scavengers of electrons or hydrogen atoms. The energy necessary for production of photocurrent in aqueous solutions of scavengers at potential of zero chrage is constant and equal to 3.4 eV.

The photocurrent is a faradaic current, it is directly proportional to light intensity and increases exponentially with the electrode potential and with the energy of light. Between the energy of red limit of photocurrent and electrode potential a linear relation holds.

In order to interpret all the experimental facts a theory is proposed based on photochemical charge-transfer between the electrode and a component of the solution. This theory in contradistinction to the theory of electron emission locates the primary act of light absorption in a surface charge-transfer complex with the solvent or a solute in which

the electrode plays the rôle of either electron donor or acceptor. The excited surface complex either is deactivated or undergoes a reaction yielding photocurrent.

The anodic photocurrent is explained by electrolytic oxidation of donor - the organic molecule - in dative state. In aqueous solutions of scavengers the charge-transfer complex is supposed to be formed with the water molecule as acceptor which in excited state bears an electron capable of reaction with the scavengers. In some cases a direct participation of the solute in charge-transfer complex with the electrode is postulated. The photocurrent in aqueous solutions without scavengers is ascribed to bimolecular reaction of excited complexes.

Experimental results were found in qualitative agreement with the proposed theory. For the three different mechanisms of photocurrent equations were derived, however, the present simple experimental arrangement did not allow their quantitative verification.

References

1. Becquerel E.: Compt.Rend.9, 145 (1839).
2. Copeland A.W., Black O.D., Garret A.B.: Chem.Rev.31, 177 (1942).
3. Paszyc S.: Wiadomosci Chemi.12, 767 (1958).
4. Mauser H., Sproesser U.: Chem.Ber.97, 2260 (1964).
5. Trümpler G.: Z.Physik.Chem.(Leipzig) 90, 385 (1915).
6. Rideal E.K., Norrish R.G.W.: Proc.Roy.Soc.(London) Ser.A 103, 342 (1923).
7. Rabinowitch E.: J.Chem.Phys.8, 551 (1940).
8. Surash J.J., Hercules D.H.: J.Phys.Chem.66, 1602 (1962).
9. Berg H., Z.Chem.2, 237 (1962).
10. Berg H., Schweiss H.: Nature 191, 1270 (1961).
11. Volmer M., Moll W.: Z.Physik.Chem.(Leipzig) 161, 401 (1932).
12. Athanasiu G.: Ann.Phys.(Paris) 4, 377 (1935).
13. Veselovsky V.I.: Zh.Fiz.Khim.22, 1427 (1948).
14. Winther C.: Z.Physik.Chem.(Leipzig) 131, 205 (1927).
15. Swensson T.: Arkiv Kemi, Mineral.Geol.7, 1 (1919).
16. Lifschitz J., Hooghoudt S.B.: Z.Physik.Chem.(Leipzig) 141, 52 (1929).
17. Audubert R.: J.Chim.Phys.27, 169 (1930).
18. Bowden F.P.: Trans.Faraday Soc.27, 505 (1931).
19. Price L.E.: Thesis. Cambridge University 1938.
20. Hillson P.J., Rideal E.K.: Proc.Roy.Soc.(London) Ser.A 199, 295 (1949).
21. Barker G,C., Gardner A.W.: Paper presented on the 14the Meeting of CITCE, Moscow 1963 (extended abstract),

22. Berg H., Schweiss H.: Electrochim.Acta 9, 425 (1964).

23. Berg H., Schweiss H.: Monatsber.Deut.Akad.Wiss.Berlin 2, 546 (1960).

24. Heyrovský M., Norrish R.G.W.: Nature 200, 880 (1963).

25. Delahay P., Srinivasan V.S.: J.Phys.Chem.70, 420 (1966).

26. Leighton P.A., Crary R.W., Schipp L.T.: J.Am.Chem.Soc.53, 3017 (1931).

27. Smoler I.: J.Electroanal.Chem.6, 465 (1963).

28. Heyrovský J., Šorm F., Forejt J.: Collection Czech.Chem. Commun.12, 11 (1947).

29. Frumkin A.N.: Z.Physik.Chem.(Leipzig) 103, 43 (1923).

30. Frumkin A.N.: J.Electroanal.Chem.9, 173 (1965).

31. Matsen F.A., Makrides A.C., Hackerman U.: J.Chem.Phys. 22, 1800 (1954).

32. Mulliken R.S.: Rec.Trav.Chim.75, 845 (1956).

33. Mulliken R.S., Person W.B.: Ann.Rev.Phys.Chem.13, 107 (1962).

34. Moelwyn-Hughes E.A.: Physical Chemistry. Pergamon Press 1957, p.1177.

35. Bisikaleva N.A.: Ukr.Khim.Zh.17, 815 (1951).

36. Abel.E.: Monatsh.Chem.83, 695 (1952).

37. Saffir P., Taube H.: J.Am.Chem.Soc.82, 13 (1960).

38. Sakurabe S., Ikeya S.: Bull.Chem.Soc.Japan 30, 662 (1957).

39. Duke F.R.: J.Am.Chem.Soc.69, 2885 (1947).

40. Drummond A.Y., Waters W.A.: J.Chem.Soc.1955, 497.

41. Levesley P., Waters W.A.: J.Chem.Soc.1955, 217.

42. Gupta K.K.S., Aditya S.: J.Electrochem.Soc.Japan,

Overseas Ed.32, 201 (1964).

43. Shiner V.J., Washuth C.R.: J.Am.Chem.Soc.81, 37 (1959).

44. Kemball C.: Proc.Roy.Soc.(London) Ser.A 190, 177 (1947).

45. Hart E.J.: Science 146, 19 (1964).

46. Thomas J.K., Gordon S., Hart E.J.: J.Phys.Chem.68, 1524 (1964).

47. Harteck P., Stewart K.: Z.Phys.Chem.(Leipzig) 181, 183 (1938).

48. Dainton F.S., James D.G.L.: J.Chim.Phys.48, C 17 (1951).

49. Dainton F.S., James D.G.L.: Trans.Faraday Soc.54, 649 (1958).

50. Markham M.C., Laidler K.J.: J.Phys.Chem.57, 363 (1953).

51. Kallmann H., Pope M.: Nature 185, 753 (1960).

52. Bohon R.L., Claussen W.F.: J.Am.Chem.Soc.73, 1571 (1951).

53. Valnev P.E.: Zh.Fiz.Khim.30, 1308 (1956).

54. Getoff N.: Discussions Faraday Soc.36, 314 (1963).

55. Rabani J., Stein G.: J.Chem.Phys.37, 1865 (1962).

56. Jortner J., Ottolenghi M., Stein G.: J.Phys.Chem.68, 247 (1964).

57. Gordon S., Hart E.J., Matheson M.S., Rabani J., Thomas J.K.: Discussions Faraday Soc.36, 193 (1963).

58. Grahame D.C.: Chem.Rev.41, 441 (1947).

59. Pascal B.: Nouveau traité de chimie minérale. Vol.10, p.434, Masson et cie, Paris 1956.

60. Rampazzo L., Cardinali M.: Ric.Sci.Rend.4, 141 (1964).

61. Levina C.D., Kalish T.V.: Zh.Fiz.Khim.36, 1926 (1962).

Contents

Preface . . . . . p. 2

Introduction 3

Experimental 11

Results 19

A. Potentiometric Measurements 19

B. Polarographic Measurements 19

Photocurrent, General Properties 21

Depemdence of Photocurrent on the Frequency of Light 25

Potential-Red Limit Diagrams 30

Cathodic Photocurrent

in Indifferent Electrolytes 33

in Specifically Active Solutions . . 37

Anodic Photocurrent 47

Discussion 56

Arguments against the Theory of Photo-emission of Electrons 56

Outline of the Charge-Transfer Theory 59

Photocurrents in the Terms of Charge--Transfer Theory 62

a) Anodic Photocurrent 64

b) Cathodic Photocurrent in Solutions of Scavengers 69

c) Cathodic Photocurrent in Indifferent Electrolytes 75

d) Cathodic Photocurrent, Special Cases . . . 77

Potentiometric Effects . . . . . p. 80

Conclusion 81

Summary 82

References 84

Contents 87

I declare that the work presented in this dissertation is original, and that every source from which any information has been derived, is stated in referemces.

I also declare that neither this dissertation nor any part of it had been submitted for a degree or diploma or other qualification at any other University.

M. Heyrovský

(*Reprinted from Nature, Vol.* 200, *No.* 4909, *pp.* 880–881, *November* 30, 1963)

Photovoltaic Phenomena in Aqueous Solutions

RESULTS of our potentiometric measurements of the photovoltaic effect in the ultra-violet region on platinum and mercury electrodes in aqueous solutions of sulphuric acid, potassium hydroxide and potassium sulphate led us to the conclusion that the observed potential changes of the illuminated electrode are caused by a competitive action of oxidizing and reducing species formed in water under the incident light.

A confirmation of this hypothesis has been found on examining the same solutions polarographically under constant irradiation by a high-pressure mercury lamp. Whereas no observable change appears on polarographic curves of deaerated solutions of potassium hydroxide and potassium sulphate when exposed to light, a rapid increase of current of the magnitude about 10^{-8} amp (Fig. 1) follows the illumination of the dropping mercury electrode in solutions of sulphuric acid. On extinguishing the light, the current falls back to its original value. The production of current on exposure to light begins to appear at potentials by about 0·6 V more positive than the rise of the reduction current due to electrolytic evolution of hydrogen, and it increases with increasing negative potential of the dropping electrode. With increasing concentration of hydrogen ions up to about 1 N the current caused by light increases; further from there it begins to diminish. In water–ethanolic solutions of sulphuric acid the photocurrent is smaller by about 1/2 than in aqueous solutions.

Qualitatively the same phenomenon was observed with solutions of perchloric, hydrochloric and acetic acids. Besides the appearance of this relatively small current on the foot of the wave the actual polarographic reduction wave of hydrogen ions is not affected by illumination. There was found no effect whatever of ultra-violet light on the foot of the polarographic reduction waves of oxygen, Cd^{4+}, Zn^{2+} or Ni^{2+} ions. Nitrous oxide dissolved under atmospheric pressure stimulates the increase of current in acid solutions and introduces an identical effect in solutions of potassium sulphate and potassium hydroxide.

The described experimental results could be interpreted on the basis of the effect of the photosensitized decomposition of water on the electrode surface. The metallic atoms in the surface of the electrode excited by the incident quanta of light transfer energy to the adsorbed molecules of water. It can be assumed that the dissociation products of water, H· and OH· radicals,

are also adsorbed at the electrode surface, and that their heat of adsorption is greater than that of the water molecule. In that case, quanta of lower energy than 118 kcal/mole (that is, light of longer wave-length than 2422 Å) can lead to splitting of the H–OH bond in water. (The potential changes in all solutions and the production of photocurrent in acid solutions were observed to a small extent also with ultra-violet light of λ above 3200 Å.) The radicals formed recombine rapidly to water, molecular hydrogen or hydrogen peroxide. The occurrence of the reaction products at the electrode surface results in a change of potential of the inert electrode, the extent and the direction of which depend on experimental conditions. However, the concentration of the electroactive species is not high enough to cause a measurable polarographic current.

In solutions of acids the hydrogen ions adsorbed at the negatively charged electrode combined with photolytically generated hydrogen atoms to form H_2^+. By this reaction the equilibrium between decomposition of water and recombination of its radicals is disturbed, and the total reaction now results partly in formation of H_2^+ and $\cdot OH$, which can both be reduced at the electrode in an extent sufficient to produce a polarographic current.

A similar mechanism occurs in the presence of N_2O which turns hydrogen atoms into OH radicals. Alcohol, on the other hand, acts as a scavenger of H and OH, changing them into water or molecular hydrogen, and thus suppresses to a certain extent the production of current.

A photosensitized decomposition of water could well account for experimental results published by other

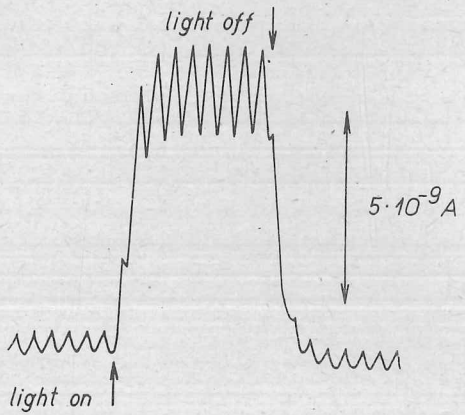

Fig. 1. Polarographic current in deaerated 1 M H_2SO_4 at constant potential −0·9 V (versus 1 M Hg_2SO_4 electrode); illumination of the dropping electrode by an ultra-violet lamp denoted by arrows

authors on photovoltaic phenomena in aqueous solutions[1–3] as well as on the acceleration of electrodeposition of hydrogen and oxygen by ultra-violet light[4–6].

M. Heyrovský
Polarographic Institute,
Czechoslovak Academy of Sciences,
Prague,
and University of Cambridge.

R. G. W. Norrish
Department of Physical Chemistry,
University of Cambridge.

[1] Swensson, T., *Arkiv Kemi, Min. och Geologi*, **7**, No. 19, 1 (1919).
[2] Lifschitz, J., and Hooghoudt, S. B., *Z. phys. Chem.*, A, **141**, 52 (1929).
[3] Audubert, R., *J. Chim. Phys.*, **27**, 169 (1930).
[4] Bowden, F. P., *Trans. Farad. Soc.*, **27**, 505 (1931).
[5] Price, L. E., Dissertation, Cambridge Univ. (1938).
[6] Hillson, P. J., and Rideal, E. K., *Proc. Roy. Soc.*, A, **199**, 295 (1949).

Printed in Great Britain by Fisher, Knight & Co., Ltd., St. Albans.

Ph. D. Dissertation 5572

(*Reprinted from Nature, Vol. 206, No. 4991, pp. 1356–1357, June 26, 1965*)

Nature of the Photoeffect in Aqueous Solutions

As has been already reported[1–3], a photocurrent is produced when a dropping mercury electrode is sufficiently strongly illuminated in solutions not absorbing the light.

Further investigation of this effect shows that in various solutions cathodic and anodic photocurrents can be obtained and that the cathodic photocurrent is particularly high if the solution contains a scavenger either of electrons or of hydrogen atoms. A plot of energy of the red limit of photocurrent against potential of the electrode gives a straight line (Fig. 1) the slope of which indicates the dependence of the photoprocess on potential; the red limit at the potential of zero charge gives the energy necessary for production of photocurrent in absence of electric field due to ionic double layer.

From an examination of a number of solutions it appears that the cathodic photocurrent is as a rule higher by more

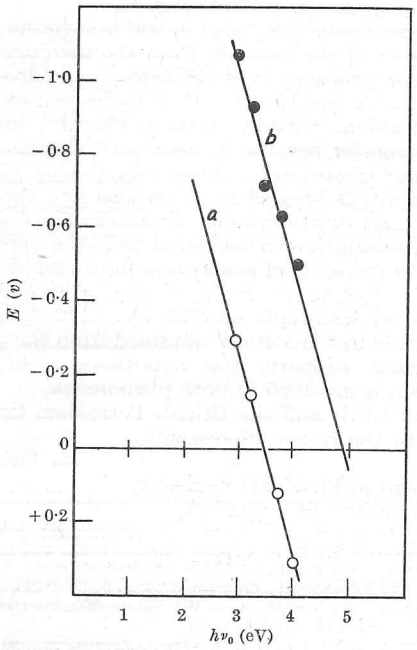

Fig. 1. Relation between the energy of red limit of photocurrent, and the electrode potential in 0·1 M LiCl saturated with N_2O. *a*, In water; *b*, in ethanol. Potentials measured from the potential of zero charge

Table 1

Solution (0·1 M unless stated otherwise)	Aqueous slope (eV/V)	Aqueous intercept (eV)	Ethanolic slope (eV/V)	Ethanolic intercept (eV)
LiCl sat. with N_2O*	1·9	3·45	1·8	4·85
LiCl + acrylonitrile	1·6	3·45	2·2	4·65
KCNS	1·1	3·35		
$Na_2S_2O_3$	1·5	3·40		
KNO_3	1·5	3·30		
$NaNO_2$†	1·9	3·40	2·3	5·15
HCl	2·6	3·30		
$HClO_4$	2·8	3·40		
H_2SO_4	2·4	3·45		
Acetic acid	2·4	3·45		
Oxalic acid	4·2	3·35	4·0	5·40

* Conc. of N_2O in aqueous solution about $2{\cdot}5 \times 10^{-2}$ M, in ethanolic about 8×10^{-2} M.

† +0·1 M KOH in aqueous solution; ethanolic solution saturated, about 4×10^{-2} M.

than one order in water than in ethanol. Table 1 compares parameters of the potential—red limit diagrams for some solutions yielding especially high photocurrents. With aqueous solutions the straight lines, although of different slopes, all have a common intercept at the potential of zero charge corresponding to 3·40 eV (within the limits of experimental error). In ethanol, on the other hand, there is a wide dispersion of the intercepts, the lowest value being 4·65 eV, slightly higher than the work function of mercury, 4·53 eV (ref. 4).

The surprisingly low value in water suggests that there the emission of the electron from the mercury surface is made easier, probably by its transfer to an adsorbed water molecule with production of a hydrogen atom and a hydroxyl anion, that is, by a mechanism known from electron transfer spectra in aqueous solutions. Dainton and James[5] discovered a linear relationship between the redox potentials of a series of cations and the energy of their red limit of absorption. From the graph illustrating this relationship it can be found that the energy corresponding to red limit of absorption for a cation with redox potential equal to potential of zero charge of mercury would be 81 kcal/mole or 3·55 eV. The fact that this value is near to the 3·40 eV obtained from the red limit of photocurrent supports the hypothesis that the same mechanism is involved in both phenomena.

I thank I.C.I. and the British Petroleum Company for support in the course of research.

M. Heyrovský

Department of Physical Chemistry,
University of Cambridge.

[1] Barker, G. C., and Gardner, A. W.: papers presented at the fourteenth meeting of C.I.T.C.E. in Moscow (August 1963), and on the Gordon conference in Santa Barbara, California (January 1964).

[2] Berg, H., and Schweiss, H., *Electrochim. Acta*, **9**, 425 (1964).

[3] Heyrovský, M., and Norrish, R. G. W., *Nature*, **200**, 880 (1963).

[4] Roller, D., *Phys. Rev.*, **36**, 738 (1930).

[5] Dainton, F. S., and James D. G. L., *Trans. Faraday Soc.*, **54**, 649 (1958).

Printed in Great Britain by Fisher, Knight & Co., Ltd., St. Albans.

Sonderdruck aus: „Zeitschr. für Physikalische Chemie", Sonderheft, 1958
Herausgegeben von H. Falkenhagen, H. Franck, F. Möglich, R. Rompe,
F. Sauerwald, K. Schwabe, A. Simon, H. Staude, E. Thilo
Akademische Verlagsgesellschaft Geest & Portig K.-G., Leipzig

Polarographisches Institut der Tschechoslowakischen Akademie der Wissenschaften, Prag 1, Vlašská 9

Depolarisationswirkungen der Aluminiumionen[1]

Von

M. Heyrovský[2]

Mit 10 Abbildungen

a) Mit angewandter Spannung

(Spannungsbedingte Polarisation)

Meistens betrachtet man die polarographischen Stufen, welche bekanntlich in schwach sauren oder neutralen Grundelektrolyten mit einer Spur eines Aluminiumsalzes bei etwa — 1,75 V (gegen die norm. Kalomelelektrode) entstehen, als einen Beweis der Abscheidung von Al^{3+}-Ionen, denn sie entspricht dem Verbrauch von 3 Elektronen und ungefähr dem Diffusionskoeffizienten des Al^{3+}-Ions. Nähere Untersuchungen der Form der Stufe (durch logarithmische Analyse) und der Lage des Halbstufenpotentials stimmen mit dieser einfachen Auffassung jedoch nicht überein [1]. Die Form der Kurve deutet auf einen irreversiblen Vorgang mit dem Richtungskoeffizienten von 50 bis 80 mV (statt 19 mV) je nach der Art des Grundelektrolyten; das Halbstufenpotential verschiebt sich mit wachsender Konzentration des Aluminiums zu negativeren Werten (um 20 bis 30 mV bei doppelter Konzentration) und wird auch durch die Konzentration und Art des Grundelektrolyten beeinflußt. Auch bei der Erhöhung des Quecksilberdruckes um 20 cm verschiebt sich das Halbstufenpotential um — 18 mV. Der Temperaturkoeffizient des Halbstufenpotentials ist hoch, fast wie bei der Wasserstoffabscheidung, + 2,2 mV pro Grad. In allen Elektrolyten, am deutlichsten aber in $LiCl$ oder $N(CH_3)_4Cl$, entstehen Maxima ohne Strömungen in der Lösung (Abb. 1).

[1] Vortrag, gehalten anläßlich des Polarographischen Kolloquiums in Dresden vom 3. bis 7. Juni 1957.

[2] Michael Heyrovský, Praha 1, Vlašská 9.

UNIVERSITY LIBRARY CAMBRIDGE

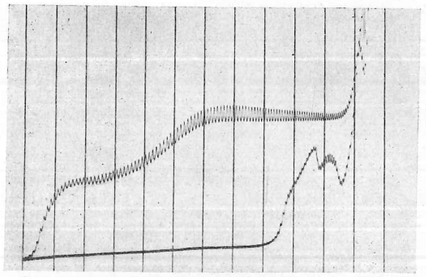

Abb. 1. Polarographische Stromspannungskurve von $3{,}85 \cdot 10^{-4}$ m $KAl(SO_4)_2$ in 0,1 *n LiCl*. Obere Kurve in Gegenwart von Luft, untere Kurve in Stickstoffatmosphäre.

Die Stromspannungskurven auf dem Kathodenstrahloszillographen zeigen bei mäßiger Geschwindigkeit der Spannungssteigung an einem Tropfen (1 V pro sec) die üblichen Maxima („peaks") (Abb. 2), welche jedoch bei der rückgängigen Kurve wieder erscheinen, obzwar sie wegen gradueller Erschöpfung des Depolarisators verschwinden sollten. Ein solches Verhalten zeigen nur Maxima der katalytischen Wasserstoffabscheidung (gemäß VALENTA [2]). Auf der rückgängigen Kurve entstehen beim Depolarisationspotential keine anodischen Ströme. Auch der Umschalter von KALOUSEK [3] zeigt kein Reduktionsprodukt an, das sich anodisch oxydieren möchte.

Das bisher erwähnte Verhalten der polarographischen Kurven beweist eher eine völlig irreversible Abscheidung (wie z. B. die des

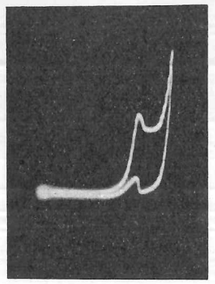

Abb. 2. Oszillographische Stromspannungskurven. Lösung $3{,}8 \cdot 10^{-3}$ *m* $Al_2(SO_4)_3$, 4 *n LiCl*, in N_2; obere Kurve von 0 bis — 2 V, untere von — 2 V zurück zu 0; 1 V pro sec.

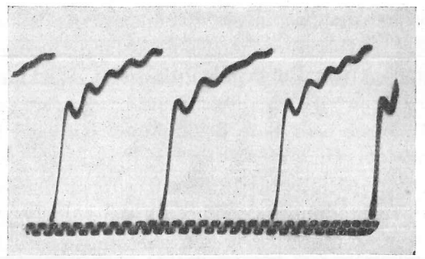

Abb. 3. *i-t*-Kurven beim halben Grenzstrom von $9 \cdot 10^{-4}$ *m* $KAl(SO_4)_2$ in 0,1 *n LiCl* in N_2, bei — 1,74 V. Die Zacken geben 0,31 sec an.

Wasserstoffs) als eine Aluminiumamalgambildung. Eine andere Anomalie zeigen auch die Strom-Zeit-Kurven des Diffusionsstromes der Aluminiumstufe. Die Kurven (Abb. 3) sind gewellt, als ob ein Vorgang periodisch die elektrolytische Abscheidung stören würde. Nach langem Elektrolysieren beim Grenzstrom des Aluminiums überzieht sich die Kapillarmündung allmählich mit festem Aluminiumhydroxyd, so daß die Kapillare zu tropfen aufhört. Das beweist, daß eines der Elektrolysenprodukte Aluminiumhydroxyd ist.

Ein anderes Merkmal einer Wasserstoffabscheidung ist das Verhalten der Aluminiumionen bei der Elektroreduktion organischer Verbindungen, wie Benzaldehyd, Azetophenon, Azobenzol, Benzil und vielen anderen. Wie RUETSCHI und TRUEMPLER [4] festgestellt haben,

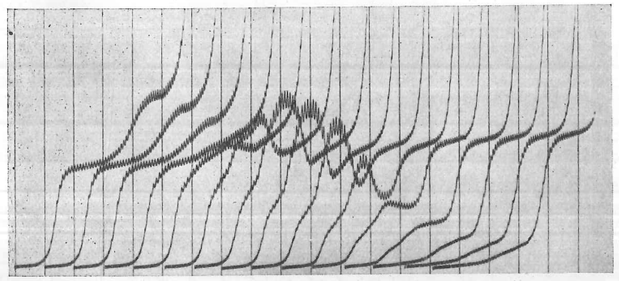

Abb. 4. Zu 5 ml $1{,}85 \cdot 10^{-4}$ *m* p-Diäthylaminobenzaldehyd in 0,1 *n KCl* wurden je 0,1 ml 10^{-3} *m* $KAl(SO_4)_2$ in N_2 zugegeben. Anfang der Kurven bei — 0,8 V.

geben Protondonatoren, wenn sie zu einer neutralen ungepufferten Lösung einer reduzierbaren organischen Verbindung zugefügt werden, eine Stufe bei positiven Potentialen. Dieselbe Wirkung geben auch Aluminiumionen, die sich in dieser Beziehung wie eine Säure verhalten (Abb. 4). Wenn man diese Wirkung mit jener der freien Wasserstoffionen vergleicht, findet man, daß z. B. eine 10^{-3}-*m*-Aluminium-Alaun-Lösung vom pH-Wert 4,12 dieselbe depolarisierende Wirkung auf organische Verbindungen ausübt wie eine 10^{-3}-*m*-Schwefelsäure von pH 2,8. Dagegen gibt 10^{-4}-*m*-Schwefelsäure von pH 4,05 (welche fast den gleichen pH-Wert wie die 10^{-3}-*m*-Alaunlösung hat) keine Stufe. Es kommt hier also nicht auf den potentiometrischen pH-Wert, sondern auf die Anzahl der Protondonatoren an. Durch Berechnung nach RUETSCHI und TRUEMPLER findet man, daß ein Al^{3+}-Ion der organischen Verbindung drei Protonen zur Verfügung stellt. Auch die katalytische Herabsetzung der Wasserstoffüberspannung durch organische Verbindungen, welche ein tertiäres oder heterocyclisches Stickstoffatom enthalten, wie Phenazinfarbstoffe und Azofarbstoffe (z. B. Phenosafranin, Safranin, Methylenblau, Methylorange, Tropaeolin), wird in einer ähnlichen Weise sowohl durch freie Wasserstoffionen als auch durch Aluminiumionen hervorgerufen (Abb. 5) [5].

Wird einer neutralen Formaldehydlösung eine Aluminiumlösung zugefügt, so entsteht beim Potential — 1,2 V eine Stufe, die zu einem kinetisch beschränkten Grenzstrome wächst. Eine ähnliche Stufe bei — 1,2 V erhält man auch, wenn zur Aldehydlösung Essigsäure zugefügt wird.

Aus dem erwähnten Verhalten der Aluminiumionen bei Depolarisationen organischer Verbindungen und auch in verschiedenen Elektro-

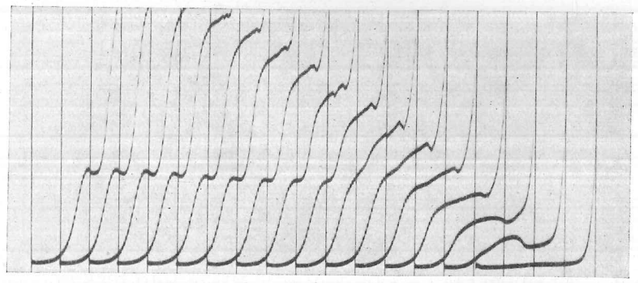

Abb. 5. Zu 5 ml $2 \cdot 10^{-4}$ *m* Phenosafranin in 0,1 *m* *KCl* wurden je 0,1 ml 10^{-2} *m* $Al_2(SO_4)_3$ in N_2 zugegeben. Anfang der Kurven bei — 1,0 V.

lyten findet man Analogien mit dem Verhalten der Wasserstoffionen in schwachen Säuren. MAŠEK [2] weist darauf hin, daß verschiedene Aquoionen, wie von Beryllium und Thorium, polarographisch als Protonendonatoren fungieren können; bei $Al^{3+}(H_2O)_6$ kann z. B. die Wasserhülle so stark polarisiert sein, daß drei Protonen ionogen gehalten werden und zur elektrolytischen Wasserstoffabscheidung führen. Die Elektrodenreaktion des Aluminiumions wäre demnach:

$$Al(H_2O)_6^{3+} + 3\,e \rightarrow Al(OH)_3 + 3\,H_2O + 3\,H.$$

Ein charakteristisches Verhalten bei der Depolarisation durch *Al*-Ionen kommt zum Vorschein an der durch den Kathodenstrahl an einem Tropfen erhaltenen Stromspannungskurve, wenn die Spannung periodisch von 0 bis — 1,8 V und zurück mit verschiedener Frequenz verläuft. VALENTA hat mit seiner periodischen Dreieckspannung nachgewiesen, daß an der ersten Kurve am neuen Tropfen die Stufe am größten ist und dann, namentlich bei größeren Frequenzen, schnell auf Null abfällt (Abb. 6). Bei Frequenzen über 20 gibt es überhaupt keine Depolarisationserscheinung der Aluminiumionen. Offenbar sind die an einer konstanten Elektrodenoberfläche vorhandenen Protonendonatoren bald erschöpft und bilden sich nur langsam aus den zudiffundierenden Aluminium-Aquokomplexen. Die durch die angelegte Spannung erhaltenen Stromspannungskurven, also die polarographischen Kurven der Aluminiumlösung, zeigen nur eine Wasserstoffabscheidung an.

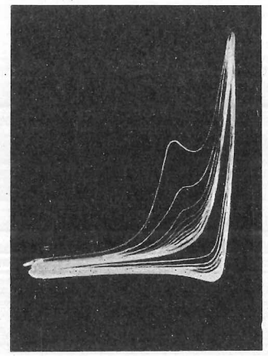

Abb. 6. Stromspannungskurven mit dem Kathodenstrahlpolarographen. 9 Spannungszyklen an einem Tropfen, Frequenz 25 Hz. Lösung $2 \cdot 10^{-3}$ *m* Al^{3+} in 0,5 *m* *LiCl*, in N_2.

b) Mit angewandtem Strom

(Strombedingte Polarisation)

Völlig verschieden sind die Ergebnisse, wenn man die Elektrolyse der Spuren von Aluminiumsalzen enthaltenden Elektrolytlösung mit konstantem Strom verfolgt. Mittels seiner Wechselstromoszillographie hat J. Heyrovsky [6] nachgewiesen, daß sich nur bei einer ziemlich großen Stromdichte (10^{-4} bis 10^{-3} A auf die Tropfenoberfläche) eine Depolarisationserscheinung der Aluminiumionen zeigt (Abb. 8), und

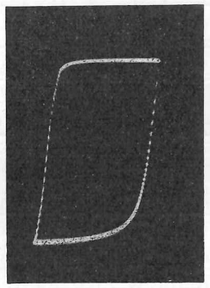

Abb. 7a. Oszillographische Potential-Zeit-Kurve einer 0,01 m $KAl(SO_4)_2$ in 6 m $LiCl$ unter Stromimpuls von $2{,}5 \cdot 10^{-6}$ A, $^1/_6$Hz.

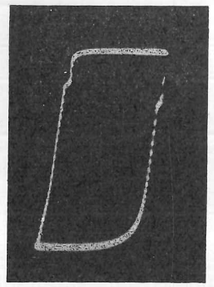

Abb. 7b. Oszillographische Potential-Zeit-Kurve derselben Lösung wie in Abb. 7a nach 3 Minuten Einwirken von Stromimpulsen $2 \cdot 10^{-4}$ A, $^1/_6$ Hz.

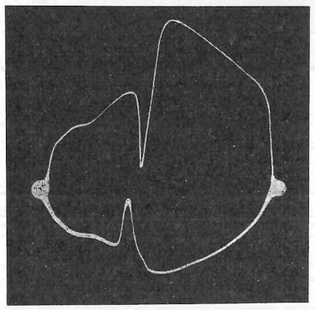

Abb. 8. Wechselstromoszillogramm $\frac{dV}{dt} - V$, 50 Hz, der Lösung $5 \cdot 10^{-3}$ m Al^{3+} in 1 m $LiCl$, i = 0,4 mA, nach 5 Sekunden Einwirkung.

zwar, je nach der Stromdichte, bei positiveren Potentialen zwischen — 1,7 bis — 1,2 V, aber nur dann, wenn in der Lösung neben den Aluminiumionen auch Lithiumionen anwesend sind. Kemula und Kublik [7] haben diese spezifische Reaktion am langsamen Tropfen nachgeprüft und gefunden, daß sich bei langem Einwirken des Wechselstromes die oszillographischen Einschnitte an den Ableitungskurven allmählich vertiefen und dadurch viel empfindlicher gegen Spuren (bis 10^{-3} m) entweder von Aluminium- oder von Lithiumionen werden.

In der vorliegenden Arbeit wurde ein an einem kurzen Platinkontakt haftender Quecksilbertropfen elektrolytisch erzeugt und als polarisierbare Elektrode benutzt, da er stärkere Ströme als die an der Kapillare hängende Tropfelektrode verträgt, ohne abzufallen. Es wurden rechteckige Impulse konstanten Gleichstromes der Stärke $2{,}5 \cdot 10^{-6}$ bis $2 \cdot 10^{-4}$ A mit einer Frequenz von $^1/_2$, $^1/_4$ und $^1/_6$ Hz angewendet. Das Potential des Tropfens gegen das Bodenpotential wird am Schirm des Oszillographen als Potential-Zeitkurve ($V - t$) veranschaulicht. Solange die Stromstärke $2{,}5 \cdot 10^{-6}$ A nicht übersteigt, ist auf der V-t-Kurve keine Verzögerung im Potentialanstieg zu beobachten (Abb. 7a, b). Nach 3 Minuten langem Einwirken von Impulsen mit der 100fachen Stromstärke ($2 \cdot 10^{-4}$ A) wird sowohl eine kathodische als auch eine anodische Verzögerung des Depolarisationspotentials sichtbar. Sie verbleibt auch, wenn die Stromstärke auf den ursprünglichen Wert ($2{,}5 \cdot 10^{-6}$ A) herabgesetzt wird. Wenn nun auf den anhaftenden Tropfen die Elektrolyse mit dem Wechselstrom einwirkt und am Leuchtschirm die Abhängigkeit $\frac{dV}{dt} - V$ aufleuchtet, kommen die bekannten, sich mit der Zeitdauer vertiefenden Einschnitte zum Vorschein (Abb. 8).

Diese nur bei gesteigerter Stromdichte auftretende Depolarisation erklärt J. Heyrovsky [6] durch Bildung des $LiAlH_4$-Komplexes. Die große Stromdichte sei der Bildung von H^--Ionen günstig, da sich dabei die Doppelschicht sehr schnell auflädt und die zur Kathode zugeführten Elektronen in die wäßrige Schicht eindringen und mit Wasser die Anionen H^- bilden; in Gegenwart von viel Li^+- und Al^{3+}-Ionen vereinigen sich diese Kationen mit den H^--Ionen zum Komplex $LiAlH_4$ früher, als sie mit Wasserstoffionen zu H_2 reagieren können. Daß sich bei Potentialen, die negativer sind als der erwähnte anodische Depolarisationsvorgang, eine adsorbierte Schicht bildet, ist aus der Erhöhung des Ladungsstromes, die eine Erniedrigung der Kapazität der Tropfelektrode durch Adsorption angibt, zu ersehen. Die An-

wesenheit des Films zeigt sich durch eine Verminderung der Einschnitte von H^+, Mn^{2+}, Fe^{2+} und Zn^{2+}, wenn diese Ionen bei Anwesenheit von Al^{3+}-Ionen dem Lithium enthaltenden Elektrolyten zugefügt werden.

Der elektrolytische Vorgang

$$Li^+ + Al^{+++} + 4\,H^+ + 8\,e \rightleftarrows LiAlH_4$$

oder die durch Li^+- und Al^{3+}-Ionen katalysierte Reaktion

$$4\,H^+ + 8\,e \rightleftarrows 4\,H^-$$

verlaufen sehr schnell, wie aus den scharfen Einschnitten der $\frac{dV}{dt} - t$-Kurve (Abb. 9) und deren Verbleiben bis zu Frequenzen von 1500 Hz hervorgeht. Wie oben angegeben, ändert sich das Depolarisationspotential dieses Vorganges gemäß der Stromdichte, und zwar liegt es bei kleineren Ladungsströmen am kathodischen Ast bei — 1,70 V und am anodischen Ast bei — 1,40 V. Bei großer Stromdichte (10^{-3} A) wird das Depolarisationspotential bis um 500 mV positiver, also sehr

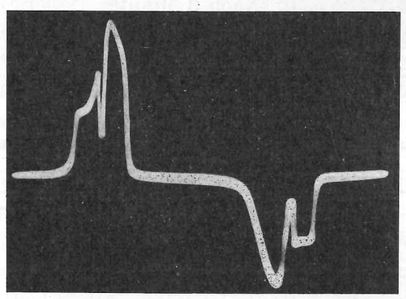

Abb. 9. Wechselstromoszillogramm $\frac{dV}{dt} - t$, 50 Hz, der Lösung $5 \cdot 10^{-3}\,m$ Al^{3+} in 1 m Li_2SO_4.

vom Abscheidungspotential der polarographischen Stromspannungskurven mit angelegter Spannung verschieden. Durch verlängerte Polarisation mittels stärkeren Wechselstromes (über 10^{-3} A) am stabil befestigten Tropfen wird die Empfindlichkeit des Erscheinens der Lithium-Aluminium-Einschnitte so weit gesteigert, daß sie noch in einem Gemisch von $10^{-6}\,m$ Al^{3+} mit 0,1 m Li^+ oder 0,1 m Al^{3+} in

Anwesenheit von $10^{-6}\,m$ Li^+ bemerkbar sind. Die Konstanz des Konzentrationsproduktes

$$[Al^{3+}] \cdot [Li^+] = 10^{-7}$$

deutet auf eine Verbindung gleicher Anzahl von Al^{3+}- und Li^+-Ionen hin. Daß nur die Höhe des Ladungsstromes für die Lithium-Aluminium-Reaktion entscheidend ist, zeigt ein Versuch, bei dem der stabile Tropfen zuerst einer Wechselstromelektrolyse mit großer Stromdichte und sofort nachher der spannungsbedingten polarographischen Elektrolyse mit auf- und absteigender Spannung unterworfen wird. Die erste dieser Stromspannungskurven zeigt sowohl die kathodische und anodische Lithium-Aluminium-Wirkung der Wechselstromkurven als auch den kathodischen Stromanstieg der polarographischen Depolarisation (also der Wasserstoffabscheidung [Abb. 10]). Bei wiederholter auf- und absteigender Spannung vermindert sich die Stromstärke dieser Wirkung und verschiebt sich zu negativeren Potentialen, um in den gewöhnlichen polarographischen Strom der Aluminiumionen überzugehen.

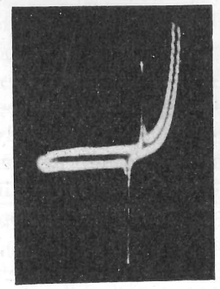

Abb. 10. Die am Kathodenstrahlpolarographen erhaltene Stromspannungskurve an einem stabilen Tropfen, der vorher durch Wechselstrom von $3 \cdot 10^{-4}$ A polarisiert wurde. Lösung $3{,}8 \cdot 10^{-3}\,m$ $Al_2(SO_4)_3$ in 4 m $LiCl$. Anstieg des Spannungsimpulses 1 V pro sec von 0 bis 2 V (obere Kurve) und zurück (untere Kurve).

Es gibt also an der Quecksilberelektrode zwei verschiedenartige Depolarisationsvorgänge der Aluminiumionen, je nachdem, ob die Elektrolyse unter Einwirkung der angewandten Spannung oder des angewandten Stromes verläuft. Im ersten Falle kommt es zur Wasserstoffabscheidung, im zweiten — und zwar nur bei Anwesenheit von

Lithiumionen und bei großer Stromdichte — bildet sich wahrscheinlich Lithium-Aluminium-Hydrid.

Es erübrigt sich zu erklären, warum sich bei langer Anwendung des Wechselstromes die Lithium-Aluminium-Einschnitte an den Ableitungskurven vertiefen und dann, nach einem viele Minuten langen Unterbrechen der Elektrolyse, wieder beim Einschalten des Wechselstromes tiefe Einschnitte erscheinen (Kemula-Kublik [7]). Während der strombedingten Polarisation kommt es bei negativen Potentialen zur Bildung und Adsorption von $LiAlH_4$ und zur Diffusion der Al^{3+}- und Li^+-Ionen an die Elektrodenoberfläche. Bei positivem Potential zerfällt das Hydrid, und die Kationen diffundieren in die Lösung, jedoch unter einem beträchtlich kleineren Konzentrationsabfall und für eine kürzere Zeit als bei den negativen Potentialen. Dadurch werden während eines jeden Zyklus des Wechselstromes die aktiven Ionen, Al^{3+} und Li^+, an der Elektrodenoberfläche angehäuft und bilden dann eher das Hydrid.

Zusammenfassung

Bei den Depolarisationswirkungen der Aluminiumionen an der polarisierbaren Quecksilberelektrode unterscheidet man zwei Arten von Elektrodenvorgängen: die eine verläuft bei gewöhnlichen polarographischen Stromspannungskurven mit angewandter Spannung oder mittels eines Kathodenstrahlpolarographen bei steigender Spannung an einem Tropfen. Die polarographische Analyse solcher Kurven, die mit angewandter Spannung ermittelt werden, zeigt, daß sich die Aluminiumionen als Protonendonatoren verhalten und nur zur Wasserstoffabscheidung führen, und zwar beim Potential von etwa — 1,7 V. Die zweite Art, die strombedingte Elektrolyse, besteht in der Anwendung eines definierten Stromes, entweder mit konstanten oder mit regelmäßig variierten Impulsen (sinusförmigen oder rechteckigen), und in der oszillographischen Messung der daraus folgenden Änderungen des Potentials, entweder als $V - t$ (Potential-Zeit-)Kurven oder Ableitungskurven $\frac{dV}{dt} - t$, $\frac{dV}{dt} - V$. Mit dieser Einrichtung erhält man kathodische und anodische Einschnitte je nach der Stromdichte von 10^{-4} A pro Oberfläche des Tropfens aufwärts, und zwar unter großen Stromdichten bei — 1,2 V, die sich beim Herabsetzen der Stromdichte bis zu — 1,7 V verschieben. Diese Depolarisationen entstehen nur bei Anwesenheit von Lithiumionen und deuten auf die Bildung des Hydrids $Li^+[AlH_4]^-$ hin, welches samt dessen Zersetzungsprodukten an der Elektrodenoberfläche adsorbiert wird.

Schrifttum

[1] Ishibashi, M., und T. Fujinaga, Proc. I. internat. polarographic Congress, Prague 1951, Part I, 106; J. chem. Soc. Japan **73** (1952) 538.
[2] Siehe Vortrag von P. Valenta.
[3] Kalousek, M., und M. Ralek, Chem. Listy **48** (1954) 808.
[4] Ruetschi, P., und G. Truempler, Helvetica chim. Acta **35** (1952) 1021, 1486, 1957.
[5] Kuta, J., Dissertation, Karls Univ., Praha 1950.
[6] Heyrovsky, J., Collection **18** (1953) 749.
[7] Kemula, W., und Z. Kublik, Roczniki Chem. **30** (1956) 1005.

CHEMICKÉ ZVESTI

OSOBITNÝ ODTLAČOK

UNIVERSITY
LIBRARY
CAMBRIDGE

VYDAVATEĽSTVO
SLOVENSKEJ AKADÉMIE VIED
BRATISLAVA

LITERATUR

1. Heyrovský J., Kalvoda R., *Oszillographische Polarographie mit Wechselstrom*, 55. Akademie-Verlag, Berlin 1960.
2. Breyer B., Hacobian S., *Australian J. Sci. Res.* ***5A***, 500 (1952).
3. Schwabe K., Jehring H., *Z. anal. Chem.* ***173***, 36 (1960).
4. Sohr H., *Chem. zvesti* ***16***, 316 (1962).
5. Kalvoda R., *J. Electroanal. Chem.* ***1***, 314 (1960).
6. Jehring H., *Vortrag z. Internat. Polarogr. Kolloquium*, Jena 1962. Monatsberichte der DAW (im Druck).
7. Jehring H., *Z. physik. Chem.* ***225***, 116 (1964).

Eingegangen am 16. September 1963

Diskussionsbeiträge

R. Kaivoda bemerkt, daß bei der Anwendung der Gleichstromkomponente die Aufladungsgeschwindigkeit der Elektrode bei kathodischem und anodischem Vorgang verschieden ist. Falls der kathodische und der anodische Strom denselben Wert hätte, wären auch die Potentialunterschiede zwischen dem kathodischen und anodischen Einschnitt kleiner.

H. Jehring betont, daß von „unsymmetrischen" Reaktionen hier nur dann gesprochen wird, falls der Potentialunterschied zwischen dem kathodischen und anodischen Einschnitt beträchtlich groß ist. Die Abhängigkeit von der Tropfzeit wurde auch bei Alkoholen untersucht: bei Alkoholen mit 6 C-Atome wurde schon eine Abhängigkeit von der Tropfdauer beobachtet. Bei größeren Molekulargewichten ist bei der Wechselspannungspolarographie immer eine längere Tropfzeit anzuwenden, sonst wird evtl. kein Peak beobachtet. Wird bei kurzer Tropfzeit kein Peak beobachtet, so bedeutet dies noch nicht, daß es nicht zur Adsorption kommt, sondern daß der Stoff nicht ausreichend andiffundieren kann. Im allgemeinen wurde beobachtet, daß stark oberflächenaktive Verbindungen langsam diffundieren, deswegen soll immer eine lange Tropfzeit oder ein stationärer Tropfen angewendet und Einstellung des Adsorptionsgleichgewichtes abgewartet werden.

Zu den elektrolytischen Reaktionen von Mangan(II)--Ionen in Anwesenheit von Sauerstoff

M. HEYROVSKÝ

Polarographisches Institut, Tschechoslowakische Akademie der Wissenschaften, Praha

Es wurden die elektrolytischen Reaktionen von sauerstoffhaltigen Mangan(II)-Lösungen mit Hilfe der oszillographischen Polarographie und anderen polarographischen Methoden verfolgt. Die Reaktionen wurden durch die Bildung von Manganhydroxid auf der Elektrodenoberfläche erklärt, das der Reduktion zum Metall oder der Oxydation zu Mangan(III)-hydroxid mit nachfolgender Rückreduktion unterliegt.

Als einer der Vorteile der oszillographischen Polarographie mit Wechselstrom gegenüber der klassischen Polarographie wird oft die Tatsache betrachtet, daß der Sauerstoff keinen Einfluß auf die Messungen ausübt. Es sind aber doch einige Beispiele bekannt, bei denen die Gestalt der Polarisationskurven durch die Sauerstoffreduktion beträchtlich beeinflußt wird. Sehr deutlich ist dieser Effekt im Falle der Reduktion des zweiwertigen Mangans in neutralen ungepufferten Lösungen zu beobachten. Das oszillographische Verhalten der Mangan(II)-Ionen in sauerstoffhaltigen Lösungen ist schon seit langem bekannt [1, 2], bisher fehlt aber eine befriedigende Erklärung der beteiligten Prozesse. Die vorliegende Arbeit stellt einen Versuch dar, eine derartige Erklärung zu bringen.

Experimenteller Teil

Alle oszillopolarographischen Messungen wurden mit einem polarographischen Oszilloskop P-4F (Konstruktion nach Dr. Vogel) durchgeführt teilweise unter Anwendung eines Adapteurs für spannungsbedingte Polarisation. Der hängende Tropfen nach Vogel wurde in Verbindung mit dem Polarecord Metrohm benutzt. Zur Registrierung der Kurven mit Umschaltung des Potentials diente ein Polarograph V 301, der mit einem elektronischen Umschalter nach Novák und Rálek gekoppelt war.

Die Lösungen wurden in einer einfachen elektrolytischen Zelle mit Bodenquecksilber als Bezugselektrode und in dem Gefäß nach Kalousek mit gesonderter gesättigter Kalomelelektrode untersucht. Alle benutzten Chemikalien (LiCl, KCl, $MnCl_2$, K_2SO_4, Na_2SO_4, $MnSO_4$, NH_4Cl, HCl) waren vom Reinheitsgrad pro analysi.

Der Sauerstoff wurde durch Durchleiten von Stickstoff aus den Lösungen vertrieben.

Ergebnisse und Diskussion

In der oszillographischen Polarographie mit Wechselstrom gibt zweiwertiges Mangan, wie schon früher beschrieben wurde, in verdünnten, nicht-

entlüfteten Lösungen von Alkalimetallsalzen eine charakteristische Kurve deren Form stark von dem angewandten Potentialbereich abhängt. Wird die Quecksilbertropfelektrode bis zu den beiden extremen Grenzpotentialen polarisiert, so entstehen auf der $dE/dt = f(E)$ Kurve zwei kathodische Einschnitte von Q^* 0,78 und 0,88 (in 1 M-LiCl), die sich mit steigender Mangankonzentration vertiefen (Abb. 1*a*). Ist die Mangankonzentration kleiner als die des Sauerstoffes, so erscheint nur der negativere Einschnitt (Abb. 2).

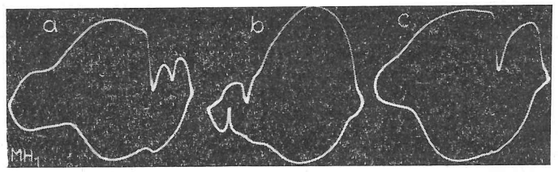

Abb. 1. 2 . 10^{-3} M-$MnCl_2$ in 0,5 M-LiCl bei Luftzutritt; i = 0,2 mA.
a) Elektrode auf die beiden extremen Grenzpotentiale polarisiert; *b*) das negative Grenzpotential erreicht nicht den Wert des zweiten negativen Einschnittes; *c*) das positive Grenzpotential wird negativer als 0,3 V (auf das Bodenquecksilber bezogen).

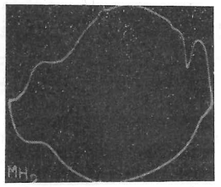

Abb. 2. 5 . 10^{-4} M-$MnCl_2$ in 0,5 M-LiCl bei Luftzutritt; i = 0,2 mA. Die Elektrode im vollen Potentialbereich polarisiert.

Wenn das negative Grenzpotential der Kurve nicht den Wert des zweiten kathodischen Einschnittes erreicht, entwickeln sich bei positiven Potentialen zwei einander gegenüber liegende Einschnitte (Abb. 1*b*), ein anodischer (Q 0,12) und ein kathodischer (Q 0,17, auf die vollentwickelte Kurve in 1 M-LiCl bezogen). Wird dagegen das positive Grenzpotential der Kurve negativer als etwa Q 0,1, so verschwindet der zweite negative kathodische Einschnitt und auf der Kurve verbleibt nur der von Q 0,78 (Abb. 1*c*). Völlig analog sind die oszillographischen Stromspannungskurven derselben Lösungen, wenn die Elektrode durch vorgegebene dreieckförmige Kippspannung polarisiert wird (Abb. 3*a*—*c*).

Nach Entfernung des Sauerstoffes aus der Lösung verschwinden die beiden positiven Einschnitte und der zweite negative kathodische. Einen gleichen

* Q bezeichnet hier die relative Lage der Spitze des Einschnittes auf der Potentialachse [10].

Effekt hat die Zugabe kleiner Mengen von Säuren oder Ammoniumsalzen (Abb. 4). Auch in Pufferlösungen erscheint auf der oszillographischen Kurve nur der erste negative kathodische Einschnitt. Die drei Einschnitte fehlen auf der Kurve, auch wenn die Lösung mit der Quecksilberstrahlelektrode elektrolysiert wird.

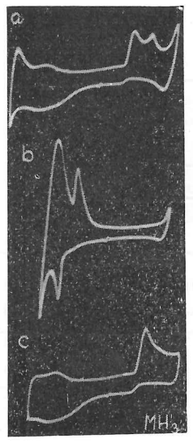

Abb. 3. $2 \cdot 10^{-3}$ M-$MnCl_2$ in 0,5 M-LiCl bei Luftzutritt. Stromspannungskurven, Elektrode mit dreieckförmiger Kippspannung polarisiert, Frequenz 50 Hz, $dE/dt = 200$ V/s; *a*, *b*, *c* — wie bei Abb. 1.

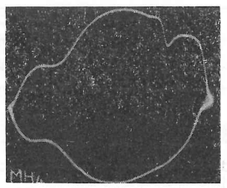

Abb. 4. $5 \cdot 10^{-4}$ M-$MnCl_2$ + + 10^{-3} M-NH_4Cl in 0,5 M-LiCl bei Luftzutritt; $i = 0{,}2$ mA.

Die Tiefe der beiden positiven und des zweiten negativen Einschnittes ist gegenüber der Ionenstärke der Grundlösung empfindlich. In Chloriden von höheren Konzentrationen als 2 M und in Sulfaten über 1 M sind die drei Einschnitte nicht mehr zu beobachten. Bei Sulfatkonzentration von rund 0,5 M entsteht bei positiven Potentialen nur der anodische Einschnitt; der gegenüberliegende kathodische erscheint erst nach dem Verdünnen. Auch die Zugabe kleiner Mengen von zwei- und dreiwertigen Kationen vermindert die drei Einschnitte.

Der erste negative kathodische Einschnitt entspricht ohne Zweifel der elektrolytischen Reduktion der freien hydratisierten Mangan(II)-Ionen. Dieser Einschnitt entsteht in allen Lösungen, die Mn^{2+}-Ionen enthalten, und sein Potential stimmt mit dem polarographischen Halbstufenpotential der Mn^{2+}--Reduktion überein. Für die entsprechende Elektrodenreaktion kann man also schreiben:

$$Mn^{2+}aq + 2e \rightarrow Mn(Hg).$$

Dieser Prozess ist teilweise reversibel, wie aus den Abbildungen 1*a*, 3*a* und 3*c* zu sehen ist. Die Reversibilität der Auflösung des Manganamalgams hängt stark von der Zusammensetzung der Lösung und von den anderen

Versuchsbedingungen ab. Wie W. Kemula und. Z. Galus [3] gezeigt haben, entstehen intermetallische Verbindungen zwischen Mangan und Quecksilber, und zur Auflösung des Mangans aus seinem Amalgam kommt es bei drei verschiedenen Potentialen — bei etwa —1,5, —0,9 und —0,4 V gegen die 0,1 N Kalomelelektrode. Ein Anzeichen der Auflösung bei —0,9 V ist auf den oszillographischen Kurven in der Nähe des Kapazitätsmaximums des Grundelektrolyten zu sehen (anodischer Ast der Kurve *1a* oder *4* im Vergleich mit *2*). Die anodische Auflösung verläuft nach der Gleichung:

$$Mn(Hg) \rightarrow Mn^{2+}aq + 2e.$$

Der zweite negative kathodische Einschnitt begleitet immer den Reduktionseinschnitt der Mn^{2+}-Ionen und wird tiefer mit steigender Mangan- und Sauerstoffkonzentration. Die Feststellung, daß nach Zugabe der Lösungen von Säuren, Ammonium-Ionen oder Puffern der Einschnitt verschwindet, führte uns zur Vermutung, daß es sich hier um die Reduktion des auf der Elektrodenoberfläche gebildeten Mangan(II)-hydroxids handelt. Ein analoger Fall wurde bei der Reduktion von Cd^{2+}-Ionen in sauerstoffhaltigen Lösungen festgestellt [4], und es ist sehr wahrscheinlich, daß auch die ähnlichen Effekte bei Zn^{2+}, Pb^{2+} [5], Fe^{2+} [6] und Co^{2+} sowie Ni^{2+} [7] durch die Reduktion der entsprechenden Hydroxide zu erklären sind.

Bei kleinen Mangankonzentrationen werden alle Mangan-Ionen an der Elektrodenoberfläche durch die OH^--Ionen gefällt und das gebildete Mangan(II)-hydroxid wird bei dem Potential des negativeren Einschnittes reduziert (Abb. 2). Die höhere Konzentration der Grundelektrolyten wirkt entweder durch Komplexierung oder Peptisierung gegen die Fällung des Manganhydroxids auf der Quecksilberoberfläche. In der gleichen Weise erklärte H. A. Laitinen [11] den Einfluß der Konzentration des Grundelektrolyten auf die Bildung von Kobalt(II)-hydroxid an der Tropfelektrode.

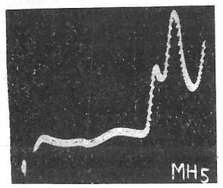

Abb. 5. $2 \cdot 10^{-3}$ M-$MnCl_2$ in 0,5 M-LiCl bei Luftzutritt. Stromspannungskurve, Elektrode mit einem einzelnen linearen Spannungsimpuls polarisiert, von 0 zu —2 V; $dE/dt = 0{,}7$ V/s.

Die oszillographischen Stromspannungskurven mit einzelnen linearen Spannungsimpulsen (single-sweep) haben gezeigt, daß nach den beiden Sauerstoffreduktionsstufen und nach dem Strommaximum der Mn^{2+}-Reduktion eine zweite Stromspitze erscheint (Abb. 5), die außer durch die oben erwähnten Reagenzien auch durch einen kleinen Gelatinezusatz unterdrückt werden

kann. Die Gelatine verhindert offensichtlich die Bildung des Manganhydroxids an der Elektrodenoberfläche. H. A. Laitinen und Mitarbeiter [11] haben denselben Effekt bei Bildung des Filmes von Kobalt(II)-hydroxid auf der Quecksilbertropfelektrode beobachtet. Das Auftreten dieses zweiten Maximums ist nicht mit dem Erreichen eines bestimmten Potentials verbunden — die Stromspitze wird durch kein elektrolytisches Oxydationsprodukt hervorgerufen. Bei Wiederholung des Impulses auf der Oberfläche des hängenden Tropfens entsteht das zweite Maximum auf der Stromspannungskurve nur dann, wenn die Anfangsspannung kleiner als 0,3 V wird. Bei dem entsprechenden Potential der Quecksilberelektrode geht das metallische Mangan aus dem Amalgam völlig in Lösung und die nachfolgenden Elektrodenprozesse laufen wieder auf der reinen Quecksilberoberfläche ab. Mit höherem Anfangswert der angelegten Spannung sieht man auf der wiederholten Kurve, daß die Sauerstoffreduktion stark vermindert ist. Infolgedessen werden die OH^--Ionen an der Elektrodenoberfläche nicht in genügend hoher Konzentration zur Bildung von Manganhydroxid erzeugt und alle Mangan-Ionen werden nur in dem positiveren Strommaximum reduziert. Die Unterdrückung der Sauerstoffreduktion an der Oberfläche aus verdünntem Manganamalgam wurde auch durch die mit dem hängenden Tropfen polarographisch registrierten Stromspannungskurven bestätigt; eine Erklärung dafür konnte jedoch nicht gefunden werden.

Einen indirekten Beweis für die Reduzierbarkeit des an der Elektrodenoberfläche sich bildenden Manganhydroxids bietet auch die klassische Polarographie. Die polarographische Reduktionsstufe der Mn^{2+}-Ionen addiert sich genau zu den zwei Stufen der Sauerstoffreduktion, nur ist das Halbstufenpotential dieser Manganstufe um 20 mV zu negativeren Werten gegen die Stufe in sauerstofffreier Lösung verschoben. Es kommt hier also nicht zur Bildung der „latenten Ströme" [8], was nur dadurch zu erklären ist, daß das in der Diffusionsschicht gefällte Manganhydroxid an der Elektrode völlig reduziert wird.

Dem zweiten, negativen kathodischen Einschnitt auf der oszillographischen Kurve entspricht also aus den oben angeführten Gründen die Reaktion

$$Mn(OH)_2 + 2e \rightarrow Mn(Hg) + 2OH^-$$

mit der vorgelagerten Bildung des Manganhydroxids:

$$O_2 + 4e + 2H_2O \rightarrow 4OH^-,$$
$$2Mn^{2+} + 4OH^- \rightarrow 2Mn(OH)_2.$$

Diese Fällung des Hydroxids spielt sich teilweise in der Elektrodendoppelschicht ab, was den Einfluß der Ionenstärke der Grundlösung auf die oszillopolarographische Einschnitte erklärt.

Der anodische Einschnitt erscheint auf der Kurve nur dann, wenn es nicht zur Reduktion des Manganhydroxids kommt; das Hydroxid bleibt also an der Elektrodenoberfläche unzerstört und kann während der anodischen Phase oxydiert werden.

Bei langsamer Polarisation des hängenden Tropfens in polarographischer Anordnung von der Spannung null zum Potential der zweiten Sauerstoffstufe und zurück erscheint auf dem anodischen Ast der Stromspannungskurve eine Stromspitze, deren Potential mit dem des oszillopolarographischen Einschnittes übereinstimmt (Abb. 6). Bei dem zweiten Polarisationszyklus entsteht bereits auch auf dem kathodischen Ast der Kurve ein scharfes Strommaximum bei demselben Potential wie der positive kathodische Einschnitt. Dieser Effekt ist nicht zu beobachten, wenn das Potential der Elektrode nicht die zweite Reduktionsstufe des Sauerstoffes erreicht. Das anodische Maximum ist also der Oxydation des Produktes einer Reaktion zwischen OH^--Ionen und Mn^{2+}-Ionen, nämlich des Mangan(II)-hydroxids, zuzuschreiben. Dieser Schluß konnte mit Hilfe des Umschalters nach Kalou-

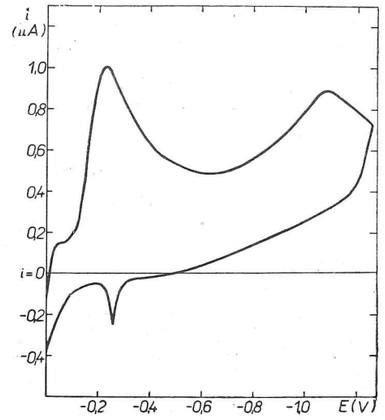

Abb. 6. 2 . 10^{-3} M-$MnCl_2$ in 0,1 M-KCl bei Luftzutritt.
Der hängende Tropfen von null zu negativen Potentialen und zurück polarisiert (gegen Bodenquecksilber); $dE/dt = 0{,}03$ V/s.

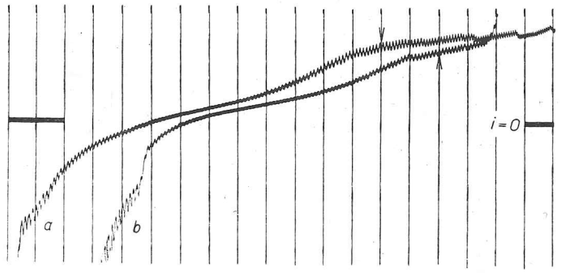

Abb. 7. Polarographische Kurven mit umgeschaltetem Potential nach Kalousek.
a) 0,1 N-KCl bei Luftzutritt; *b*) 2 . 10^{-3} M-$MnCl_2$ in 0,1 N-KCl bei Luftzutritt, 100 mV/Absz., von 0 V, $S = 1/40$; gegen Bodenquecksilber; Frequenz der Umschaltung 4 Hz, Hilfspotential —1,3 V (auf den Kurven bezeichnet). Anfang der Kurve *b* um zwei Abszissen verschoben. Galvanometer im Stromzweig des veränderlichen Potentials.

sek bestätigt werden. Das bei dem Potential der zweiten Sauerstoffstufe in der Diffusionsschicht entstandene Manganhydroxid gibt bei Umschaltung eine anodische Stufe, die wieder bei dem Potential des anodischen Einschnittes liegt (Abb. 7). Für den mit dem anodischen Einschnitt verbundenen Prozess läßt sich also schreiben:

$$Mn(OH)_2 \rightarrow Mn(OH)_2^+ + e,$$
$$Mn(OH)_2^+ + Y^{n-} \rightarrow Mn(OH)_2Y^{(n-1)-}.$$

In verdünnten Lösungen steht für Y^{n-} wahrscheinlich wieder OH^-, in konzentrierteren Sulfatlösungen werden die Hydroxylionen gegen Sulfat-Ionen vertauscht.

Der positive kathodische Einschnitt gehört, wie aus dem obenangeführten folgt, der Rückreduktion des Mangan(III)-hydroxids zum Mangan(II)-hydroxid. In Sulfatlösungen, in denen die Bildung des Mangan(III)-hydroxids nach der Oxydation verhindert wird, tritt dieser Einschnitt nicht auf.

Bei Wiederholung der einzelnen linearen Spannungsimpulse auf dem hängenden Tropfen erscheint, wenn das Potential der Elektrode nicht den Wert der Manganreduktion erreicht, auf der Stromspannungskurve bei dem Potential des oszillopolarographischen Einschnittes eine Spitze, die offenbar auch dieser Reduktion entspricht. In älteren Lösungen, in denen die Existenz von Hydrolyseprodukten, unter anderem auch des Mangan(III)-hydroxids, anzunehmen ist, entsteht diese Spitze schon auf der ersten Kurve (Abb. 8). Für den positiven kathodischen Einschnitt gilt also die umgekehrte Reaktion wie für den anodischen:

$$Mn(OH)_3 + e \rightarrow Mn(OH)_2 + OH^-.$$

Nach den Berechnungen von W. M. Latimer [9] ist für die Reaktion

$$Mn(OH)_2 + OH^- \rightleftarrows Mn(OH)_3 + e$$

das Potential von etwa —0,23 V gegen die 0,1 M-KCl-Elektrode zu erwarten.

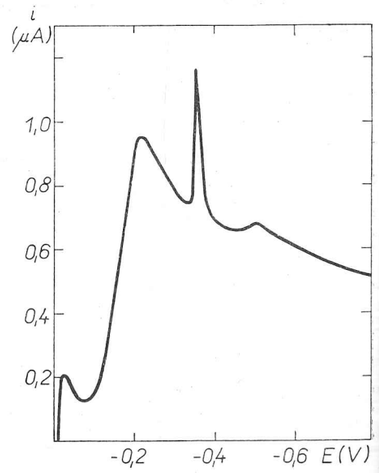

Abb. 8. $2 \cdot 10^{-3}$ M-$MnCl_2$ in 0,1 M-KCl, hydrolysierte Lösung, bei Luftzutritt. Kurve mit dem hängenden Tropfen aufgenommen, Potentiale gegen Bodenquecksilber; $dE/dt = 0{,}03$ V/s.

Ein genauer Vergleich dieses Wertes mit dem experimentell gemessenen setzt eine eingehendere Studie der Elektrodenreaktion des Manganhydroxids voraus, die den Rahmen dieser qualitativen Mitteilung überschreitet.

PRÍSPEVOK K ELEKTROLYTICKÝM REAKCIÁM IÓNOV Mn^{2+} ZA PRÍTOMNOSTI KYSLÍKA

M. Heyrovský

Polarografický ústav, Československá akadémia vied, Praha

Oscilografickou polarografiou, ako aj inými polarografickými metódami sa sledovali elektrolytické reakcie iónov Mn^{2+} v roztokoch obsahujúcich kyslík. Reakcie sa objasnili tvorbou hydroxidu mangánatého na povrchu elektródy. Vzniknutý hydroxid podlieha redukcii na kov alebo oxydácii na hydroxid manganitý.

К ЭЛЕКТРОЛИТИЧЕСКИМ РЕАКЦИЯМ ИОНОВ МАРГАНЦА(II) В ПРИСУТСТВИИ КИСЛОРОДА

М. Гейровски

Полярографический институт, Чехословацкая академия наук, Прага

Методом осциллографической полярографии и другими полярографическими методами исследовались электролитические реакции двухвалентного марганца в растворах, содержащих кислород. Реакции были объяснены образованием на поверхности электрода гидроокиси марганца(II), подвергающейся восстановлению до металла или окислению до гидроокиси марганца(III).

Preložil I. Smoler

LITERATUR

1. Bieber R., Trümpler G., *Helv. Chim. Acta* ***30***, 971 (1947).
2. Heyrovský J., Forejt J., *Oscilografická polarografie*, 111. Státní nakladatelství technické literatury, Praha 1953.
3. Kemula W., Galus Z., *Roczniki Chem.* ***36***, 1223 (1962).
4. Kaufman D. C., Loveland J. W., Elving P. J., *J. Phys. Chem.* ***63***, 217 (1959).
5. Behr B., Chodkowski J., *Roczniki Chem.* ***26***, 650 (1952).
6. Heyrovský J., *Anal. Chim. Acta* ***8***, 283 (1953).
7. Kemula W., Kublik Z., *Roczniki Chem.* ***30***, 1259 (1956).
8. Kemula W., *Sprawozd. Tow. Nauk. Warz.*, Wydz. III. ***40***, 3 (1947).
9. Latimer W. M., *Oxidation Potentials*, 2nd ed., 237. Prentice-Hall, New York 1952.
10. Heyrovský J., Kalvoda R., *Oszillographische Polarographie mit Wechselstrom*, 88. Akademie-Verlag, Berlin 1960.
11. Laitinen H. A., Frank A. J., Kivalo P., *J. Am. Chem. Soc.* ***75***, 2865 (1953).

Eingegangen am 16. September 1963

Diskussionsbeiträge

R. Kalvoda bemerkt, daß der Einfluß des Sauerstoffes auch bei einigen organischen Verbindungen wie zweiwertige Fenole beobachtet wurde. Bei der Reduktion des Sauerstoffes in neutraler Lösung wird die Elektrodenoberfläche alkalisch. In diesem alkalischen Milieu werden die zweiwertigen Fenole oxydiert; diese werden dann bei dem folgenden kathodischen Vorgang elektrolytisch reduziert.

M. Schulz macht aufmerksam auf den Einfluß von H_2O_2 auf Mn, Fe sowie auch zweiwertige Fenole.

M. Heyrovský antwortet, daß er keinen bedeutendsten Einfluß von H_2O_2 auf die beschriebenen Erscheinungen beobachtet hat.

POLAROGRAPHISCHE STUDIE DES DREIWERTIGEN CHROMS IN ALKALISCHER LÖSUNG

M. HEYROVSKÝ

Reprinted from Collection Czechoslov. Chem. Commun. *29*, 1344—1349 (1964)

Collection of Czechoslovak Chemical Communications. Vol. 29 (1964). — Published under the auspices of the Czechoslovak Academy of Sciences by the Publishing House of the Czechoslovak Acad. Sci., Vodičkova 40, Prague 1. — Address of the Editor: Institute of Organic Chemistry and Biochemistry, Czechoslovak Academy of Sciences, Na cvičišti 2, Prague 6.
Annual subscription Kčs 300·—, US $ 33·60, £ 12, single issue Kčs 25·—.
Subscriptions from abroad, except from socialist countries, may be sent to ACADEMIC PRESS Inc. (London) Limited, Berkeley Square House, Berkeley Square, London, W. 1, or to ACADEMIC PRESS Inc., Publishers, 111, Fifth Avenue New York 3, N. Y., or to ARTIA, P. O. Box 790, Smečky 30, Prague 1, Czechoslovakia.
Rozšiřuje Poštovní novinová služba, objednávky a předplatné přijímá PNS — ústřední expedice tisku, administrace, odborného tisku, Jindřišská ul. 14, Praha 1. Lze také objednat u každého poštovního úřadu nebo doručovatele. Objednávky do zahraničí vyřizuje PNS — ústřední expedice tisku, odd. vývoz tisku, Jindřišská 14, Praha 1.

POLAROGRAPHISCHE STUDIE DES DREIWERTIGEN CHROMS IN ALKALISCHER LÖSUNG

M. HEYROVSKÝ

Polarographisches Institut, Tschechoslowakische Akademie der Wissenschaften, Prag

Eingegangen am 17. Juni 1963

Die polarographische Stufe der Oxydation des Chromits zu Chromat wird beschrieben. Ihr Grenzstrom ist durch die Diffusionsgeschwindigkeit des Depolarisators bestimmt und sinkt mit der Zeit. Aus dem zeitlichen Abfall der Stufe folgt, daß das Chromit in der Lösung einer Reaktion zweiter Ordnung unter Bildung eines zweikernigen Komplexes unterliegt.

Bei der Untersuchung alkalischer Lösungen von Chrom(III)-salzen mit Hilfe der Methoden der oszillographischen Polarographie[1,2] wurde festgestellt, daß an der Oberfläche der Tropfelektrode, wenn diese bis zum Potential der Quecksilberauflösung polarisiert wird, Chromat entsteht, das bei negativeren Potentialen der Reduktion unterliegt. Da die Oxydation des dreiwertigen Chroms an der Quecksilberelektrode bisher nicht beschrieben wurde, haben wir uns die Aufgabe gestellt, diese Reaktion mit Hilfe der klassischen Polarographie zu erforschen. Die polarographische Untersuchung der alkalischen Lösungen des dreiwertigen Chroms versprach außerdem, neue Erkenntnisse über das chemische Verhalten der Chromite zu bringen, das bisher nicht ganz geklärt war.

Experimenteller Teil

Die polarographischen Kurven wurden mit dem Polarographen Yanagimoto PA-101 registriert. Die angewandte Kapillare vom Typus nach Smoler hatte bei 50 cm hoher Quecksilbersäule die Ausflußgeschwindigkeit $m = 0{,}68$ mg/s und die Tropfzeit von 4,37 s in 1N-KCl-Lösung beim Potential der gesättigten Kalomelelektrode.

Die Chrom(III)-Lösungen wurden direkt im Elektrolysegefäß durch Pipettieren von 0,1 oder 0,01M Kaliumchromalaun zu einer vorher entlüfteten Hydroxid-Lösung dargestellt.

Die Untersuchungen wurden in einem Kalousek-Gefäß mit getrennter gesättigter Kalomelelektrode vorgenommen, das sich in einem auf die Temperatur von 20°C thermostatisierten Wasserbad befand. Der Luftsauerstoff wurde durch Durchperlen mit Stickstoff aus den Lösungen vertrieben. Die angewandten Chemikalien vom Reinheitsgrad *pro analysi* waren durchwegs Erzeugnisse der Firma Lachema.

Ergebnisse und Diskussion

Polarographisches Verhalten der Chromite

Alkalische Lösungen von dreiwertigem Chrom geben eine polarographische Oxydationsstufe (Abb. 1), deren Halbstufenpotential um weniger als 100 mV vor dem anodischen Strom der Quecksilberauflösung liegt. Um die Stufe messen zu können, wurden die Kurven im Maßstab von 10 mV/cm registriert. Im untersuchten Konzentrationsbereich von $1 \cdot 10^{-4}$ bis $5 \cdot 10^{-3}$M und bei mindestens 50fachem Laugenüberschuß ist die Höhe der Stufe der Konzentration des Chroms direkt proportional und unabhängig von der der Hydroxidionen. Vermindert man das Konzentrationsverhältnis der OH^--Ionen zu den Chrom(III)-Ionen, so sinkt die Stufe und verschwindet schließlich beim Konzentrationsverhältnis 10 : 1 praktisch von der Kurve. Angefangen von 10^{-3} molarer und höherer Konzentration erscheint auf dem Grenzstrom der Stufe ein Abfall, dessen Natur nicht näher untersucht wurde.

Die Abhängigkeit von der Höhe der Quecksilbersäule zeigt an, daß der Grenzstrom nur durch die Diffusionsgeschwindigkeit des Depolarisators bestimmt ist. Die Höhe der Stufe ist gleich der Gesamthöhe der zweistufigen kathodischen Dreielektronenwelle in 0,1M-$NaClO_4$-Lösung mit gleicher Konzentration an Chrom(III)-salz – sie ent-

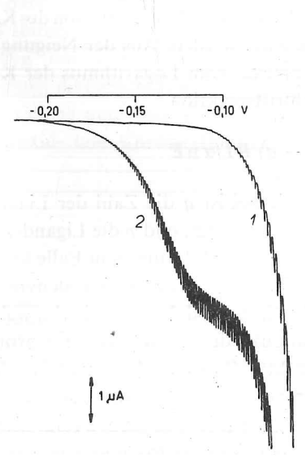

Abb. 1
Polarographische Stufe der anodischen Oxydation des Chromits
0,1M-KOH, Konzentration des $KCr(SO_4)_2$: *1* 0; 2 $5 \cdot 10^{-4}$M. Kurvenbeginn −0,2 V, SKE.

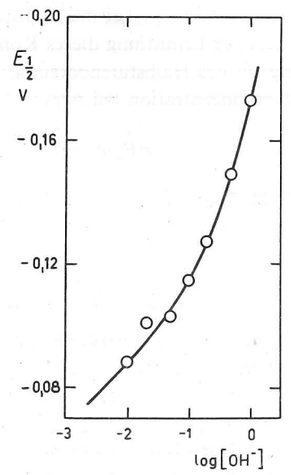

Abb. 2
Abhängigkeit des Halbstufenpotentials des Chromits von der Hydroxidionenkonzentration bei konstanter Ionenstärke
Lösung von $5 \cdot 10^{-4}$M-$KCr(SO_4)_2$ in KOH, durch Natriumnitrat auf $\mu = 1$ ergänzt.

spricht folglich einer Dreielektronen-Oxydation. Die logarithmische Analyse ergibt eine Gerade; der Reziprokwert ihrer Neigung beträgt in 10^{-2}, 10^{-1} und 1M-KOH 30 mV. Hieraus ergibt sich für den Koeffizienten α der Wert 2/3 (bei n = 3). Aus der Differenz der Halbstufenpotentiale der Oxydation des Chromits zu Chromat und der Reduktion des Chromats zu Chromit[3], die etwa 0,7 V beträgt, ist der stark irreversible Charakter der Durchtrittsreaktion erkennbar. In Anwesenheit eines indifferenten Elektrolyten (KNO_3, $NaClO_4$) verschiebt sich die Stufe nach positiven Potentialen. Die Abhängigkeit des Halbstufenpotentials von der Hydroxidionenkonzentration bei konstanter Ionenstärke ist in Abb. 2 dargestellt.

Auf Grund der Ergebnisse von Scholder und Plätsch[4] kann angenommen werden, daß in einer frisch bereiteten alkalischen Lösung von dreiwertigem Chrom je nach den Konzentrationsverhältnissen mehrere Chrom(III)-Komplexe existieren, die sich untereinander im Gleichgewicht befinden:

$$[(H_2O)_2Cr(OH)_4]^-,\quad [(H_2O)Cr(OH)_5]^{2-},\quad [Cr(OH)_6]^{3-},\quad [(H_2O)Cr(OH)_7]^{4-},$$

$$[Cr(OH)_8]^{5-}$$

(die Natriumsalze der letzten drei Komplexe wurden im kristallinen Zustand dargestellt).

Ist das Gleichgewicht zwischen den Komplexen mobil und überwiegt bei der betrachteten Hydroxidionenkonzentration stets ein bestimmter Komplex gegenüber den anderen, so kann die Abhängigkeit des Halbstufenpotentials von der Konzentration des Komplexbildners zur Ermittlung dieses Komplexes benutzt werden. Aus der Neigung der Abhängigkeit des Halbstufenpotentials des Komplexes vom Logarithmus der Komplexbildnerkonzentration bei irreversibler Durchtrittsreaktion

$$\mathrm{d}E_{\frac{1}{4}}/\mathrm{d}\log[X^-] = -(p-q)\,RT/\alpha\,nF$$

kann die Differenz $(p - q)$ ermittelt werden. Hierbei ist q die Zahl der Liganden des Komplexes, der direkt der Durchtrittsreaktion unterliegt, und p die Ligandenzahl des Komplexes, der in der betrachteten Lösung überwiegt[5]. In unserem Falle können wir versuchen, an Hand eines Vergleichs der Struktur der für den Elektrodenvorgang in Frage kommenden Komplexe den Wert q zu bestimmen, d. h. zu ermitteln, welcher Komplex direkt oxydiert wird. Dem Reaktionsprodukt, dem tetraedrischen Chromat-Anion, steht das Tetrahydroxochromit-Ion strukturell am nächsten; es ist wahrscheinlich, daß eben dieser Komplex der Durchtrittsreaktion unterliegt, und wir können deshalb q gleich 4 setzen. Aus der Neigung der Kurve in Abb. 2 folgt hierauf, daß in $5 \cdot 10^{-4}$M Lösung von Chrom(III)-Ionen bei einer Hydroxidionenkonzentration der Größenordnung von 10^{-2}M das Pentahydroxochromit-Anion die überwiegende Komplexform ist ($\mathrm{d}E_{\frac{1}{4}}/\mathrm{d}\log[OH]^- = 30$ mV). Bei zehnmal höherer Laugenkonzentration ist es das Hexahydroxochromit-Anion ($-\mathrm{d}E_{\frac{1}{4}}/\mathrm{d}\log[OH^-] = 60$ mV) und in Kaliumhydroxid von etwa 1M Konzentration überwiegt das Heptahydroxochromit über den übrigen Komplexen ($-\mathrm{d}E_{\frac{1}{4}}/\mathrm{d}\log[OH^-] = 90$ mV). Zum gleichen Ergebnis in bezug auf das Mengenverhältnis der einzelnen Chrom(III)-komplexe in der

Lösung führt auch die Methode von Koryta[6], bei der der Strom bei konstantem Potential in Abhängigkeit von der Konzentration des Komplexbildners gemessen wird.

Sind also die oben angeführten Voraussetzungen über die Eigenschaften des Systems der Chrom(III)-komplexe richtig, so können wir für die elektrolytische Oxydation des dreiwertigen Chroms in alkalischem Milieu folgende Bruttoreaktion ansetzen:

$$[(H_2O)_2Cr(OH)_4]^- + 4\,OH^- \rightarrow CrO_4^{2-} + 3\,e + 6\,H_2O\,.$$

Verfolgung der Reaktion in der Lösung

Bei der Untersuchung des polarographischen Verhaltens der Chromite wurde beobachtet, daß ihre anodische Stufe mit der Zeit sinkt. Dieser Effekt ist augenscheinlich die Folge des bekannten Alterns der Chrom(III)-Lösungen[7], auf das zum Beispiel auch der Abfall der Anfangsgeschwindigkeit bei der Oxydation mit Wasserstoffperoxid zurückzuführen ist[8]. Der Abfall der polarographischen Stufe ist im gesamten untersuchten Konzentrationsbereich im Hinblick auf das Chrom durch die Beziehung für Reaktionen zweiter Ordnung bestimmt (Abb. 3). Die Geschwindigkeitskonstanten dieser Reaktion wurden durch die graphische Methode ermittelt. Sie haben nur formale Bedeutung, da sie sich immer nur auf eine bestimmte Verteilung der Komplexe beziehen, deren absolute Konzentration nicht bekannt ist und sich je nach der Konzentration der Hydroxid- und Chrom(III)-Ionen ändert.

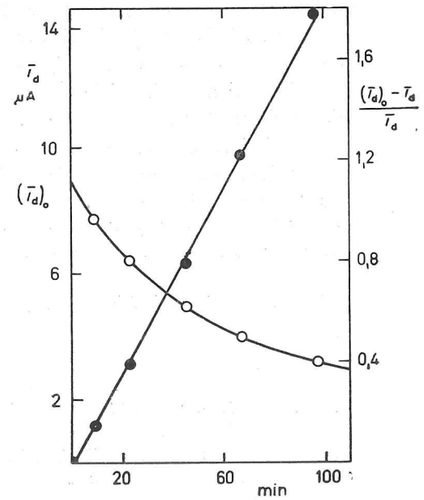

Abb. 3
Zeitlicher Abfall des Chromit-Grenzstromes $9 \cdot 10^{-4}$M-$KCr(SO_4)_2$ in $9 \cdot 10^{-2}$M-KOH ○ Zeitliche Änderung der Stufenhöhe; ● lineare Abhängigkeit des Ausdruckes. $[(\bar{i}_d)_0 - \bar{i}_d]/\bar{i}_d$ von der Zeit; der lineare Verlauf entspricht einer Reaktion zweiter Ordnung.

Mit wachsender Hydroxidionenkonzentration sinkt der Wert der Reaktionsgeschwindigkeitskonstante (Tab. I). Dies läßt sich dadurch erklären, daß die Komplexe mit niedrigerer Zahl an Hydroxid-Liganden leichter der chemischen Reaktion unterliegen.

Tabelle I

Abhängigkeit der Dimerisationsgeschwindigkeitskonstante des Chromits von der Hydroxidionenkonzentration bei konstanter Konzentration von 10^{-3}M-$KCr(SO_4)_2$

$[OH^-]$ mol l^{-1}	$5 . 10^{-2}$	$1 . 10^{-1}$	$1{,}5 . 10^{-1}$	1
$k . 10^2$ l mol^{-1} s^{-1}	38	21	11	6,5

Die Chrom(III)-komplexe sind befähigt, sich vermittells von Diolbrücken miteinander zu verbinden[9]. Diese Brücken kommen zwischen Komplex-Ionen zustande, die in *cis*-Stellung ein Wassermolekül und eine OH-Gruppe tragen[10,11]; derartige Ionen sind in unserem Falle das Tetra- und Pentahydroxochromit.

Im Hinblick auf die elektrische Ladung des Komplexes kann erwartet werden, daß sich die Dimerisation am schnellsten zwischen zwei Tetrahydroxochromit-Teilchen vollziehen wird; der Pentahydroxokomplex wird wahrscheinlich bei höherer Laugenkonzentration in der Reaktion zur Geltung kommen. Komplexe mit höherer Zahl an OH-Liganden kommen für die Reaktion bereits nicht mehr in Betracht; dies erklärt die relative Beständigkeit der Chromite in konzentrierten Laugenlösungen[12]. Das zweikernige Chromit ist in dem an der Quecksilberelektrode zugänglichen Potentialbereich bereits nicht mehr oxydierbar. Infolgedessen ist es nicht möglich, seine weitere Reaktion in der Lösung polarographisch zu verfolgen. Es ist sehr wahrscheinlich, daß es, ähnlich wie bei der Hydrolyse der Chrom(III)-salze[13], zur stufenweisen Bildung großer mehrkerniger Komplexe kolloidalen Charakters kommt. Das Anfangsstadium des Alterns von wäßrigen Chrom(III)-Lösungen beruht demnach nicht auf der Abscheidung von Chrom(III)-hydroxid, sondern auf der Bildung mehrkerniger Komplexe vermittels von Diolbrücken.

Frau V. Kailová spreche ich für die Anfertigung der Abbildungen meinen Dank aus.

Literatur

1. Heyrovský J. im Buche: *Advances in Polarography* (I. S. Longmuir Ed.), Bd. 1, S. 18. Pergamon Press, London 1960.
2. Heyrovský M.: Chem. zvesti *14*, 834 (1960).
3. Lingane J. J., Kolthoff I. M.: J. Am. Chem. Soc. *62*, 852 (1940).
4. Scholder R., Pätsch R.: Z. anorg. u. allgem. Chem. *220*, 411 (1934).
5. Matsuda H., Ayabe Y.: Bull. Chem. Soc. Japan *29*, 134 (1956).
6. Koryta J.: diese Zeitschrift *24*, 3057 (1959).
7. Fricke R., Windhausen O.: Z. anorg. u. allgem. Chem. *132*, 273 (1924).
8. Baloga M. R., Earley J. E.: J. Am. Chem. Soc. *83*, 4906 (1961).
9. Pfeiffer P., Stern R.: Z. anorg. Chem. *58*, 240, 280 (1908).
10. Hein F.: *Chemische Koordinationslehre*, S. 176. Hirzel, Leipzig 1954.

11. Grant D. M., Hamm R. E.: J. Am. Chem. Soc. *78*, 3006 (1956).
12. Nekrasov B. V.: *Kurs obščej chimii*, 9. Aufl., S. 333. Gostechizdat, Moskau 1952.
13. Hückel W.: *Structural Chemistry of Inorganic Compounds*, S. 232. Elsevier, New York 1950.

Übersetzt von H. Bažantová.

Резюме

М. Гейровский: *Полярографическое изучение трехвалентного хрома в щелочном растворе.* Описана полярографическая волна окисления хромита до хромата. Предельный ток последней управляется скоростью диффузии деполяризатора и падает во времени. Из падения высоты волны во времени вытекает, что хромит подвергается в растворе реакции второго порядка с образованием двухядерного комплекса.

MERKURIERUNG VON KETONEN AN DER QUECKSILBERTROPFELEKTRODE

M. HEYROVSKÝ

Collection of Czechoslovak Chemical Communications. Vol. 28 (1963) — Published under the auspices of the Czechoslovak Academy of Science by the Publishing House of the Czechoslovak Acad. Sci., Vodičkova 40, Prague 1. — Address of the Editor: Institute of Organic Chemistry and Biochemistry, Czechoslovak Academy of Science, Na cvičišti 2, Prague 6.

Annual subscription Kčs 300·—, US $ 33·60, £ 12, single issue Kčs 25·—.

Subscriptions from abroad, except from socialist countries, may be sent to ACADEMIC PRESS Inc. (London) Limited, Berkeley Square House, Berkeley Square, London, W. 1, or to ACADEMIC PRESS Inc., Publishers, 111 Fifth Avenue, New York 3, N.Y., or to ARTIA, P.O.Box 790, Smečky 30, Prague 1, Czechoslovakia.

Rozšiřuje Poštovní novinová služba, objednávky a předplatné přijímá Poštovní novinový úřad — ústřední administrace PNS, Jindřišská 14, Praha 1. Lze také objednat u každého poštovního úřadu nebo doručovatele.

Reprinted from Collection Czechoslov. Chem. Commun. *28*, 26—35 (1963)

MERKURIERUNG VON KETONEN AN DER QUECKSILBERTROPFELEKTRODE

M. HEYROVSKÝ

Polarographisches Institut, Tschechoslowakische Akademie der Wissenschaften, Prag

Eingegangen am 11. Januar 1962

Ketone bilden in alkalischem Milieu eine anodische polarographische Stufe, die der Bildung einer Organoquecksilberverbindung entspricht. Der zugehörige Strom ist durch die Geschwindigkeit der autokatalysierten chemischen Reaktion bestimmt, die der Durchtrittsreaktion vorgelagert ist. Auf Grund der Vorstellung, daß die Bildung der Enolform des Ketons der geschwindigkeitsbestimmende Schritt der Merkurierung ist, wurde die Enolisierungsgeschwindigkeit des Acetons aus den polarographischen Messungen berechnet. Sie stimmt größenordnungsgemäß mit den Literaturangaben überein, die aus Messungen der Halogenierungsgeschwindigkeit gewonnen wurden.

In Ketonen, die Wasserstoffatome in α-Stellung enthalten, lassen sich diese leicht durch Quecksilber ersetzen[1,2]. Die Ergebnisse der oszillopolarographischen Beobachtungen[3] haben gezeigt, daß diese Reaktion in alkalischem Milieu an der Quecksilbertropfelektrode abläuft. Aus Vorversuchen ging hervor, daß das polarographische Studium dieser Reaktion neue Erkenntnisse über den Mechanismus der Merkurierung bringen wird.

Experimenteller Teil

Die polarographischen Kurven wurden mit den Polarographen der Typen Zbrojovka V 301, Radiometer PO 4 und Yanagimoto PA-101 registriert. Als Umschalter diente die von Kalousek und Rálek[4] beschriebene Einrichtung. Die *i–t*-Kurven wurden mit dem von Němec und Smoler[5] entwickelten Gerät unter Verwendung eines Saitengalvanometers aufgenommen.

Die Kapillarelektrode besaß bei 100 cm Behälterhöhe die Ausflußgeschwindigkeit $m = 2{,}15 \cdot 10^{-3}$ g s^{-1} und ihre Tropfzeit betrug bei Kurzschluß der Tropfelektrode mit der gesättigten Kalomelelektrode $t_1 = 3{,}68$ s. Als stationäre Elektrode diente die von Vogel[6] beschriebene Elektrodentype, als vibrierende Platinelektrode die Elektrode nach Jenšovský[7].

Alle Messungen wurden in einem Kalousek-Gefäß mit gesättigter Kalomelelektrode durchgeführt. Die Lösungen haben wir durch einen Stickstoffstrom vom Sauerstoff befreit. Der dazu benutzte Stickstoff wurde dabei vorher durch eine Waschflasche mit einer Lösung geleitet, die die gleiche Ketonkonzentration wie die Untersuchungslösung enthielt. Die Messungen wurden bei der Temperatur von 22°C vorgenommen.

Die geprüften Ketone hatten wir durch Destillation gereinigt, das Aceton wurde zweimal aus Kaliumpermanganat destilliert. Die anorganischen Präparate waren von analytischer Reinheit.

Das merkurierte Aceton war nach Morton und Penner[8] dargestellt worden und in Form des

Nitrates oder Jodids isoliert. Das Nitrat ist in Aceton sehr gut löslich, den polarographischen Ergebnissen gemäß lösen sich in Wasser bei der Temperatur von 20°C etwa 1,5 g Substanz in 1 Liter und in Äthanol etwa 0,5 g im Liter.

Ergebnisse

Aceton liefert eine anodische polarographische Stufe mit Halbstufenpotential −0,23 V (ges. KE) (Abb. 1). Diese Stufe erscheint nur in alkalischen Lösungen und wächst mit steigender Hydroxydkonzentration (Abb. 2). Bei konstanter Kaliumhydroxydkonzentration hat die Abhängigkeit der Stufenhöhe von der Acetonkonzentration einen parabelförmigen Verlauf (Abb. 3). In 1M-KOH folgt diese Abhängigkeit in den Grenzen von 10^{-3} bis 10^{-2}M Aceton der Beziehung $i_l = [CH_3COCH_3]^2/_{60}$ A.

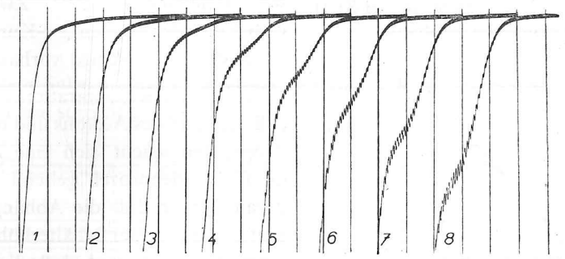

Abb. 1
Anodische Stufe bei wachsender Acetonkonzentration
1M-KOH; Acetonkonzentration: *1* 0; *2* 2 . 10^{-3}M; *3* 4 . 10^{-3}M; *4* 6 . 10^{-3}M; *5* 8 . 10^{-3}M; *6* 10 . . 10^{-3}M; *7* 12 . 10^{-3}M; *8* 14 . 10^{-3}M. Kurvenbeginn bei −0,4 V; 50 mV/Absz.; Empf. 1 : 20.

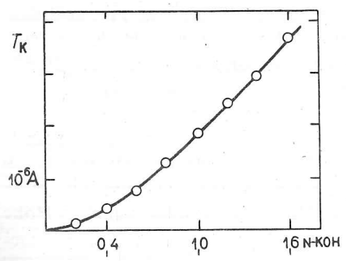

Abb. 2
Grenzstrom von 10^{-2}M Aceton in Abhängigkeit von der Kaliumhydroxydkonzentration

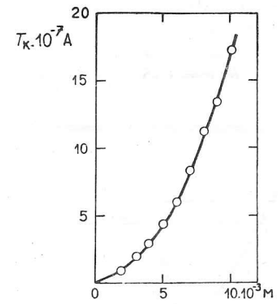

Abb. 3
Grenzstrom in Abhängigkeit von der Acetonkonzentration in 1M-KOH

Meßbare Stufen gewinnt man, wenn die Konzentration des Hydroxyds größer als 0,1M und die des Acetons größer als 10^{-3}M ist.

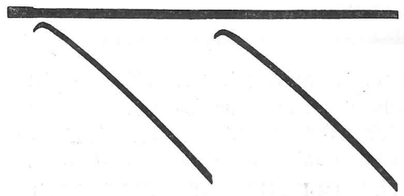

Abb. 4
Erste und zweite *i–t*-Kurve bei der Konzentration von 10^{-2}M Aceton in 1M-KOH am Grenzstrom registriert

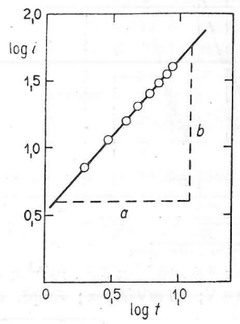

Abb. 5
Logarithmische Analyse der *i–t*-Kurven aus Abb. 4
$b : a = 1{,}15$.

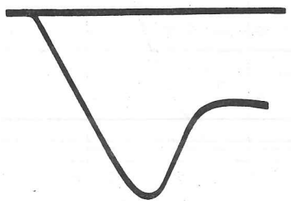

Abb. 6
i–t-Kurven bei der Konzentration von $8 \cdot 10^{-2}$M Aceton in 1M-KOH am Grenzstrom registriert

Der Anstieg der Stufenhöhe mit sinkender Quecksilbersäule zeugt von autokatasyliertem Charakter des Stromes. Im Einklang damit ist auch die Gestalt der bei dem Potential des Grenzstromes registrierten *i–t*-Kurven, die die Zeitabhängigkeit des momentanen Stromes ausdrücken (Abb. 4). Die Abhängigkeit des Logarithmus des momentanen Stromes vom Logarithmus der Zeit ist linear (Abb. 5) und entspricht der Beziehung $i \sim t^{1{,}15}$. Zwischen der ersten und der zweiten *i–t*-Kurve ist kein merklicher Unterschied vorhanden.

Bei höheren Konzentrationen der Hydroxylionen und des Acetons und bei längeren Tropfzeiten macht sich eine Adsorption im Elektrodenprozeß geltend. Das geht daraus hervor, daß die Abhängigkeit der Stufenhöhe von der Behälterhöhe ein Maximum durchläuft und daß die Stufe bei hohen Konzentrationen mit abnehmender Quecksilbersäule sinkt. Auch die Gestalt der *i–t*-Kurven erweist, daß der ursprüngliche autokatalytische Prozeß durch Adsorption gehemmt ist (Abb. 6).

Die Höhe der anodischen Stufe des Acetons wächst beträchtlich mit der Temperatur; bei 25°C haben wir für den Grenzstrom den Temperaturkoeffizienten $(\mathrm{d}\bar{i}_l/\mathrm{d}T \,.\, 1/\bar{i}_l)_{25°} = 6{,}8\ \mathrm{grad}^{-1}$ gefunden.

Gelatine erniedrigt die Acetonstufe dermaßen, daß bei $4 \cdot 10^{-2}$M Aceton schon 10^{-2}% Gelatine genügen, um die Stufe auf die Hälfte ihrer ursprünglichen Höhe zu unterdrücken (Abb. 7). Durch den Gelatinezusatz verliert der Strom seinen autokatalytischen Charakter, wie aus der Höhenabhängigkeit und aus den *i–t*-Kurven hervorgeht.

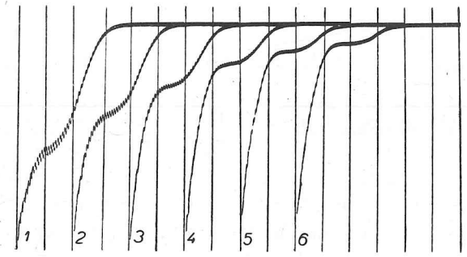

Abb. 7
Einfluß von Gelatine auf die anodische Stufe des Acetons
Lösung von $4 \cdot 10^{-2}$M Aceton in 1M-KOH; Gelatinekonzentration: *1* 0; *2* $0{,}5 \cdot 10^{-2}$%; *3* $1{,}0 \cdot 10^{-2}$%; *4* $1{,}5 \cdot 10^{-2}$%; *5* $2{,}0 \cdot 10^{-2}$%; *6* $2{,}5 \cdot 10^{-2}$%. 50 mV/Absz., Empf. 1 : 150, Kurvenbeginn bei −0,4 V.

Verschiedene Salze üben eine spezifische Wirkung auf den Grenzstrom des Acetons aus (Abb. 8); am stärksten wird die Stufe durch Kaliumbromid herabgesetzt, weniger durch Kaliumchlorid und -nitrat; Phosphat und Sulfat erhöhen umgekehrt die Stufe. Durch die Gegenwart von Äthanol in der Lösung wird die Höhe des Grenzstromes vermindert.

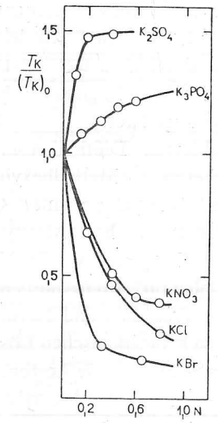

Abb. 8
Einfluß von Anionen auf den Grenzstrom des Acetons, ausgedrückt durch das Verhältnis der Stufenhöhe in 1M-KOH-Lösung mit dem betreffenden Salz zur Stufenhöhe in reinem 1M-KOH

Die mit dem Kalousek-Umschalter gewonnenen Ergebnisse zeigen, daß das beim

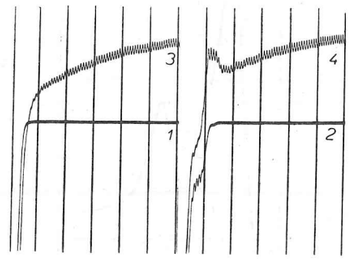

Abb. 9
Anodische Stufe des Acetons mit dem Kalousek-Umschalter
Kurve *1* 1M-KOH; *2* $4 \cdot 10^{-2}$M Aceton in 1M-KOH; *3* 1M-KOH, umgeschaltete Kurve, $E_{\mathrm{Hilfs.}} = -0{,}14$ V; *4* $4 \cdot 10^{-2}$M Aceton in 1M-KOH, umgeschaltete Kurve, $E_{\mathrm{Hilfs.}} = -0{,}14$ V; $f = 25$ Hz; 200 mV / Absz., Empf.: 1 : 100.

Potential der anodischen Stufe entstandene Produkt reversibel an der Elektrode reduziert wird. Bei höheren Umschaltfrequenzen (etwa von 20 Hz an) bildet sich am Anfang des kathodischen Teiles der umgeschalteten Stufe ein kleines Maximum (Abb. 9).

Auch die Versuche mit der stationären Tropfenelektrode führen zu den gleichen Schlüssen über die Reversibilität der anodischen Reaktion. Der anodische Strom, der der Bildung des Oxydationsproduktes entspricht, geht kontinuierlich in eine der Reduktion dieses Produktes angehörende kathodische Strompitze mit dem Maximum bei −0,30 V (ges. KE) über, die von einer kleinen Stromspitze beim Potential −0,47 V gefolgt wird (Abb. 10). Beläßt man die stationäre Elektrode 1 – 2 min auf dem Potential der Bildung des Oxydationsproduktes und bringt sie dann nach 1 – 5 minutiger Unterbrechung der Polarisation auf negativere Potentiale, so verschiebt sich das gegenseitige Höhenverhältnis der ersten und zweiten Stromspitze zugunsten der zweiten, und zwar ungefähr von 3 : 1 auf 7 : 10, wobei beide Stromspitzen bei denselben Potentialen bleiben. Bei höherer Acetonkonzentration (0,3M in 1M-KOH) oder in Gegenwart organischer Lösungsmittel bleibt die zweite Stromspitze auf der Kurve aus. Aus diesem Verhalten und aus der festgestellten Tatsache, daß das Produkt der anodischen Reaktion an der Elektrode adsorbiert wird, kann geschlossen werden, daß die zweite kathodische Stromspitze der Reduktion des anodisch gebildeten Depolarisators angehört, der im adsorbierten Zustand vorliegt. Diese Vorstellung ist im Einklang mit der Deutung der Adsorptionsstufen in der klassischen Polarographie.

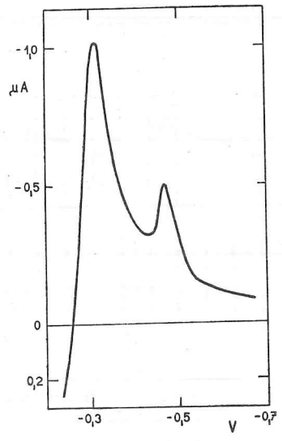

Abb. 10
Polarographische Kurve des Acetons mit dem hängenden Quecksilbertropfen
1M-NaOH, 0,1M Aceton; Geschwindigkeit der Polarisationsveränderung −400 mV/min.

Die mit der vibrierenden Platinelektrode in Laugelösungen erhaltenen Polarisationskurven wiesen nach der Zugabe von Aceton keine Veränderungen auf.

Methyläthylketon, Diäthylketon, Methylisopropylketon, Methylhexylketon, Methylnonylketon, Cyclopentanon, Cyclohexanon, Diacetonalkohol, Mesityloxyd, Acetophenon, Phenylaceton, Propiophenon, Butyrophenon, Brenztraubensäure, Phenylbrenztraubensäure und Lävulinsäure verhalten sich in alkalischen Lösungen polarographisch analog wie Aceton. Benzaldehyd, Benzophenon, Phenylglyoxalsäure, Malonsäure, Äthylacetat, Acetonitril und Phenylisopropylketon lieferten keine anodische Stufe in alkalischer Lösung. Harnstoff, Acetamid und Urethan bilden eine anodische Stufe mit abweichenden Eigenschaften.

Diskussion

Die beschriebenen Versuche haben zur Vermutung geführt, daß das Quecksilber bei dem Potential der anodischen Stufe in Lösung geht und eine Organoquecksilberverbindung mit dem Keton bildet. Diese Vermutung wird auch durch den Versuch unterstützt, in welchem wir chemisch dargestelltes merkuriertes Aceton von der Zusammensetzung $CH_3COCH_2HgNO_3$ der alkalischen Acetonlösung zugesetzt haben. Auf der polarographischen Kurve (Abb. 11) erschien eine einzige anodisch–kathodische Stufe; ihr anodischer Teil entspricht der autokatalysierten Bildung des merkurierten Acetons und ihr kathodischer Teil dem Strom, der durch die Diffusion dieses Stoffes aus der Lösung zur Elektrode gegeben ist.

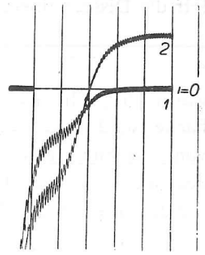

Abb. 11
Einfluß des merkurierten Acetons auf die Stufe der Merkurierung des Acetons
Kurve *1* 5 ml 10^{-2}M Aceton in 1M-KOH; Kurve *2* nach Zusatz von 0,1 ml gesättigter Acetonylmerkurinitrat-Lösung. Kurvenbeginn bei −0,4 V. 50 mV/Absz., Empf. 1 : 30.

Über den Mechanismus der Merkurierung wird angenommen, daß das Quecksilber, ähnlich wie das Brom bei der Bromierung, mit der Enolform des Ketons reagiert[1,2]. Vollzieht sich die eigentliche Reaktion des Enols mit dem Quecksilber genügend schnell, so ist die Gesamtgeschwindigkeit der Merkurierung durch die Enolisierungsgeschwindigkeit bestimmt. In unserem Fall, in welchem es sich unseren Vorstellungen nach um die Reaktion des Enolat-Anions mit dem Quecksilber-Kation im alkalischen Milieu handelt, können wir die Geschwindigkeit der sauren Dissoziation des Ketons als den Prozeß betrachten, der den anodischen Strom bestimmt. Der autokatalytische Charakter des Stromes ist wahrscheinlich darauf zurückzuführen, daß die Dissoziationsgeschwindigkeit des Ketons durch die katalytische Wirkung des eigentlichen Reaktionsproduktes, des merkurierten Acetons, erhöht wird. Dieses Katalysationsvermögen tritt deutlich zutage, wenn man der alkalischen Acetonlösung chemisch dargestelltes merkuriertes Aceton zugibt (Abb. 11): bei 10^{-4} molarer Konzentration des zugesetzten Produktes wächst die anodische Stufe von 10^{-2}M Aceton in 1M-KOH etwa um 100% an; eine weitere Konzentrationserhöhung hat keine Veränderung der Stufenhöhe mehr zur Folge.

Wir nehmen an, daß die Merkurierung an der Quecksilbertropfelektrode über die nachstehende Reaktionsfolge abläuft:

$$CH_3COCH_3 + OH^- \rightleftharpoons CH_3COCH_2^- + H_2O \qquad (1)$$

$$Hg - 2e \rightleftharpoons Hg^{2+} \qquad (2)$$

$$CH_3COCH_2^- + Hg^{2+} \rightleftharpoons CH_3COCH_2Hg^+ \qquad (3)$$

$$CH_3COCH_2Hg^+ + OH^- \rightleftharpoons CH_3COCH_2HgOH \qquad (4)$$

Der Strom ist durch die Reaktion (*1*) bestimmt, die der Durchtrittsreaktion (*2*) vorgelagert ist; die Reaktion (*3*) halten wir für sehr schnell.

Bei konstanter Hydroxylionenkonzentration, die hundert- bis tausendmal höher ist als die Acetonkonzentration, folgt die Dissoziation praktisch der Gleichung für Reaktionen erster Ordnung, und wir können anstelle der Gleichung (*1*) formal schreiben:

$$CH_3COCH_3 \underset{k_{-1}}{\overset{k_1}{\rightleftharpoons}} CH_3COCH_2^- . \qquad (5)$$

Für die Dissoziationsgeschwindigkeitskonstante k_1 gilt hier

$$k_1 = k_1'[OH^-] + k_1''[OH^-][M]_0 , \qquad (6)$$

worin $[M]_0$ die Konzentration des Reaktionsproduktes an der Elektrodenoberfläche ist, d. h. des merkurierten Acetons. Das zweite Glied auf der rechten Seite von Gleichung (*6*) drückt also den autokatalytischen Charakter der Merkurierung des Acetons an der Quecksilbertropfelektrode aus. Das Konzentrationsverhältnis der dissoziierten und der nicht dissoziierten Form bezeichnen wir mit K:

$$K = k_1/k_{-1} = [CH_3COCH_2^-]/[CH_3COCH_3] . \qquad (7)$$

In dieser Formulierung stellt die Merkurierung des Acetons vom polarographischen Gesichtspunkt einen völlig analogen Fall wie die Reduktion des Formaldehyds in ungepuffertem Milieu dar, der von Brdička[9] und Koutecký[10] gelöst worden ist. Daß dieser Vergleich berechtigt ist, geht daraus hervor, daß bei niedrigeren Acetonkonzentrationen und kürzeren Tropfzeiten (wenn keine Adsorption zur Geltung kommt) der Grenzstrom des Acetons mit dem Quadrat der Konzentration wächst, wie es beim Formaldehyd der Fall ist[10]. Der momentane Strom ist beim Formaldehyd[10] proportional $t^{7/6}$, d. h. $t^{1,17}$; beim Aceton wurde experimentell der Exponent 1,15 gefunden.

Nach der Näherungslösung[9] gilt für die mittleren polarographischen Grenzströme der Merkurierung des Acetons, $\bar{i}_k$, die Beziehung:

$$[\bar{i}_k/(\bar{i}_d - \bar{i}_k)]^2 = 0{,}661K \,.\, t \,.\, [OH^-]\,(k_1' + k_1''[CH_3COCH_3] \,.\, \bar{i}_k/\bar{i}_d \,.\, \sqrt{D_A/D_M}) . \quad (8)$$

$\bar{i}_d$ ist der hypothetische Diffusionsgrenzstrom des Acetons, t_1 die Tropfzeit, D_A der Diffusionskoeffizient des Acetons und D_M der Diffusionskoeffizient des merkurierten Acetons. Stellen wir $[\bar{i}_k/(\bar{i}_d - \bar{i}_k)]^2$ in Abhängigkeit vom Produkt $[CH_3COCH_3] \,.\, \bar{i}_k/\bar{i}_d$ für verschiedene Acetonkonzentrationen graphisch dar, so erhalten wir eine Gerade (Abb. 12), deren Neigung sich mit der Hydroxylionenkonzentration ändert.

Im Konzentrationsbereich von 10^{-3} bis 10^{-2}M Aceton in 1M-KOH entspricht den experimentellen Werten eine Gerade (Abb. 12), die die Gleichung erfüllt:

$$[\bar{i}_k/(\bar{i}_d - \bar{i}_k)]^2 = 8 \,.\, 10^{-6} + 1{,}72[CH_3COCH_3] \,.\, \bar{i}_k/\bar{i}_d . \qquad (8a)$$

Aus den Gleichungen (*8*) und (*8a*) können wir nach Einsetzen der bekannten Werte die unbekannten Größen berechnen. Beim Einsetzen in Gleichung (*8*) haben wir in Analogie zu strukturverwandten Verbindungen für Aceton schätzungsweise den Diffusionskoeffizienten $D_A = 1{,}1 \,.\, 10^{-5}\ cm^2\ s^{-1}$ und für das merkurierte Aceton $D_M = 0{,}85 \,.\, 10^{-5}\ cm^2\ s^{-1}$ gewählt. Beim Potential des Grenzstromes des Acetons in 1M-KOH und bei der Behälterhöhe von 140 cm betrug die Tropfzeit $t_1 = 2{,}8$ s, die Ausflußgeschwindigkeit bei der gegebenen Höhe $m = 3{,}0 \,.\, 10^{-3}\ g\ s^{-1}$. Bei unseren experimentellen Bedingungen war der hypothetische Diffusionsstrom nach der Ilkovič-Gleichung durch die Beziehung $\bar{i}_d = 0{,}96 \,.\, 10^{-3}[CH_3COCH_3]$ A gegeben. Für die durch das Verhältnis

$$[CH_3COCH_2^-]\,[H_3O^+]/[H_2O]\,[CH_3COCH_3]$$

definierte saure Dissoziationskonstante der Ketoform des Acetons gibt Bell[11] bei der Temperatur von 25°C den Wert 10^{-20} an. Für unsere Konstante K ergibt sich hieraus

$$K = [CH_3COCH_2^-]/[CH_3COCH_3] = \\ = 10^{-20} \,.\, [H_2O]/[H_3O^+] = 55 \,.\, 10^{-6} \,.\, [OH^-].$$

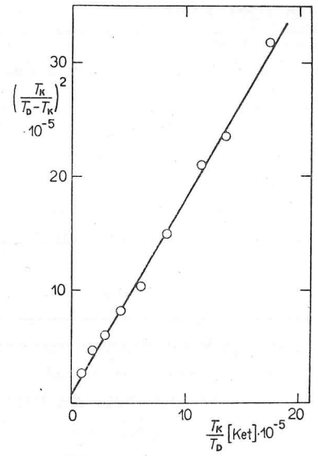

Abb. 12
Graphische Darstellung der Beziehung (*8*) für $2 \,.\, 10^{-3}$ bis 10^{-2}M Aceton in 1M-KOH

Aus den Gleichungen (*8*) und (*8a*) erhalten wir nach Einsetzen für k_1' bei 1M-KOH:

$$k_1' = 8 \,.\, 10^{-6}/0{,}661Kt_1[OH^-] = 7{,}8 \,.\, 10^{-2}\ s^{-1}\ l\ mol^{-1} = 4{,}7\ min^{-1}\ l\ mol^{-1} .$$

Die Konstante k_1' sollte von der Laugekonzentration unabhängig sein. Zur Kontrolle haben wir die Messung noch in 0,8M-KOH durchgeführt, wobei die durch die Experimentalpunkte durchgelegte Gerade der Gleichung entsprach:

$$[\bar{i}_k/(\bar{i}_d - \bar{i}_k)]^2 = 5 \,.\, 10^{-6} + 1{,}40 \,.\, [CH_3COCH_3] \,.\, \bar{i}_k/\bar{i}_d . \qquad (8b)$$

Durch den gleichen Vorgang haben wir aus diesem Versuch für k_1' den Wert 7,6 . $10^{-2}\ s^{-1}\ l\ mol^{-1}$ erhalten, der mit dem Ergebnis in 1M-KOH gut übereinstimmt. Für die gleiche Konstante bei der Temperatur von 25°C geben Dawson und Spivey[12] den Wert $7\ min^{-1}\ l\ mol^{-1}$ und Bell und Lidwell[13] den Wert $15\ min^{-1}\ l\ mol^{-1}$ an; beide Werte wurden aus Messungen der Jodierungsgeschwindigkeit des Acetons gewonnen.

Den Wert der katalytischen Konstante k_1'' für 1M-KOH erhalten wir aus dem zweiten Glied der Gleichung (*8a*):

$$k_1'' = 1{,}72/0{,}661 \,.\, K \,.\, t_1 \,.\, [OH^-] \,.\, \sqrt{D_A/D_M} = 1{,}7 \,.\, 10^4/1{,}13 =$$
$$= 1{,}5 \,.\, 10^4 \, s^{-1} \, l^2 \, mol^{-2} \,.$$

Die Konstante k_1'' läßt sich auch durch Vergleich der oben angeführten empirisch gefundenen Beziehung mit dem theoretischen Näherungsausdruck für die Konzentrationsabhängigkeit des Grenzstromes berechnen. Auf diesem Weg ergibt sich für 1M-KOH $k_1'' = 1{,}45 \,.\, 10^4 \, s^{-1} \, l^2 \, mol^{-2}$.

In 0,8M KOH-Lösung ist der für die Konstante k_1'' gefundene Wert etwas größer, und zwar $1{,}95 \,.\, 10^4 \, s^{-1} \, l^2 \, mol^{-2}$. Diese Unstimmigkeit läßt sich wahrscheinlich dadurch erklären, daß die katalytische Aktivität des merkurierten Acetons bei höheren Laugekonzentrationen geringer ist. Derselben Ursache kann auch der ungewöhnliche Verlauf der Abhängigkeit der Stufenhöhe von der Laugekonzentration zugeschrieben werden (Abb. 2).

Die Erscheinung, daß die polarographische Stufe nur bis zu einem bestimmten Grenzwert mit der Zugabe des merkurierten Acetons wächst, läßt sich dadurch erklären, daß die Adsorption des Reaktionsproduktes an der Elektrodenoberfläche bei der großen Geschwindigkeit der gesamten Reaktion zu stören beginnt. Die gleiche Erscheinung tritt bei höheren Aceton- oder Laugekonzentrationen ein. Daß Organoquecksilberverbindungen leicht adsorbiert werden, ist schon aus der klassischen Polarographie bekannt[14].

Der resultierende Wert für die Dissoziationsgeschwindigkeitskonstante des Acetons zeigt, daß die Dicke der Reaktionsschicht an der Elektrode die Moleküldimensionen genügend übersteigt, so daß es berechtigt war, für die der Durchtrittsreaktion vorgelagerte chemische Reaktion die Beziehungen aus der homogenen Reaktionskinetik zu benutzen.

Pedersen[15,16] hat festgestellt, daß die saure Dissoziation des Ketons durch Schwermetall-Ionen katalysiert wird. Es scheint, daß bei den Quecksilber-Ionen ein analoger Fall vorliegt; nach den polarographischen Ergebnissen wirkt wahrscheinlich der zwischen den Quecksilber-Ionen und dem Anion der Enolform des Ketons ausgebildete Komplex katalytisch. Aus den bisherigen Resultaten lassen sich allerdings noch keine Schlüsse über den eingehenden Mechanismus der Katalyse ziehen; der Einfluß des Anions auf die Stufenhöhe deutet darauf hin, daß die katalytische Aktivität in beträchtlichem Maß von der Zusammensetzung des Komplexes abhängt.

Das Strommaximum auf der umgeschalteten Kurve erscheint im Potentialgebiet, in welchem die anodische Stufe der normalen Kurve beginnt, also bei Potentialen, bei denen die rückläufige Reaktion noch zur Geltung kommt (es handelt sich um eine reversible Stufe). In diesem Gebiet wird während beider Umschaltphasen eine gewisse Menge des katalytisch hoch wirksamen komplexen Kations an der Elektrodenoberfläche erneuert und so die Depolarisatormenge erhöht. Bei negativeren Potentialen, bei denen die Rückreaktion bereits nicht mehr verläuft, werden in der „Arbeitsphase" des Umschaltens sämtliche Kationen an der Elektrodenoberfläche reduziert, dadurch nimmt der Katalysator wesentlich ab und der resultierende Strom sinkt. Bei niedrigeren Frequenzen wird das Kation nicht so häufig an der Elektrodenoberfläche erneuert und seine Aktivität durch die Adsorption vermindert weshalb kein Maximum entsteht.

Die übrigen Ketone unterliegen in ähnlicher Weise wie Aceton an der Tropfelektrode der Dissoziation und Merkurierung. Ketone, die keinen sauren Wasserstoff enthalten, liefern keine polarographische Reaktion. Phenylisopropylketon ist wahrscheinlich aus sterischen Gründen polarographisch inaktiv.

Dr. O. Exner spreche ich für die Darstellung und die Zurverfügungstellung des merkurierten Acetons und zahlreicher Ketone sowie für die wertvollen Diskussionen meinen aufrichtigen Dank aus und ebenso auch Dr. P. Zuman für die Überlassung einiger Präparate und die Hinweise zu dieser Arbeit.

Fräulein V. Skálová danke ich für die Anfertigung der Abbildungen.

Literatur

1. Rochow E. G., Hurd D. T., Lewis R. N.: *The Chemistry of Organometallic Compounds*, S. 112. Wiley, New York 1957.
2. Sidgwick N. V.: *The Chemical Elements and their Compounds*, S. 302. Oxford Univ. Press, 1950.
3. Heyrovský M.: Chem. zvesti *16*, 338 (1962).
4. Kalousek M., Rálek M.: diese Zeitschrift *19*, 1099 (1954); Chem. listy *48*, 808 (1954).
5. Němec L., Smoler I.: Chem. listy *51*, 1958 (1957).
6. Říha J. im Buche: *Progress in Polarography*, Bd. 2, S. 383. Interscience, New York 1961.
7. Jenšovský L.: Chem. Tech. (Berlin) *8*, 360 (1956).
8. Morton A. A., Penner M. P.: J. Am. Chem. Soc. *73*, 3300 (1951).
9. Brdička R.: diese Zeitschrift *20*, 387 (1955); Chem. listy *48*, 1458 (1954).
10. Koutecký J.: diese Zeitschrift *21*, 652 (1956); Chem. listy *49*, 1621 (1955).
11. Bell R. P.: Trans. Faraday Soc. *39*, 253 (1943).
12. Dawson H. M., Spivey E.: J. Chem. Soc. *1930*, 2180.
13. Bell R. P., Lidwell O. M.: Proc. Roy. Soc. (London) *176*, 88 (1940).
14. Benesch R. E., Benesch R.: J. Phys. Chem. *56*, 648 (1952).
15. Pedersen K. J.: Acta Chem. Scand. *2*, 252 (1948).
16. Pedersen K. J.: Acta Chem. Scand. *2*, 385 (1948).

Übersetzt von H. Bažantová.

Резюме

М. Гейровский: *Меркурирование кетонов на ртутном капельном электроде.* Кетоны дают в щелочной среде анодную полярографическую волну, соответствующую образованию ртутноорганического соединения. Соответствующий ток управляется скоростью автокатализированной химической реакции, предшествующей собственно электродному процессу. На основании представления, что реакцией, определяющей скорость меркурирования, является образование энольной формы кетона, из полярографических измерений рассчитана константа скорости энолизации ацетона, значение которой хорошо совпадает со значениями, приведенными в литературе и рассчитанными на основании измерения скорости галоидирования.

EFFECT OF ANTIOXIDANTS ON OXIDATION OF METHYL OLEATE

M. H. Chahine, F. A. El-Shobaki and M. Heyrovský

UNIVERSITY
LIBRARY
CAMBRIDGE

Collection of Czechoslovak Chemical Communications. Vol. 27 (1962). — Published under the auspices of the Czechoslovak Academy of Science by the Publishing House of the Czechoslovak Acad. Sci., Vodičkova 40, Prague 1. — Address of the Editor: Institute of Organic Chemistry and Biochemistry, Czechoslovak Academy of Science, Na cvičišti 2 Prague 6. — Annual subscription Kčs 300.—, US $ 30.20, £ 10/15/8, single issue Kčs 25.—. Subscription orders should be addressed to ARTIA, 30 Ve smečkách, Prague 1, Czechoslovakia. — Printed by Knihtisk 05, Prague.

Rozšiřuje Poštovní novinová služba, objednávky a předplatné přijímá Poštovní novinový úřad — ústřední administrace PNS, Jindřišská 14, Praha 1. Lze také objednat u každého poštovního úřadu nebo doručovatele.

Reprinted from Collection Czechoslov. Chem. Commun. *27*, 2216—2219 (1962)

EFFECT OF ANTIOXIDANTS ON OXIDATION OF METHYL OLEATE

M. H. Chahine, F. A. El-Shobaki and M. Heyrovský

Fats and Oils Unit, National Research Centre, Cairo, UAR and Polarographic Institute, Czechoslovak Academy of Science, Prague

Received January 12th, 1962

It has been shown by Kuta and Quackenbush[1] on their polarographic investigations and chemical peroxide value measurements that the presence of antioxidants introduced a lag phase in oxidation of lard without changing qualitatively the types of the present oxidation products. We have used the same methods to compare the protecting ability of various antioxidants on oxidation of methyl oleate, at 63° and 100°C.

Experimental

Materials

Methyl oleate was prepared by esterifying pure oleic acid (Merck) with methanol in presence of sulfuric acid[2]. The acid free, dry ester was subjected to fractional distillation under vacuum. The fraction which boiled at 166·8°/2 mm was collected (iodine number 85·4) and was stored in a refrigerator.

The *antioxidants* 3,5-di-t-butyl-4-hydroxytoluene, butylated hydroxyanisole (mixture of 3-t-butyl-4-hydroxyanisole and 2-t-butyl-4-hydroxyanisole) and propyl gallate were supplied by Eastman, Kingsport, Tenn., USA. Mixed tocopherols (concentrate containing mainly α and γ tocopherols in equal proportions in addition to small amounts of β and δ forms) were manufactured by Distillation Products Industries, Rochester, N. Y., USA. Gossypol was prepared from butanone extracts of cottenseed, as described by King and Thurber[3] and purified by crystallization from diethylether and xylene. Crystalline gossypol melted at 184°C. For $C_{30}H_{30}O_8$ (518·0) calculated 69·42% C, 6·05% H; found 69·48% C, 5·83% H. Dianilinogossypol was prepared as described by Clark[4]. After repeated crystallization from benzene, free of thiphene, it melted at 302°C. For $C_{42}H_{40}N_2O_6$ (668·1) calculated 75·11% C, 6·32% H, 4·32% N; found 75·40% C, 6·00% H, 4·20% N.

Kinetic Measurements

Each of the tested antioxidants was incorporated at a concentration of 0·05% in 70 g of peroxide free methyl oleate by the aid of 10 ml of anhydrous diethyl ether; in case of dianilinogossypol chloroform was used[5].

The test tubes containing the examined ester were immersed in a thermostated paraffine oil bath. The oxidation reaction was conducted by bubbling oxygen at a constant rate through the reaction mixture. In the experiment performed at 100°C which lasted 165 hours a 2 ml sample was withdrawn every three hours from each test tube. At 63°C a 1 ml sample was being taken twice a day for about 900 hours.

Analytical Method

The peroxide value, expressed in milliequivalents per kilogram, was determined as follows[6]. A weighed sample (0·2 g) was placed in a stoppered flask, flushed with carbon dioxide, and dissolved in 25 ml of a mixture of chloroform–acetic acid (2 : 3). After swirling for two minutes 1 ml of freshy prepared saturated potassium iodide solution was added. After five minutes 75 ml of distilled water were added and the liberated iodine was immediately titrated with 0·01N-$Na_2S_2O_3$.

The polarographic procedure was essentially that described by Kuta and Quackenbush[1]. Polarograms of samples of oxidized methyl oleate were obtained using a 0·3M solution of LiCl in a methanol–benzene mixture (1 : 1). Conducting the analyses at 63°C we had to incorporate 0·01% ethylhydroxycellulose into the solution in order to suppress maxima; after recording the polarographic curve of the deaerated 5 ml of blank solution 0·095 g of sample was added, dissolved on stirring by passing a stream of nitrogen through the cell, and the polarographic curve was taken. At 100°C no maximum suppressor was necessary, and 0·19 g of sample were taken. The polarograms were obtained on a Radiometer polarograph PO 3.

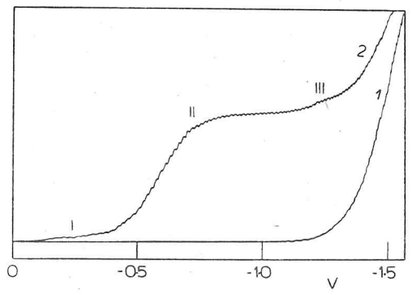

Fig. 1
Polarographic Curve of Oxidised Methyl Oleate
1 5 ml of blank solution, *2* added 0·095 g of sample containing mixed tocopherols after 241 hours of oxidation. From $E = 0$, sens. = 1 : 5000.

Results und Discussion

The polarographic curves of autoxidized methyl oleate are of the type shown on Fig. 1. The reduction wave I, which appears from the beginning of oxidation together with the wave II (comp. Fig. 1), but reaches only about 10% height of it, belongs probably to peroxidic com-

pounds[7,8]. Wave II, most prominent during the whole process, is due to the prevailing primary oxidation product, a mixture of the isomers of methyl hydroperoxide oleate[7,9,10]. The height of this wave was followed and was found to show the same general trend as the peroxide values. After the maximum of peroxide values was reached, there appeared on the polarographic curve a third wave III, indicating presence of further oxidation products in the mixture, probably of unsaturated aldehydes[7]. The shape of polarographic curves in pure oxidized methyl oleate does not differ from those obtained in presence of any of the antioxidants examined, which confirms[1] that no one of the antioxidants changes the mechanism of oxidation.

The course of oxidation is represented on Fig. 2 and 3 showing the simultaneous changes of peroxide value and of the height of hydroperoxidic wave during the time of oxidation.

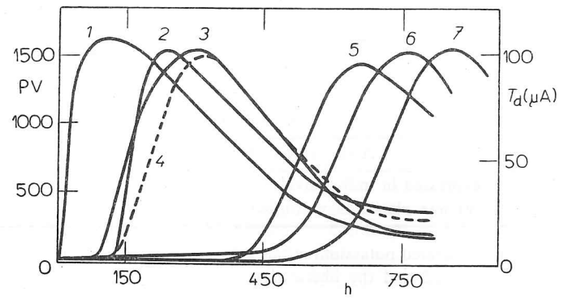

Fig. 2
Peroxidic Values (P. V.) and Heights of Polarographic Hydroperoxide Wave during Oxidation at 63°C
1 Pure methyl oleate, *2* methyloleate and gossypol, *3* methyl oleate and mixed tocopherols, *4* methyl oleate and dianilinogossypol, *5* methyl oleate and propylgallate, *6* methyl oleate and butylated hydroxyanisole, *7* methyl oleate and 3,5-di-t-butyl-4-hydroxytoluene.

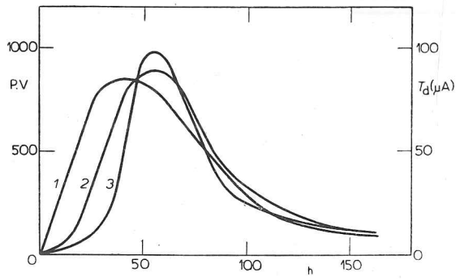

Fig. 3
Peroxidic Values (P. V.) and Heights of Polarographic Hydroperoxide Wave during Oxidation at 100°C
1 Pure methyl oleate, *2* methyl oleate and propylgallate, *3* methyl oleate and butylated hydroxyanisole.

At 63°C (Fig. 2) there is a considerable difference in the induction periods of the pure methyl oleate and methyl oleate with antioxidants, and moreover various antioxidants increase the induction period in various extent. The difference between the two groups of curves with antioxidants of higher (2—4) and lower (5—7) molecular weight could be accounted for by the difference in molar concentrations; the same weight of antioxidants being taken the ligher ones are more concentrated, and hence more effective in removing free radicals. But within these groups of curves the cause of the differences has to be sought in the specific activity of each antioxidant.

At 100°C (Fig. 3) the peroxide curves do not differ much from each other. Even here the shortest induction period appears with antioxidants of higher molecular weight, but the differences are small. This might be explained by the high rate of destruction of antioxidants at 100°C as well as by the fact, that a higher temperatures other oxidation mechanisms have to be taken into consideration (as direct reaction of oxygen with the double bound[11]), where the antioxidants play no role.

References

1. Kuta E. J., Quackenbush F. W.: J. Am. Oil Chemists' Soc. *37*, 148 (1960).
2. Hilditch T. P.: *The Chemical Constitution of Natural Fats*. Chapman & Hall, London 1947.
3. King W. H., Thurber F. H.: J. Am. Oil Chemists' Soc. *30*, 70 (1953).
4. Clark E. P.: J. Biol. Chem. *76*, 229 (1928).
5. King W. H., Thurber F. H.: J. Am. Oil Chemists' Soc. *33*, 169 (1956).
6. Tollenaar F. D.: *Central Institute for Nutrition Research T. N. O., Utrecht, Report No. R 307 E.*
7. Willits C. O., Ricciuti C., Knight H. B., Swern D.: Anal. Chem. *24*, 785 (1952).
8. Swern D., Coleman J. E., Knight H. B., Ricciuti C., Willits C. O., Eddy C. R.: J. Am. Chem. Soc. *75*, 3135 (1953).
9. Willits C. O., Ricciuti C., Ogg C. L., Morris S. G., Riemenschneider R. W.: J. Am. Oil Chemists' Soc. *30*, 420 (1953).
10. Swift C. E., Dollear F. G., O'Connor R. T.: Oil & Soap *23*, 355 (1946).
11. Gunstone F. D., Hilditch T. P.: J. Chem. Soc. *1945*, 836.

Резюме

М. Г. Чахин, Ф. А. Эл-Шобаки и М. Гейровский: *Влияние антиоксидантов на окисление метилового эфира олеиновой кислоты.* Авторами изучена противоокислительная способность различных антиоксидантов по отношению к метиловому эфиру олеиновой кислоты при 63 и 100°C.

CHEMICKÉ ZVESTI

SLOVENSKEJ AKADÉMIE VIED

SEPARÁTNY VÝTLAČOK

VYDAVATEĽSTVO
SLOVENSKEJ AKADÉMIE VIED
BRATISLAVA

Organische Elektrochemie, Dresden 1942, 227. — 10. Heyrovský J., Kalvoda R., *Oszillographische Polarographie*, Berlin 1960, 87.

11. Kalvoda R., Macků J., Micka K., Z. phys. Chem. (Leipzig) Sonderheft 66 (1958). — 12. Vogel J., bisher nicht veröffentlicht. — 13. Kalvoda R., Macků J., Collection *21*, 493 (1956); Chem. listy *49*, 1565 (1955). — 14. Benesch R., Benesch R. E., J. Am. Chem. Soc. *73*, 3391 (1951). — 15. Vojíř V., Collection *16—17*, 488 (1951—1952); Chem. listy *46*, 129 (1952). — 16. Rice F. O., Evering B. L., J. Am. Chem. Soc. *56*, 2105 (1934).

Dr. Robert Kalvoda, Praha 1, Vlašská 9, Polarografický ústav ČSAV.

Diskussionsbeiträge

J. Dévay fügt zu, dass man vielleicht durch die Erhöhung der Wechselstromfrequenz die Bildungsgeschwindigkeit des Artefaktes feststellen könnte.

OSZILLOPOLAROGRAPHISCHES VERHALTEN DER KETONE IN ALKALISCHEN LÖSUNGEN

MICHAEL HEYROVSKÝ

Polarographisches Institut an der Tschechoslowakischen Akademie der Wissenschaften in Praha

Ketony mající na α-uhlíku vodíkové atomy vykazují v roztocích alkalických louhů na křivce $dE/dt = f_1(E)$ katodický zářez o hodnotě Q 0,2.

Bei der Polarisation der Quecksilbertropfelektrode mittels Wechselstrom in Lösungen alkalischer Hydroxyde weisen die rein aliphatischen gesättigten Ketone in Konzentrationen der Ordnung 10^{-4} M, je nach ihrer Adsorptivität, nur Kapazitätseffekte auf. Der an die Ketogruppe gebundene aromatische Kern bringt in die oszillopolarographische Ableitungskurve zu den Kapazitätseinschnitten noch elektrolytische Einschnitte zu [1].

Falls die Konzentrationen der Ketone auf 10^{-3} M bis 10^{-1} M erhöht werden, entsteht auf der Ableitungskurve ein neuer Einschnitt. Dieser wurde von J. Heyrovský [2] bei Aceton beobachtet. Da dieses Verhalten für alle Ketoverbindungen, die in α-Stellung zur CO-Gruppe Wasserstoffatome enthalten, charakteristisch ist, wurde die Reaktion näher untersucht.

Experimenteller Teil

Oszillopolarographische Messungen wurden mit dem Polaroskop P 576 und mit einem universalen polarographischen Oszillographen P-4F durchgeführt. Als polarisierbare Elektrode wurde die tropfende und strömende Quecksilberelektrode und der hängende Quecksilbertropfen nach J. Vogel verwendet. Zur Verfolgung der polarographischen Kurven diente der Polarograph V 301 und der Polarograph Yanagimoto PA 101.

Als Grundelektrolyt wurden wässrige und wässrig-äthanolische Lösungen von KOH und NaOH der Reinheit p. a benutzt. Die Ketoverbindungen wurden durch Destillation gereinigt; Aceton zweimal mit Kaliumpermanganat destilliert.

Ergebnisse und Diskussion

Aceton bildet auf der $dE/dt = f_1(E)$-Kurve einen irreversiblen kathodischen Einschnitt von Q-Wert etwa 0,2. Das Erscheinen dieses Einschnittes hängt von der Konzentration der Lauge folgendermassen ab: In einer 0,1 M Lauge ist der Einschnitt von der Konzentration des Acetons 0,2 M; in 1 M Lauge von $5 \cdot 10^{-2}$ M (Abb. 1) und in 5 M Lauge von $2 \cdot 10^{-2}$ M messbar. Mit Erhöhung der Konzentration des Acetons wird der Einschnitt tiefer; in 1 M Lauge und 0,25 M Aceton entsteht neben dem ersten ein positiverer kleiner Einschnitt von Q etwa 0,1. Dabei erscheinen auch Ausbuchtungen der Kurve wegen Veränderung der Differentialkapazität. Die beiden Einschnitte hängen stark von der Gleichstromkomponente des polarisierenden Stromes ab. Wenn das Potential der Elektrode den positiven Grenzwert, d. h. die elektrolytische Auflösung des Quecksilbers unter

der Bildung von Quecksilber(II)oxyd, nicht erreicht, verschwinden die Einschnitte (Abb. 2). Diese Wirkung ist nur in konzentrierteren alkalischen Lösungen zu beobachten; im neutralen oder sauren Milieu kommen diese positiven kathodischen Einschnitte nicht vor.

Völlig analog ist das Verhalten der höheren Acetonhomologe: es wurden Methyläthylketon, Diäthylketon, Methyl*iso*propylketon, Metyl-*n*-hexylketon und Methyl-*n*-nonylketon untersucht. Alle geben in alkoholischen Laugen positive kathodische Ein-

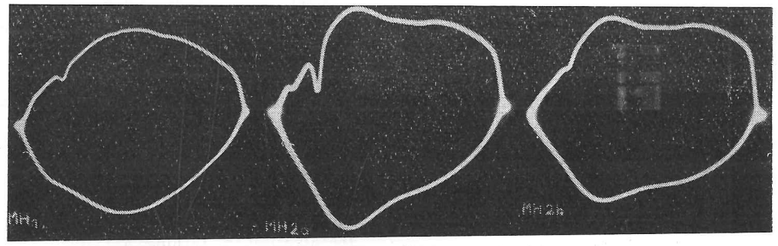

Abb. 1. $dE/dt = f_1(E)$-Kurve von 0,1 M-Aceton in 1 M-KOH. — Abb. 2. $dE/dt = f_1(E)$-Kurve von 0,25 M Aceton in 1 M-KOH. *a*) die Elektrode ist polarisiert im ganzen Potentialbereich; *b*) das Potential der Elektrode erreicht nicht völlig den positiven Grenzwert.

schnitte von Q 0,2 und 0,1, die mit dem positiven Grenzpotential verbunden sind; bei den grösseren Molekülen der Ketone ist hier die Kapazitätswirkung viel stärker als bei Aceton ausgeprägt.

Dieselben Einschnitte erscheinen auf der Kurve von Cyclopentanon und Cyclohexanon (Abb. 3), Diacetonalkohol (Abb. 4), Mesityloxyd und Phenylaceton in beinahe denselben Konzentrationsverhältnissen wie bei Aceton. In der Reihe Acetophenon (Abb. 5),

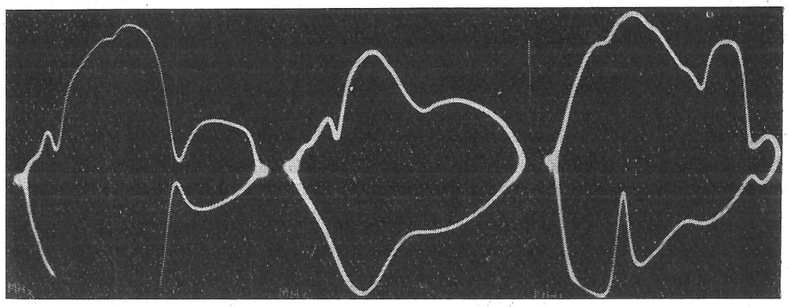

Abb. 3. $dE/dt = f_1(E)$-Kurve von $5 \cdot 10^{-2}$ M Cyclohexanon in 1 M-KOH. — Abb. 4. $dE/dt = f_1(E)$-Kurve von $5 \cdot 10^{-2}$ M Diacetonalkohol in 1 M-KOH. — Abb. 5. $dE/dt = f_1(E)$-Kurve von $1 \cdot 10^{-3}$ M Acetophenon in 1 M-KOH.

Propiophenon, Butyrophenon sind in millinormalen Lösungen neben grossen elektrolytischen und Kapazitätseinschnitten auch die positiven kathodischen Einschnitte sichtbar, die mit dem positiven Grenzpotential zusammenhängen.

Auch verschiedene Ketosäuren, wie Brenztraubensäure (Abb. 6), Phenylbrenztraubensäure und Lävulinsäure geben neben anderen auch die für die Ketogruppe charakteristischen Einschnitte.

Acetylaceton als Diketon unterscheidet sich von den Monoketonen verschieden in dem Sinne, dass in einer Lösung schon in der Konzentration $5 \cdot 10^{-4}$ M in 1 M-KOH zwei gleiche gut messbare Einschnitte von Q-Werten 0,27 und 0,49 entstehen (Abb. 7). Das Vorkommen beider Einschnitte ist wieder durch das Erreichen des positiven Grenzpotentials bedingt.

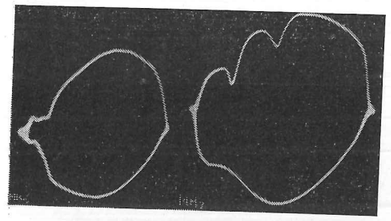

Abb. 6. $dE/dt = f_1(E)$-Kurve von $5 \cdot 10^{-2}$ M Brenztraubensäure in 1 M-KOH. (Das negative Grenzpotential ist durch Reduktion der Brenztraubensäure gegeben.) — Abb. 7. $dE/dt = f_1(E)$-Kurve von $1 \cdot 10^{-3}$ M Acetylaceton in 1 M-KOH.

Mit Phenyl*iso*propylketon, Benzaldehyd, Benzophenon, Phenylglyoxalsäure, Malonsäure und Äthylacetat konnten die typischen Einschnitte in keinem Konzentrationsverhältnis beobachtet werden.

Neben Ketonen bilden auch einige Amide (Harnstoff, Acetamid, Urethan) in der alkalischen Lösung auf der Ableitungskurve irreversible kathodische Einschnitte, die auch von dem positiven Grenzpotential abhängen. Dagegen weist Acetonitril auf der Ableitungskurve in Kalilauge keine Wirkung auf.

Auf den polarographischen Kurven aller dieser Verbindungen erscheinen in alkalischen Lösungen anodische Stufen bei etwa —0,2 V (GKE). Andere polarographische Messungen [3] erklären diese Stufen bei positiven Potentialen durch das Auflösen des Quecksilbers unter Bildung einer Organoquecksilberverbindung. Diese Hypothese wird dadurch gestützt, dass mit einer vibrierenden Platinelektrode die Ketoverbindungen in Alkalilauge weder polarographische noch oszillopolarographische Effekte zeigen.

Der Merkurierung unterliegen die Ketone in ihrer enolischen Form [4], die mit der Keto-Form in alkalischen Lösungen im Gleichgewicht steht. Die Gleichgewichtskonzentration der Enol-Form steigt mit steigendem pH der Grundlösung, liegt aber immer im Gebiete von Prozenten und Bruchteilen der Prozenten der analytischen Konzentration. Dadurch wird die scheinbare kleine Empfindlichkeit der polarographischen Reaktion erklärt.

Bei der Polarisation der Elektrode durch Wechselstrom ist auf der Ableitungskurve die anodische Bildung der Organoquecksilberverbindungen nicht zu beobachten, weil sie sich zu nahe dem positiven Grenzpotential abspielt, bei dem sich das Quecksilber auflöst. In der folgenden kathodischen Phase wird das Quecksilber aus den Produkten der anodischen Merkurierung wieder reduziert.

Versuche mit dem Kalousek-Umschalter und mit dem hängenden Tropfen zeigen, dass das bei den Potentialen der anodischen Stufe entstandene Produkt reversibel reduziert wird. Es handelt sich hier wahrscheinlich um einfache Quecksilberverbindungen mit der Gruppe $[—\overset{|}{\underset{\|}{C}}—\overset{|}{\underset{O}{C}}—Hg]^+$. Falls man aber die Elektrode zu noch positiveren Potentialen polarisiert, entstehen auf ihrer Oberfläche unter der Wirkung von Quecksilber(II)hydroxyd, bzw. -oxyd. Verbindungen, in denen das Quecksilber fester gehalten wird,

voraussichtlich in der Gruppe $—\overset{|}{\underset{\|}{C}}—\overset{|}{\underset{O}{C}}—Hg—O—$. Die Reduktion dieser Bindungen verläuft dann irreversibel, bei negativeren Potentialen. Diese Reduktion entspricht den Einschnitten auf den oszillopolarographischen Ableitungskurven. Die Einschnitte entstehen bei verschiedenen Substanzen bei demselben Potential, was auf Reduktion derselben funktionellen Gruppe hinweist.

Wegen geringer Empfindlichkeit ist die beschriebene oszillopolarographische Reaktion zur quantitativen Bestimmung (mit der Ausnahme der β-Diketone) nicht geeignet. Sie könnte aber vielleicht als konstitutioneller Beweis für die Ketogruppe mit Wasserstoffatomen am α-Kohlenstoffatom dienen, gleich wie es für die chemische Reaktion dieser organischen Substanzen mit der alkoholischen Lösung von Quecksilber(II)chlorid und Natriumethoxyd vorgeschlagen wurde [5].

Herrn Dr. O. Exner bin ich für die Darstellung zahlreicher Verbindungen und für wertvolle Diskussionen verbunden; Herrn Dr. P. Zuman gebührt mein Dank für die Überlassung einiger Ketoderivate.

Zusammenfassung

Ketoverbindungen, die am α-C-Atom Wasserstoffatome enthalten, bieten in alkalischen Lösungen einen kathodischen Einschnitt auf der $dE/dt = f_1(E)$-Kurve vom Q 0,2. Dieser Einschnitt hängt mit der Bildung einer Organoquecksilberverbindung zusammen.

ОСЦИЛЛОПОЛЯРОГРАФИЧЕСКОЕ ПОВЕДЕНИЕ КЕТОНОВ В ЩЕЛОЧНЫХ РАСТВОРАХ

МИХАЕЛ ГЕЙРОВСКИ

Полярографический институт Чехословацкой академии наук в Праге

Кетоны, имеющие на α-углероде водородные атомы, дают в растворах едких щелочей на кривой $dE/dt = f_1(E)$ катодный зубец со значением Q 0,2.

LITERATUR

1. Molnár L., *Dissertation*, Chemisches Institut der Slowakischen Akademie der Wissenschaften, Bratislava 1959. — 2. Heyrovský J., *Oszillographische Polarographie mit Wechselstrom*, Abhandl. Deutsch. Akad. der Wiss. zu Berlin, Berlin 1959. — 3. Heyrovský M., bisher nicht veröffentlicht. — 4. Rochow E. G., Hurd D. T., Lewis R. N., *The Chemistry of Organometallic Compounds*, New York 1957, 112. — 5. Connor R., van Campen J. H., J. Am. Chem. Soc. *58*, 1131 (1936).

Dr. Michael Heyrovský, Praha 1, Vlašská 9, Polarografický ústav ČSAV.

Diskussionsbeiträge

P. Zuman ist der Meinung, dass es sich wahrscheinlich bei der Reaktion der Amide mit dem Quecksilber um eine Bildung von Chelatverbindungen handelt.

M. Heyrovský ergänzt, dass beim Verfolgen des Mechanismus der oszillopolarographischen Elektroreduktionen bei extrem positiven oder negativen Potentialen immer noch eine andere polarographische Methode herangezogen werden muss.

CHEMICKÉ ZVESTI XVI, 4–5 — Bratislava 1962

OSZILLOPOLAROGRAPHISCHER NACHWEIS VON ELEKTROLYTISCHEN, HYDROLYTISCHEN UND PHOTOLYTISCHEN FOLGEREAKTIONEN

HERMANN BERG

Institut für Mikrobiologie und experimentelle Therapie Jena
der Deutschen Akademie der Wissenschaften zu Berlin

U sloučeniny typu etyleniminobenzochinonu (Bayer E-39) je sledován průběh elektrolytických, hydrolytických a fotolytických reakcí.

Gegenüber der Gleichspannungspolarographie ermöglicht die oszillographische Polarographie mit Wechselstrom häufiger den Nachweis von Produkten der Durchtrittsreaktion sowie von kurzlebigen Reaktanten im Verlauf von Lösungsreaktionen. Aus diesen Gründen wurde diese Methode herangezogen für die Aufklärung mehrerer Folgereaktionen von Äthylenimino-Benzochinonen, insbesondere des 2,5-Bis-(äthylenimino)-3,6-bis-(*n*-propoxy)-benzochinons-(1,4) (*I*), einem unter der Bezeichnung Bayer E-39 bekannten Cytostatikum. Sein Polarogramm weist die reversible Chinonstufe ($E_{1/2} = -0{,}23$ V gegen NKE, pH 7) und bei -1 V eine irreversible Welle auf, deren Grenzstrom pH-abhängig ist [1, 2]. Es konnte durch präparative Reduktion [3] gezeigt werden, dass nur die protonisierten Äthyleniminogruppen nacheinander reduziert werden. Im Oszillopolarogramm $dE/dt = f_1(E)$ findet man in diesem negativen Potentialbereich eine *L*-förmige kathodische Einbuchtung, während bei positiven Potentialen drei reversible Einschnitte erscheinen [1]. Ihre Ursachen und ihre Änderungen durch hydrolytische oder photolytische Reaktionen sollen nun geschildert werden.

Experimenteller Teil

Die Oszillogramme wurden mit dem Polaroskop P 574 unter grösster Dehnung der Potentialachse aufgenommen, so dass überwiegend nur der positive Ausschnitt im Bild erscheint.

Die Grundlösungen bestanden aus Phosphatpuffer oder Schwefelsäure (0,1 N, 0,01 N) mit einem Gehalt von 0,6 M-Na_2SO_4 zur Verminderung des Zellwiderstandes. Die Konzentrationen des Bayer E-39 lagen zwischen $5 \cdot 10^{-5}$ M und $5 \cdot 10^{-4}$ M; in letzterem Fall enthielten die Grundlösungen 10 % Vol. Methanol.

Temperierbare Messzellen fanden Verwendung und zwar für die Tropfelektrode eine Schliffzelle [4] (Bodenquecksilber), für die strömende Elektrode eine Überlaufzelle [5] (Bodenquecksilber) und zur Bestrahlung eine Quarzzelle (NKE), umgeben von U-förmigem Hg-Brenner [6].

Vergleichspolarogramme wurden mit dem LP 55, Absorptionsspektren mit dem Photometer SP 700 oder dem Zeiss-Monochromator aufgenommen.

Ergebnisse

Die elektrolytischen Vorgänge sollen vorangestellt werden, da sie auch als Indikator für die Lösungsreaktionen dienen.

CHARGING CURRENT IN POLAROGRAPHY WITH DISCONTINUOUSLY CHANGED POTENTIAL

M. HEYROVSKÝ

Collection of Czechoslovak Chemical Communications. Vol. 26 (1961). — Published under the auspices of the Czechoslovak Academy of Science by the Publishing House of the Czechoslovak Acad. Sci., Vodičkova 40, Prague 1. — Address of the Editor: Institute of Organic Chemistry and Biochemistry, Czechoslovak Academy of Science, Na cvičišti 2, Prague 6. — Annual subscription Kčs 300.—, US $ 20.20, £ 10/15/8, single issue Kčs 25.—. Subscription orders should be addressed to ARTIA, 30 Ve smečkách, Prague 1, Czechoslovakia. — Printed by Knihtisk 05, Prague.

Rozšiřuje Poštovní novinová služba, objednávky a předplatné přijímá Poštovní novinový úřad — ústřední administrace PNS, Jindřišská 14, Praha 1. Lze také objednat u každého poštovního úřadu nebo doručovatele.

Reprinted from Collection Czechoslov. Chem. Commun. *26*, 3164—3167 (1961).

CHARGING CURRENT IN POLAROGRAPHY WITH DISCONTINUOUSLY CHANGED POTENTIAL

M. Heyrovský

Polarographic Institute, Czechoslovak Academy of Science, Prague

Received October 24th, 1960

The polarographic method of dicsontinuously changed potential using the switch of Kalousek[1] is currently used for the investigation of electrode processes: it shows the degree of reversibility, helps to identify the reaction products and may indicate adsorption of the depolarizer[2]. An equation was deduced for the mean electrolytic current[3], but no paper has yet dealt with the charging

current obtained with the switch.* It can be expected that because of the repeated charging of the electrode to different potentials during the drop-life, the charging current will be much higher than in ordinary polarography, and that changes of capacity of the electrode double layer due to adsorption or desorption of surface active substances will cause considerable changes of current, comparable with polarographic reduction or oxidation waves. In order to distinguish the mean charging current from the mean electrolytic current obtained with the switch an expression for the charging current has been deduced and checked experimentally.

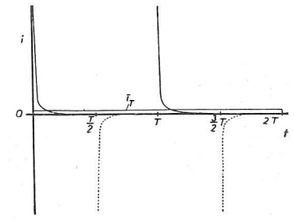

Fig. 1
Instantaneous Charging Current During two Periods of Commutation and the Mean Current $\bar{i}_T$
Dotted lines indicate current not recorded by the galvanometer.

Theoretical

The electrode is charged with a periodic rectangular voltage of frequency f from an auxiliary potential E_A to potential E (given by the position of the sliding contact on the potentiometer of the polarograph) in the first half of the period T ($T = 1/f$) and back in the second half-period, the current being recorded by the galvanometer only during the first part of the cycle (Fig. 1). The capacity of the electrode C is considered constant during one half-period; this approximation is valid only when the relative change of the electrode surface during one half-period, is negligible i. e. with higher frequencies of commutation, especially towards the end of the drop life. The instantaneous current charging the electrode in the first half-period is given by the formula

$$i = \frac{\Delta E}{R} \exp\left(-\frac{t}{RC}\right) \qquad (1)$$

where $\Delta E = E - E_A$ and R is the total resistance of the polarising circuit (which is usually less than 1 kΩ). The mean current over the whole period is then

$$\bar{i}_T = \frac{1}{T}\int_0^{T/2} \frac{\Delta E}{R} \exp\left(-\frac{t}{RC}\right) dt = f\Delta E \,.\, C - f\Delta E \exp\left(-\frac{T}{2RC}\right)$$

Since under polarographic conditions the second term is negligibly small, the equation for the mean current in one period becomes

$$\bar{i}_T = f \,.\, \Delta E \,.\, C \qquad (2)$$

To obtain the mean current during the whole drop life t_1, we replace the term C in the equation (2) by the product of specific capacity C_1 ($F\,cm^{-2}$) and mean surface of the dropping electrode $\bar{q} = 0.51\ m^{2/3}t_1^{2/3}$ (cm^2), where m is the rate of flow of mercury ($g\,s^{-1}$). The resulting mean charging current recorded polarographically with the Kalousek's switch is given in absolute units as

$$\bar{i} = 0{\cdot}51 \,.\, f \,.\, \Delta E \,.\, C_1 \,.\, m^{2/3} \,.\, t_1^{2/3} \qquad (3)$$

Experimental

All chemicals used were reagent grade (*pro analysi*). Curves were recorded using an electronic switch constructed according to Rálek and Novák[4] in conjunction with the Model V 301 polaro-

* Matsuda[8] calculated from a general equation the mean alternating charging current for polarography with a superimposed square-wave voltage of a small amplitude.

graph. The switch worked with frequencies 2; 2·6; 3·5; 4·9; 8·8; 11; 15·4; 19; 21·8; 30 and 39·8 cs^{-1}. The solutions were examined in the Kalousek cell with a saturated calomel reference electrode.

Results and Discussion

The validity of eq. (*2*) was proved by joining a condenser of 0·25 μF and 1 μF to the apparatus instead of the electrolytic cell and registering the resulting current. The obtained straight lines fitted the equation (*2*) within the limits of experimental error (about 3%, mainly due to inconstancy of frequency) in the whole available range of frequencies. Equation (*3*) was checked using pure 0·1M solutions of KCl, Na_2SO_4, HCl and NaOH.

Like in ordinary polarography the charging current of a pure supporting electrolyte obtained with the switch is given by a curve consisting of two almost linear branches of different slopes on each side of the electrocapillary maximum. Unlike in ordinary polarography it crosses the galvanometer zero line at the potential at which the difference ΔE of the commutated potentials becomes zero. In accordance with the formula the current was found to increase linearly with the frequency of commutation in all examined solutions within the whole frequency range. According to (3) the current should be independent of the pressure of mercury, which was also found to be the case.

After substituting known and experimentally measured quantities into equation (*3*) we may calculate the specific capacity C_1. The resulting values obtained from the negative branches of the curves are 14·9 $\mu F/cm^2$ for 0·1M-HCl, 15·2 $\mu F/cm^2$ for 0·1M-NaOH, 16·3 $\mu F/cm^2$ for 0·1M-KCl and 17·1 $\mu F/cm^2$ for 0·1M-Na_2SO_4. These data do not differ much from integral capacities given in literature[5,6].

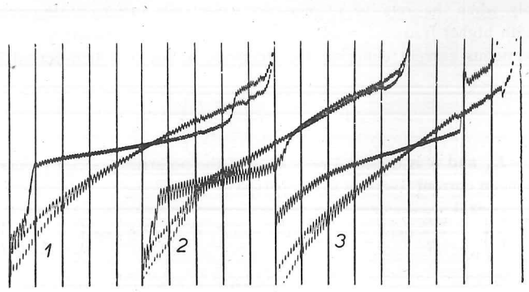

Fig. 2
Charging Current in Presence of Surface Active Substances
200 mV/absc.; $f = 11$ c s^{-1}; free from oxygen. *1* 0·1M-Na_2SO_4 alone and with 4 . 10^{-4}M tetrabutylammonium sulphate added; $\Delta E_0 = -1{\cdot}0$ V; sens. 1 : 40; from 0V . *2* 0·1M-KCl alone and with 1 . 10^{-3}M octanol added; $\Delta E_0 = -1{\cdot}2$ V; sens. 1 : 40 from 0 V. *3* 0·1M-NaOH alone and with 0·25M pyridine added; $\Delta E_0 = -1{\cdot}2$ V; sens. 1 : 30; from −0·2 V.

The presence of surface active substances in aqueous solutions is marked on the curves by a decrease of the absolute value of charging current in the potential region where adsorption on the electrode surface takes place and by its sudden increase when the substance desorbs. Record of the charging current thus presents waves denoting adsorption and desorption (Fig. 2). The behaviour of these waves was followed with solutions of pyridine in 0·1M-NaOH, of tetrabutylammonium sulphate in 0·1M-Na_2SO_4 and of octanol in 0·1M-KCl. The adsorption-desorption waves obtained with

the switch obey equation (*3*): they are directly proportional to the frequency of commutation and do not depend on the mercury pressure. However, the capacity C_1 is here a function of ΔE_0, specific for each substance, and cannot be substituted by the values of the integral capacity.

Koutecký[3] has deduced in his theoretical treatment that the mean electrolytic current obtained with the switch for a reversible electrode process at high frequencies and long drop times is independent of the mercury pressure and proportional to the square root of the frequency of commutation *f*. In the present paper the independence of the mercury pressure and a direct proportionality to the first power of frequency for the case of charging current is shown. Thus the change of frequency of commutation permits to distinguish between the two different currents. There appears a formal analogy in polarographic techniques: A linear dependence is obtained when plotting the diffusion current intensity *a*) in ordinary polarography against the square root of the height of the mercury reservoir, *b*) in polarography with Kalousek's switch against the square root of the frequency of commutation and *c*) in oscillographic polarography with applied voltage[7] against the square root of the rate of change of potential dE/dt. The charging current, on the other hand, gives a linear plot with the first power of these values.

References

1. Kalousek M.: This Journal *13*, 105 (1948).
2. Kalousek M., Rálek M.: This Journal *19*, 1099 (1954); Chem. listy *48*, 808 (1954).
3. Koutecký J.: This Journal *21*, 433 (1956); Chem. listy *49*, 1454 (1955).
4. Rálek M., Novák L.: This Journal *21*, 248 (1956); Chem. listy *49*, 557 (1955).
5. Grahame D. C.: Chem. Revs *41*, 441 (1947).
6. Frumkin A. N., Bagockij V. S., Iofa Z. A., Kabanov B. M.: *Kinetika elektrodnych processov*, p. 17. Izd. Moscov. univ., Moscow 1952.
7. Loveland J. W., Elving P. J.: Chem. Revs *51*, 67 (1952).
8. Matsuda H.: Z. Elektrochem. *62*, 977 (1958).

Translated by the Author.

Резюме

М. Гейровский: *Зарядный ток в полярографии с прерывисто изменяющимся потенциалом.* При полярографии с прерывисто изменяющимся потенциалом при помощи переключателя Калоусека зарядный ток играет гораздо более важную роль, чем в классической полярографии. Выведено и экспериментально проверено выражение для среднего зарядного тока, позволяющее различать его от среднего электролитического тока.

CHEMICKÉ ZVESTI

SLOVENSKEJ AKADÉMIE VIED

SEPARÁTNY VÝTLAČOK

VYDAVATEĽSTVO
SLOVENSKEJ AKADÉMIE VIED
BRATISLAVA

THEORY OF THE OSCILLOGRAPHIC POLAROGRAPHY WITH A. C. CURRENT

KAREL MICKA

Polarographic Institute, Czechoslovak Academy of Sciences, Praha

Summary

The theory of the oscillographic polarography starts from the general integral equation describing reversible processes at the mercury electrode during the polarization by means of the current of an arbitrary time course. The solution of this equation can be carried out rigorously for the sineshaped a. c. current in three limiting cases: *1.* the specific charge of the electrode is negligible, *2.* the faradayic current is negligible, *3.* the changes of the electrode potential are small. From the three limiting solutions the approximate equation describing the true state of the electrode during the polarization by means of the a. c. current can be derived. From this equation follow all the used functions, $E = f(t)$, $\mathrm{d}E/\mathrm{d}t = \mathrm{f}'(t)$ and $\mathrm{d}E/\mathrm{d}t = \mathrm{f}_1(E)$ in agreement with the experiments. The potential of the peak of the incision at the curve $\mathrm{d}E/\mathrm{d}t = \mathrm{f}_1(E)$ is equal to the half-wave potential of the depolarizer. The relative depth of the incision (equal to the ratio between the depth of the incision and the height of the curve without the depolarizer) is decreased slowly with increasing frequency of the a. c. current; with increasing temperature it is either slightly increased or remains unchanged. The capacity effects are defined like all changes of the shape of the curve $\mathrm{d}E/\mathrm{d}t = \mathrm{f}_1(E)$ caused by the change of the differential capacity of mercury.

From the theory it follows how these effects can be distinguished from the incisions caused by the depolarizer. Further the significance of the d. c. component of the current is elucidated which, according to the theory, is necessary for compensation of the losses of the reduction products at the electrode. In the ideal case when these losses do not occur, it is fully sufficient to polarize the mercury electrode by the a. c. current without the d. c. component to obtain a rightly developed curve $\mathrm{d}E/\mathrm{d}t = \mathrm{f}_1(E)$ on the screen of the polaroscope. The losses of the reduction products are caused by the instability of the amalgams, by the vibrations of the mercury electrode or also by the irreversibility of the electrode process, and are manifested by the tendency of the electrode potential to shift towards the more positive values.

LITERATURA

1. Micka K., Collection *24*, 3708 (1959); Z. physik. Chem. *206*, 345 (1957). — 2. Heyrovský J., Kalvoda R., *Oszillographische Polarographie mit Wechselstrom*, Berlin 1960.

Adresa autora:

Prom. chemik Karel Micka, kandidát chemických věd, Praha 1, Vlašská 9, Polarografický ústav ČSAV.

ARTEFAKTY V OSCILOGRAFICKÉ POLAROGRAFII

MICHAEL HEYROVSKÝ
Polarografický ústav Československé akademie věd v Praze

Je diskutována podstata a vznik tzv. artefaktů pozorovaných při polarisaci rtuťové kapkové elektrody střídavým proudem. Je upozorněno na různé typy artefaktů.

V oscilografické polarografii se setkáváme často s výsledky, které nelze vysvětlit prostým srovnáním s daty známými z klasické polarografie. Příčina tkví v rozdílném způsobu polarisace kapkové elektrody u obou metod.

Je tu jednak rozdíl v nabíjecích proudech. Střední nabíjecí proud v klasické polarografii, řádu 10^{-7} A, je obvykle zanedbatelný proti elektrolytickému. Naproti tomu v oscilografické polarografii vnuceným střídavým proudem je nabíjecí proud stejného řádu s elektrolytickým, a proto každá změna diferenciální kapacity, ať již způsobená přítomností povrchově aktivní látky nebo jen změnou základního elektrolytu v roztoku, se zřetelně projeví na křivkách. Tyto změny jsou souhrnně označovány jako kapacitní efekty. Kapacitní efekty způsobené adsorpcí jsou patrné v klasické polarografii jen při nejvyšších citlivostech nebo za použití tryskavé elektrody.

Druhý bod, v němž se obě metody liší, je rozdílný rozsah potenciálové změny na jedné kapce. V polarografii roste každá rtuťová kapka při prakticky konstantním potenciálu (maximální změna asi 20 mV během růstu kapky); difusní vrstva kolem elektrody je tvořena pouze depolarisátorem a zplodinou jeho elektrodové reakce vznikající při daném potenciálu. S odkápnutím odnese kapka zplodiny reakce s sebou a na novém povrchu probíhá celý děj opět podle vloženého potenciálu, bez ohledu na děje, jež proběhly na předchozích kapkách. (Toto platí zcela přesně u vodorovné kapiláry, kde nenastává přenos koncentrační polarisace.) V oscilografické polarografii naproti tomu se během růstu jedné kapky změní potenciál ve velkém rozsahu — obyčejně kolem 2 V; při střídavé polarisaci s frekvencí 50 c/s se tato změna od 0 do 2 V a zpět opakuje asi 200 krát na jediném povrchu. Produkty reakce, která proběhla při určitém potenciálu, zůstávají v difusní vrstvě i při další polarisaci a mohou se buď samy účastnit jiné elektrodové reakce, nebo se chemicky přeměnit na novou látku elektrodově aktivní.

Takové látky, které nejsou obsaženy v původním systému roztok—elektroda, ale vznikají na elektrodě teprve během její polarisace, nazýváme obecně artefakty [1] (doslova: látky uměle vytvořené). V klasické polarografii na vznik a povahu těchto látek usuzujeme nepřímo z tvaru vln a ze závislostí půlvlnových potenciálů na různých faktorech. Přímo se projeví některé z nich při použití Kalouskova přepínače nebo stálé visící kapky; jejich působení je však zcela typické pro oscilopolarografické metody.

V některých případech, zejména u organických depolarisátorů, vzniká na elektrodě tak velký počet artefaktů, že se oscilopolarografické výsledky stávají nepřehlednými. Například alkalický roztok nitrobenzenu [2], dávající jednu polarografickou redukční vlnu, poskytuje při elektrolyse střídavým proudem na křivce $dE/dt = f_1(E)$ sedm zářezů (čtyři katodické a tři anodické), z nichž jeden přísluší redukci nitrobenzenu a ostatní různým artefaktům (oscilogram 1).

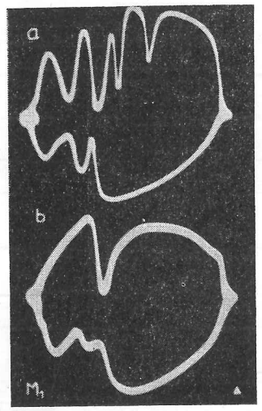

Oscilogram 1. Oscilopolarografické křivky $dE/dt = f_1(E)$ 10^{-3} M nitrobenzenu v 1 M-KOH. *a*) na kapkové, *b*) na tryskavé elektrodě.

Podle způsobu, jakým artefakty na elektrodě vznikly, můžeme rozeznávat artefakty elektrochemické a chemické. Elektrochemické, kterých je většina, jsou přímé produkty elektrodové reakce; chemické vznikají z nich následnou reakcí. Tak například při zmíněné redukci nitrobenzenu v alkalickém prostředí vznikají na kapce nitrosobenzen a fenylhydroxylamin [3] jako elektrolytické artefakty reagující spolu za tvorby chemického artefaktu, azoxybenzenu, který se dále redukuje ireversibilně na azobenzen.

Jakýmsi přechodem mezi elektrochemickými a chemickými artefakty jsou sloučeniny se rtutí, které vznikají na elektrodě reakcí složek roztoku nebo artefaktů s ionty rtuti vysílanými z elektrody při positivních potenciálech. Z těchto sloučenin se při negativnějších potenciálech redukuje rtuť. Na polarografických křivkách je možno v takových případech pozorovat jen anodické vlny tvorby sloučenin se rtutí; při potenciálech, kde by došlo k jejich redukci, tyto sloučeniny na povrchu kapek již nejsou. Sem patří především účinky komplexotvorných látek, jako kyanidových iontů [4] (oscilogram 2), komplexonu aj., ale také acetylenu [5] a některých ketonů v alkalickém prostředí [6], kde dochází k tvorbě organortuťných sloučenin.

Artefakty se na elektrodě mohou projevovat různým způsobem: buď se oxydují, nebo redukují, nebo jen mění kapacitu elektrody bez přenosu elektrického náboje; u mnoha případů je elektrodová reakce artefaktů spojená s adsorpcí.

Výklad oscilopolarografických efektů je často obtížný; k jednoznačnému závěru je možno zpravidla dojít teprve na základě výsledků několika pokusných metod. Vycháa-

zíme ze srovnání s klasickou polarografií: zářezy na oscilopolarografických derivačních křivkách, které není možno podle potenciálu přiřadit polarografickým vlnám, přísluší buď kapacitním efektům, nebo artefaktům. Kapacitní efekty způsobené povrchově aktivními látkami z roztoku lze snadno určit srovnáním s křivkami čistého základního elektrolytu, nejlépe pomocí metody srovnávacích titrací [7]; v oblasti adsorpce je derivační křivka vlivem snížené kapacity elektrody zvýšena.

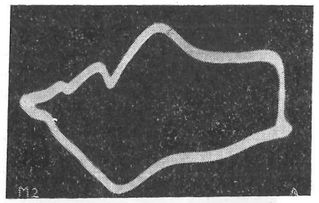

Oscilogram 2. Oscilopolarografická křivka $dE/dt = f_1(E)$ 5 . 10^{-4} M-KCN v 1 M acetátovém pufru.

Při srovnávání oscilopolarografických a polarografických výsledků se setkáme také s případy, kdy polarografické vlně neodpovídá žádný zářez na oscilopolarografické křivce. Dochází k tomu tehdy, když produkt elektrodového děje zůstává u povrchu elektrody a brání vlastní reakci. Takový je případ iontů hliníku, kde hydroxyd hlinitý jako zplodina reakce zůstává adsorbován na kapce a brzdí další redukci [8]. Když zaznamenáváme jednotlivě za sebou první, druhý a další polarisační cykly, dostaneme na první křivce zářez, který je na druhé menší a na páte až šesté zmizí úplně.

Při reversibilní elektrodové reakci leží zářez artefaktu na opačné větvi křivky při témže potenciálu jako zářez původního depolarisátoru. Z pouhé oscilopolarografické křivky však nemůžeme říci, je-li depolarisátor v roztoku v oxydované formě a artefakt na elektrodě v redukované anebo obráceně, nebo kolik procent depolarisátoru je v roztoku v oxydované a kolik v redukované formě. V tomto směru jsme odkázáni na klasickou polarografii.

Leží-li dva zářezy na křivce $dE/dt = f_1(E)$ proti sobě při témže potenciálu, může též jít o dva různé, nezávislé procesy, zvláště jsou-li zářezy rozdílné svým vzhledem.

Artefakty vznikající ireversibilní reakcí je snáze identifikovat. Jako vodítko tu může sloužit reakce křivky na změnu stejnosměrné složky proudu: zpolarisujeme-li elektrodu tak, že potenciál nedosáhne hodnoty, při níž dochází k primární elektrodové reakci, netvoří se dále artefakt a zářez příslušející artefaktu zmizí. Nedosáhne-li elektroda potenciálu redukce zinku, zmizí zářez oxydace zinkové amalgámy. Z toho vyplývá, že hloubka zářezu artefaktu je citlivá na nastavení stejnosměrné složky. To je zejména patrno, nastává-li primární děj při jednom z krajních potenciálů. Trojmocný chrom, například [9], tvoří v louhu chromitan, jenž se ireversibilně oxyduje na chroman při potenciálech o málo negativnějších než potenciál rozpouštění rtuti — na křivce $dE/dt = f_1(E)$ se tato reakce ani neprojeví. (Na oscilogramu 3 je uvedena křivka $i = f_2(E)$ pořízená s trojúhelníkovým střídavým napětím frekvence 50 c/s.) Chroman se pak v katodické fáze následujícího cyklu redukuje zpět na chromitan. Není-li elektroda polarisována k dostatečně positivním potenciálům (tj. nesvítí-li jasně levý okrajový bod křivky $dE/dt = f_1(E)$ na obrazovce), katodický zářez chromanu se neobjeví. Je tedy zřejmé, že pro získání reprodukovatelných výsledků při analytickém využití oscilopolarografických křivek je třeba

vhodnou volbou střídavé a stejnosměrné složky proudu polarisovat elektrodu v maximálním rozsahu potenciálů — tj. tak, aby okrajové body křivky zůstaly po celou dobu kapky na mezných potenciálech rozpouštění rtuti a vylučování kationtu základního elektrolytu.

K objasnění povahy artefaktu přispívá sledování změn křivky při změně koncentrace nebo složení základního elektrolytu. Změnou základního elektrolytu měníme jednak

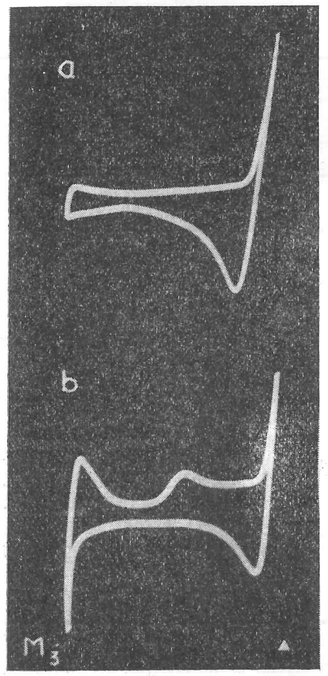

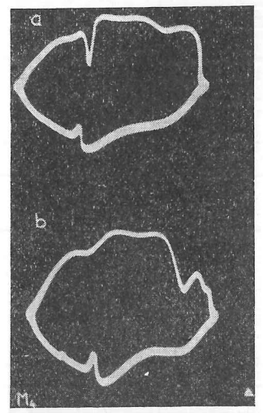

Oscilogram 3. Oscilopolarografické křivky $i = f_2(E)$ 10^{-3} M-$CrCl_3$ v 1 M-KOH. Elektroda polarisována střídavým trojúhelníkovým napětím frekvence 50 c/s; potenciál (*a*) nedosahuje, (*b*) dosahuje anodické oxydace.

Oscilogram 4. Oscilopolarografické křivky $dE/dt = f_1(E)$ 5 . 10^{-4} M-CS_2 v 1 M acetátovém pufru. (*a*) na kapkové, (*b*) na tryskavé elektrodě.

látku, která se může s depolarisátorem podílet na tvorbě artefaktu, jednak měníme potenciálové meze, jichž může elektroda při polarisaci dosáhnout; omezováním potenciálů přídavkem různých elektrolytů v nadbytku můžeme určit potenciál, při kterém ke vzniku artefaktu dochází. Sirouhlík, jehož oscilopolarografické zářezy jsou způsobeny sirníkovými ionty [10], produkty primární redukce sirouhlíku, dává v různých roztocích přibližně stejný efekt, pokud potenciál elektrody dosahuje dostatečně negativních hodnot. Při nadbytku zinečnatých iontů v roztoku zmizí zářezy sirouhlíku, protože nemůže dojít k primární redukci sirouhlíku na sirník, která nastává při —1,25 V, když zinečnaté ionty se redukují při —1,05 V (v octanovém pufru, SKE) (oscilogram 4). S acetylenem naproti tomu dostaneme zářez redukce sloučeniny se rtutí jen v koncentrovaných louzích [5] a ionty hlinité se projevují složitým artefaktem výhradně za přítomnosti lithia v roztoku [11]. Změna základního elektrolytu může tedy způsobit zásadní změnu

v chování látky na elektrodě. Aceton dává v alkalickém roztoku artefakt — sloučeninu se rtutí tvořící se při positivních potenciálech; v kyselině vzniká z acetonu artefakt naopak při negativních potenciálech, spojený se značným kapacitním efektem [12] (oscilogram 5).

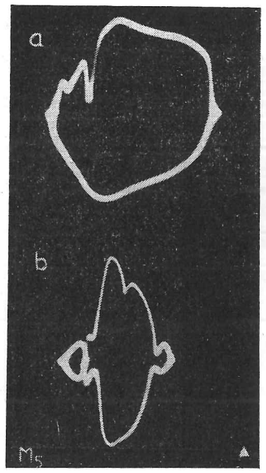

Oscilogram 5. Oscilopolarografické křivky $dE/dt = f_1(E)$ 10^{-3} M acetonu. (*a*) v 1 M-KOH, (*b*) v 1 M-HCl.

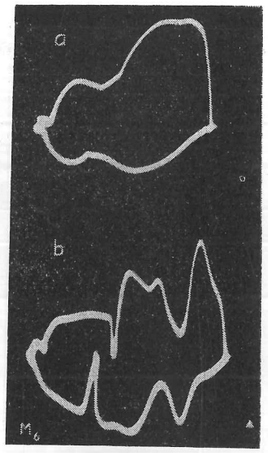

Oscilogram 6. Oscilopolarografické křivky $dE/dt = f_1(E)$ 10^{-2} N-$FeSO_4$ v 1 M-KCl. (*a*) za nepřístupu vzduchu, (*b*) na vzduchu.

Je-li v roztoku přítomen kyslík, dochází na elektrodě k jeho redukci, i když to není z křivek patrno, a zplodiny této redukce — peroxyd vodíku a hydroxylové ionty — mohou s depolarisátorem tvořit různé artefakty. To pozorujeme například s ionty železnatými, manganatými [4], kobaltnatými a s kadmiem a olovem v neutrálních základních elektrolytech; po odstranění kyslíku se křivka zjednoduší (oscilogram 6).

S pomocí Kalouskova přepínače si můžeme ověřit vznik jednoduchých artefaktů při určitém konstantním potenciálu. Cenné informace o mechanismu oscilopolarografických efektů podávají již zmíněné křivky, zaznamenané při jednotlivých polarisačních cyklech metodou podle R. Kalvody a J. Macků [13]. Tyto křivky nám ukazují, že některé artefakty se objevují teprve po prvním cyklu a s opakováním polarisace se hromadí na elektrodě, jak je tomu například u hliníku za přítomnosti lithia [14]. Jiné artefakty vzniknou v prvním cyklu a opakovanou polarisací jejich efekt mizí — tento případ pozorujeme například u thiosíranu [13], kde se na první křivce objeví šest zářezů, z nichž po několika cyklech zbude jeden (oscilogram 7).

Cennou pomocí při studiu elektrodových procesů je tryskavá elektroda. Rychlá obnova povrchu elektrody tu dovoluje proběhnout jen nejjednodušším reakcím, odpadá hromadění reakčních zplodin a reakce mezi nimi. Křivky s tryskavou elektrodou jsou proto zpravidla jednodušší než křivky téhož roztoku zaznamenané s kapkovou elektrodou (srov. oscilogram 1). Z artefaktů se na tryskavé elektrodě mohou uplatnit jen jednoduché

artefakty elektrochemické a sloučeniny se rtutí. Zdviháním rezervoáru rtuti zvyšujeme průtokovou rychlost a zkracujeme dobu, po kterou se artefakty mohou udržet na elektrodě; jejich zářezy se následkem toho zmenšují a případně úplně vymizí (oscilogram 8; srovnej též positivní katodický zářez na oscilogramu 4*a*—*b*). Některé děje jsou naopak lépe patrny s tryskavou elektrodou, kde se nemohou dostatečně uplatnit brzdivé účinky

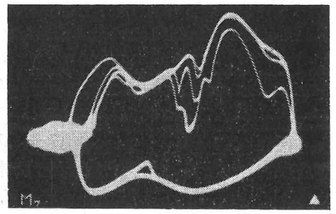

Oscilogram 7. Oscilopolarografické křivky $dE/dt = f_1(E)$ 10^{-3} M-$Na_2S_2O_3$ ve 2 M-KCl. Zaznamenáno prvních 5 křivek.

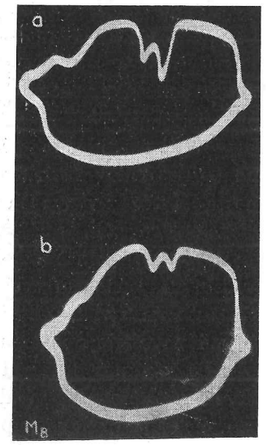

Oscilogram 8. Oscilopolarografické křivky $dE/dt = f_1(E)$ acetylenu v 5 M-NaOH. (*a*) na kapkové, (*b*) na tryskavé elektrodě.

reakčních produktů. Například zářez redukce sirouhlíku, vedle nápadného zářezu artefaktu — sirníkových iontů — sotva patrný na kapkové elektrodě, na tryskavé elektrodě se projeví velmi výrazně (oscilogram 4).

Jsou-li artefakty dostatečně stálé, je možno k jejich sledování použít stálou rtuťovou elektrodu o malém povrchu, jakou je visící kapka (nejlépe v úpravě podle J. Vogela [15]), a registrovat křivky v klasickém polarografickém zapojení. Touto cestou lze

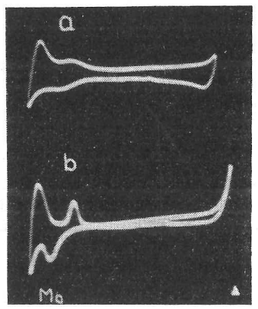

Oscilogram 9. Oscilopolarografické křivky $i = f_2(E)$ 1 M-$MgCl_2$. Elektroda polarisována střídavým trojúhelníkovým napětím frekvence 50 c/s; potenciál (*a*) nedosahuje, (*b*) dosahuje vylučování vodíku.

například zachytit též artefakty vznikající v hořečnatých solích jako základních elektrolytech, zpolarisujeme-li elektrodu k dostatečně negativním potenciálům, kde při redukci hořečnatých iontů dochází k vývoji vodíku. Hydroxylové ionty vzniklé při tom na povrchu elektrody vytvoří chemický artefakt — sraženinu hydroxydu hořečnatého, která zůstává dále naadsorbovaná na elektrodě a dává adsorpční a desorpční zářezy na positivní straně od elektrokapilárního maxima. Zvláště silný je tento efekt v roztocích nitrátů, kde redukcí nitrátových iontů vzniká velké množství iontů OH^-. Za přítomnosti iontů amonných, kdy se hydroxyd hořečnatý nesráží, nedochází k tvorbě artefaktu a zářezy se neobjeví. Jde zde o častý případ elektrodové reakce kombinované s chemickou reakcí a s adsorpcí, odlišný od dějů čistě elektrolytických nebo adsorpčních. (Na oscilogramu 9 je popsaný efekt ukázán na i—E křivce, kde je lépe patrný než na křivce $dE/dt = f_1(E)$.)

Jak vyplývá z uvedených příkladů, artefakty hrají v mechanismech elektrodových dějů v oscilografické polarografii prvořadou úlohu. Jsou to látky měnící vlastnosti elektrody v průběhu elektrolysy; jejich působení nespadá v úvahu v klasické polarografii, jejíž jednou z předností je, že povrch elektrody zůstává stále čerstvý. Oscilografická polarografie však přinesla možnost sledovat reprodukovatelným způsobem změny nastávající na elektrodě během elektrolysy a využít tyto změny i k analytickým účelům. V tomto směru na oscilografickou polarografii navazuje v poslední době použití stálé rtuťové kapky v polarografii. Podrobnější výzkum elektrodových reakcí, k nimž dochází v oscilopolarografických metodách, by mohl pomoci i při studiu procesů na pevných elektrodách, jichž je rtuťová kapková elektroda ideálním modelem.

АРТЕФАКТЫ В ОСЦИЛЛОГРАФИЧЕСКОЙ ПОЛЯРОГРАФИИ

МИХАЕЛ ГЕЙРОВСКИ
Полярографический институт Чехословацкой академии наук
в Праге

Выводы

В осциллографической полярографии называем артефактом вещество, которое не содержит раствор, но возникает на электроде в ходе его поляризации и проявляется на осциллографических кривых. Творение артефактов часто является одной из причин разности результатов приобретенных осциллографическим и полярографическим методами. Сравнением результатов приобретенных осциллографическим и полярографическим методами или с переключателем Калоуска при различных частотах, изучением первых кривых, сравнением кривых приобретенных с капельным и струйчатым электродами и наблюдением влияния постоянной слагаемой тока и состава фона на осциллографическую кривую, можно отличить, принадлежит-ли эффект веществу присутному в растворе или артефакту.

Более подробное исследование разрешает классифицировать артефакты до нескольких групп. По возникновению можно отличить артефакты электрохимические и химические, или первичные и вторичные; по поведению восстанавливающиеся или окисляющиеся и артефакты адсорбционные.

ARTEFAKTE IN DER OSZILLOGRAPHISCHEN POLAROGRAPHIE

MICHAEL HEYROVSKÝ
Polarographisches Institut
an der Tschechoslowakischen Akademie der Wissenschaften in Praha

Zusammenfassung

Als Artefakte bezeichnen wir in der oszillographischen Polarographie jene Verbindungen, die in der untersuchten Lösung nicht anwesend sind, sondern die erst im Verlaufe der Polarisation der Elektrode an deren Oberfläche entstehen und Einschnitte an den oszillopolarographischen Kurven bieten. Die Bildung der Artefakte ist einer der Gründe der oft unterschiedlichen Resultate der oszillographischen Methode von der klassischen Polarographie. Durch den Vergleich der oszillographischen Resultate mit der klassischen Polarographie und dem Umschalter nach Kalousek bei verschiedenen Frequenzen, durch Vergleich der Kurven, die mit der tropfenden und strömenden Elektrode aufgenommen wurden, durch das Studium der „ersten" Kurven und Verfolgen des Einflusses der Gleichstromkomponente und der Zusammensetzung der Grundlösung auf die oszillographische Kurve können wir unterscheiden, ob der Einschnitt der Verbindung die in der Lösung anwesend ist oder einem Artefakt gehört.

Ein ausführliches Studium ermöglicht es, die Artefakte in mehrere Gruppen einzuteilen. Dem Ursprung nach können wir elektrochemische und chemische, event. primare und sekundare Artefakte unterscheiden; nach dem Verhalten können wir die Artefakte auf reduzierbare oder oxydierbare und adsorptive teilen.

ARTEFACTS IN OSCILLOGRAPHIC POLAROGRAPHY

MICHAEL HEYROVSKÝ
Polarographic Institute, Czechoslovak Academy of Sciences, Praha

Summary

Substances which are not present in the solution, but which are formed at the electrode in the course of its polarization and cause changes of the oscillographic curves are called in oscillographic polarography artefacts. The formation of artefacts is one of the reasons of the frequent difference between the results of the oscillographic methods and those of the classical polarography. By comparing the oscillographic results with the classical polarography and with the commutator according to Kalousek using various frequencies, by studying the first curves, by comparing the curves obtained with the dropping and the streaming electrode and by following the influence of the d. c. component and of the composition of the supporting electrolyte on the oscillographic curve it can be distinguished, whether the effect is caused by a substance present in the solution or by an artefact.

A more detailed study enables us to classify the artefacts into several groups. According to their origin electrochemical and chemical, event. primary and secondary artefacts can be distinguished; according to the behaviour we know reducible, oxidizable and adsorptive artefacts.

LITERATURA

1. Heyrovský J., Forejt J., *Oscilografická polarografie*, Praha 1953, 97. — 2. Ibid. 105. — 3. Volke J., Chem. zvesti *14*, 807 (1960). — 4. Heyrovský J., Techn. práca *5*, 475 (1953). — 5. Heyrovský J., Techn. práca *6*, 603 (1954). — 6. Heyrovský M., Nepublikováno. — 7. Kalvoda R., Macků J., Chem. listy *48*, 254 (1954); Collection *20*, 257 (1955). — 8. Heyrovský M., Z. physik. Chem. (Sonderheft) *1958*, 97. — 9. Heyrovský M., Nepublikováno. — 10. Heyrovský J., Forejt J., *Oscilografická polarografie*, Praha 1953, 96.

11. Heyrovský J., Chem. listy *47*, 1762 (1953); Collection *18*, 749 (1953). — 12. Heyrovský J., *Oszillographische Polarographie mit Wechselstrom*, Berlin 1959, 10. — 13. Kalvoda R., Macků J., Chem. listy *49*, 1565 (1955); Collection *21*, 493 (1956). — 14. Heyrovský M., Proc. 2. Internat. polarograph. Congress, Cambridge (v tisku). — 15. Vogel J., *Kandidátská disertace*, Polarografický ústav ČSAV, Praha 1960.

Adresa autora:

Prom. chemik Michael Heyrovský, Praha 1, Vlašská 9, Polarografický ústav ČSAV.

POLAROGRAPHIC WAVE OF ALUMINIUM

M. Heyrovský

Collection of Czechoslovak Chemical Communications, Vol. 25 (1960). – Published under the auspices of the Czechoslovak Academy of Science by the Publishing House of the Czechoslovak Acad. Sci., Vodičkova 40, Prague 2. – Address of the Editor: Institute of Chemistry, Czechoslovak Academy of Science, Na cvičišti 2, Prague 6. – Annual subscription Kčs 300·–, Rbl 120·80, US $ 30·20, £ 10/15/8, single issue Kčs 25·– Subscription orders should be addressed to ARTIA, 30 Ve smečkách, Prague 2, Czechoslovakia. – Printed by Knihtisk 05, Prague.

Zájemcům v ČSR dodává Poštovní novinový úřad, Jindřišská 14, Praha 3.

Reprinted from Collection Czechoslov. Chem. Commun. *25*, 3120—3136 (1960).

POLAROGRAPHIC WAVE OF ALUMINIUM

M. Heyrovský
Polarographic Institute, Czechoslovak Academy of Science, Prague

Received February 8th, 1960

To Academician J. Heyrovský on his 70th birthday.

Experimental data are given to prove that the polarographic wave of aluminium ions on the dropping electrode does not consist in reduction of cation to metallic state, but that three protons of the hexaquoaluminium ion are reduced. By various polarographic techniques catalytic activity of the reaction product, the aluminium hydroxide, in electrolytic evolution of hydrogen is revealed and all differences between the aluminium wave and the waves of ordinary acids are explained.

It is a known fact in technical electrochemistry that aluminium cannot be electrodeposited from aqueus solutions[1]. The aqueous solutions of aluminium ions, on the other hand, give a polarographic reduction wave, described as early as in 1931 [2] and since then often used for the analytical determination of aluminium[3–18]. Several authors have noticed the anomalous behaviour of this wave which does not correspond to the simple deposition of a metal[19,20].

It was suggested to explain the aluminium wave through the evolution of hydrogen[21–23], but no satisfactory scheme of electrode mechanism was given.

In papers published independently by two authors [24–27] the evolution of hydrogen was accounted for by the acidic properties of the hydrated aluminium ion in aqueous solutions. According to them the electrode reaction consists in reduction of three hydrogen ions from the hexaquoaluminium complex, which is thus changed into non-reducible aluminium hydroxide. This hypothesis fits in principle the experimental data, but it cannot explain all properties of the aluminium wave. Later on the present author tried to take direct reduction of aluminium into account for a better fitting explanation[28], but neither this was satisfactory.

The experiments described in the present paper prove that the polarographic wave of aluminium ions is due to the reduction of hydrions from the aquocomplex proceeding under the catalytic action of the reaction product, aluminium hydroxide, adsorbed at the electrode surface.

Aluminium hydroxide which is adsorbed at the electrode in the electrode process is shown to be the cause of all differences between the aluminium wave and the simple wave of proton reduction from an ordinary acid. The similarity of the polarographic behaviour of aluminium ion with that of some other cations shows that the conclusions drawn from the case of aluminium are of a more general validity.

Experimental

Chemicals and Apparatus

All experiments were carried out with solutions of $KAl(SO_4)_2.12\,H_2O$, p. a.; important results were then checked with aluminium chloride and sulphate of high purity. The salts used as supporting electrolytes and the organic compounds were of reagent grade.

Aluminium amalgam was prepared according to the method described by Heyrovský[29] by boiling mercury with strips of 99,99% Al in the atmosphere of pure dry nitrogen. The flask in

which the amalgam was prepared served, after cooling, directly as a reservoir for the dropping electrode; the reservoir was joined to a capillary tube of a wide boring (about 0·2 mm). The wide boring was necessary, because a narrow capillary was easily blocked by aluminium hydroxide. The drop-time was consequently short, about 0·2 s.

Most of the experiments were made in the Kalousek cell with a separated saturated calomel electrode. All the solutions were deprived of oxygen by passing pure nitrogen through the cell. The surface of the dropping mercury electrode was observed by means of a binocular microscope through a plane round window in the wall of the cell according to Šerák[30] with a separated saturated calomel electrode.

For streaming electrode the arrangement described by Kůta[31] was applied. In these experiments thallous sulphate was added to the solutions and the thallium wave was registered from which correction on the potential drop i. R was made. The resistance of the whole polarizing circuit and of the cell was found to be 400 Ω.

The hanging mercury-drop electrode was of the type described by Kemula[32] in Vogel's[33] modification.

Polarographic curves were registered using V 301 and LP 55 polarographs; oscillographic curves were followed with the P 576 polaroscope Křižík and the voltage impulse polarographic oscilloscope designed by Valenta[34]. The investigation of polarographic reversibility was carried out with the commutator by Kalousek and Rálek[35]. The *i–t* curves were followed on the N 522 oscilloscope Křižík and registered with a string galvanometer by means of an adapter for polarographic *i–t* curves devised by Němec and Smoler[36].

To keep the temperature constant a simple thermostat was used; the results of measurements at varying temperature are corrected for the temperature dependence of the potential of saturated calomel electrode.

Logarithmic analysis of *i–t* curves was done after the correction for the charging current.

The A. C. polarographic curves were drawn point by point with the use of a simple circuit[37] consisting of the V 301 polarograph, *RC* alternating voltage generator Tesla and an alternating milivoltmeter Tesla.

For plotting electrocapillary curves the drop-time of ten drops was measured at every 50 mV of the voltage applied to the dropping mercury electrode. Mean values of three independent measurements were used for the construction of the parabola; from this curve the derivative was obtained by graphical method.

pH-values were measured using a Phillips GM pH-meter with a glass electrode. The data of potentials are given against the saturated calomel electrode.

Results

Unbuffered aqueous solutions of aluminium salts, slightly acidic because of hydrolysis, give a polarographic reduction wave the shape and position of which depend remarkably on the composition of the solution (Fig. 1). In 0·1N solutions of salts of alkali metals or alkaline earth metals the waves are very

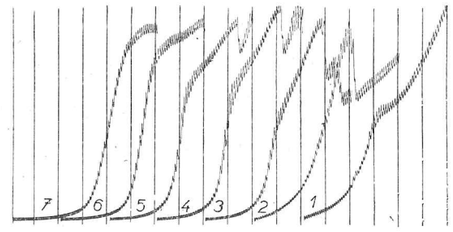

Fig. 1
Curves of Al^{3+} in 0,1M-LiCl at Various Concentrations
Concentration of $KAl(SO_4)_2$: *1* 5 . 10^{-5}M; *2* 1 . 10^{-4}; *3* 3 . 10^{-4}; *4* 5 . 10^{-4}; *5* 7 . 10^{-4}; *6* 2 . 10^{-3}; *7* 4 . 10^{-3}M; from −1,3 V; 100 mV/absc., sensitivity reduced stepwisely from 1 : 3 to 1 : 200.

similar; for investigation of the electrode process lithium or tetramethylammonium salts are most suitable as supporting electrolytes.

At concentrations of the order of 10^{-5}M of aluminium salt the wave with a half-wave potential at $-1{\cdot}58$ V is purely diffusion-controlled. Its logarithmic analysis gives two straight linear parts the slopes of which are 132 mV (at more positive potentials) and 84 mV, respectively. The wave height corresponds according to the Ilkovič equation to a 3-electron reduction. With increasing temperature between 10° and 60°C the limiting current increases by 1·2% per degree and the half-wave potential shifts to positive values by $+3{\cdot}6$ mV per degree.

From the concentration of about $6 \cdot 10^{-5}$M at the rising part of the curve there appears a maximum, falling abruptly down to the limiting current at more negative potentials. The current at maximum is a linear function of the square root of the height of mercury reservoir the dependence showing a kinetic component of the current.

On *i–t* curves obtained at potentials at which the polarographic curve exceeds the height of the limiting diffusion current there appears at first a slight undulation indicating an adsorption process. The undulation changes into sharp cuts the number of which increases as the potential approaches the summit of the maximum. The shape of these *i–t* curves is not exactly reproducible; between the first and the following drops (Fig. 2) there is no essential difference. After the fall of the maximum the shape of *i–t* curves indicates adsorption taking place at the beginning of the drop-time. In the potential range of the maximum one observes a mild streaming of the solution in small whirls round the surface of the electrode, without any uniform direction, resembling the streaming characteristic for catalytic processes.

This maximum is suppressed by gelatine or by a small concentration of lanthanum ions. The maximum relative height of the current peak is reached at the concentration of about $1{\cdot}7 \cdot 10^{-4}$M-Al^{3+}, when the maximum current attains almost twice the value of the limiting current. At higher concentrations the ratio of maximum to the limiting current decreases, but the occurrence of the maximum remains characteristic for the aluminium wave.

The maximum is highly sensitive to the presence of hydrions or proton donors in the solution (Fig. 3). Hydrogen ions from stronger acids, reduced at potentials more positive than is the maximum, cause an increase of the

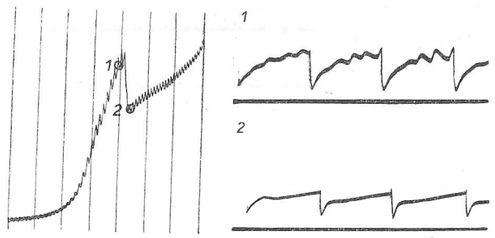

Fig. 2
i–t Curves Registered at Denoted Potentials
$1{\cdot}2 \cdot 10^{-4}$M-$KAl(SO_4)_2$ in 0,1M-LiCl.

maximum by more than 100% at a concentration 5times higher than that of aluminium ions. The increase of maximum with addition of strong acid is not linear — it reaches a limit which is practically obtained at a tenfold excess of hydrions over aluminium ions. Weak acids giving the hydrogen wave at potentials more negative or giving no wave at all (e. g. boric acid, phenol or ammonium ions) raise the maximum to the same extent but at concentrations 10 to 50times greater as compared to strong acids. In acetate buffer solution the whole wave of aluminium ions disappears in a drawn-out curve due to the reduction of hydrogen ions (cf.[23]).

At the concentration of about $1{\cdot}7 \cdot 10^{-4}$M of aluminium ions there appears at the foot of the wave a steep increase of current which at higher aluminium concentrations extends to the whole ascending part of the curve. From the dependence on the mercury pressure it follows that this increase is of an autocatalytic nature: by lowering the mercury reservoir the current at the foot increases (Fig. 4). The autocatalytic nature is clearly demonstrated by the *i–t*

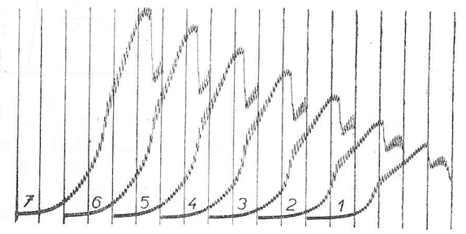

Fig. 3
Effect of Weak Acid on Maximum Height
1 $3 \cdot 10^{-4}$M–$KAl(SO_4)_2$ in 0·1M-LiCl. 10^{-2}M acetic acid added to 5 ml of the solution: *2* 0·1 ml; *3* 0·2 ml; *4* 0·3 ml; *5* 0·4 ml; *6* 0·5 ml; *7* 0·6 ml. From $-1{\cdot}3$ V; 100 mV/absc.; $S = 1 : 40$.

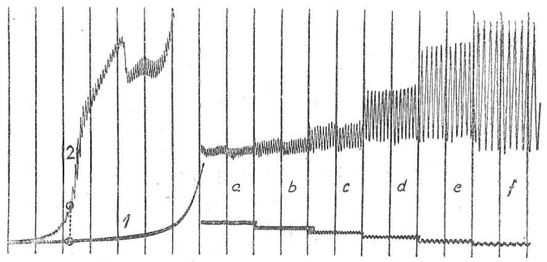

Fig. 4
Dependence of Current at Denoted Constant Potential on the Height of Mercury Reservoir
1 0·1M-LiCl; *2* in presence of $3{\cdot}5 \cdot 10^{-4}$M-$KAl(SO_4)_2$. Height of mercury head: *a* 121 cm; *b* 100 cm; *c* 84 cm; *d* 64 cm; e 49 cm; *f* 36 cm. Sensitivity: *1*, *2* 1 : 20, *a*—*f* 1 : 10.

curves (Fig. 5); their shape corresponds to the equation $i = k \,.\, t^a$, where a attains the value of 1·25. When the potential gets gradually more negative, the autocatalytic increase of current is slowed down at the end of the drop-time; then it rises again and finally the shape of the curve results in the form of damped oscillations. In the region of potentials of the maximum (cf. Fig. 1) on polarographic curves the regular oscillations on i–t curves change into irregular acute cuts, the number of which increases towards the highest point of the maximum. Besides the autocatalytic part on the polarographic curves there appears a second rounded maximum (cf. Fig. 1) of a catalytic nature which is evident from the dependence on the mercury pressure and from the i–t curves. If constant potential of the second maximum is applied to the electrode, the current falls after an interval of about 10 drops to the height of a three-electron reduction and then its value remains virtually constant, only with slight irregular oscillations (Fig. 6). When using a horizontal capillary the registered current-voltage curve shows instead of the second maximum a wave merging into the current of deposition of Li^+ ions.

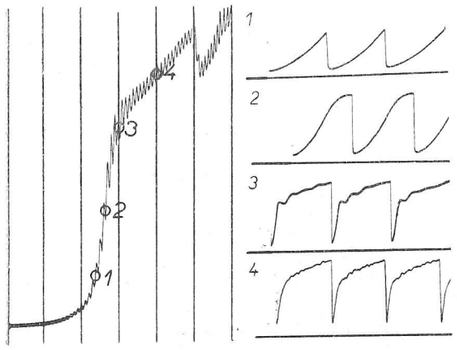

Fig. 5
i–t Curves Registered at Denoted Potentials
$4 \,.\, 10^{-4}$M-$KAl(SO_4)_2$ in 0,1M-LiCl.

Polarographic curves and sequences of i–t curves closely similar to the curves due to aluminium ions are obtained for beryllium and scandium with the only difference that the wave for scandium is by about 50 mV and the wave for beryllium by 140 mV more negative (Fig. 7).

Autocatalytic shape of i–t curves changing into oscillations with increasing negative potential was observed also for lanthanum and some rare earth metals (tried with Pr, Nd, Sm). Thorium gives no autocatalytic reaction at potential of the foot of the wave, but on the limiting current the i–t curves have the same structure of irregular oscillations of high frequency as with aluminium.

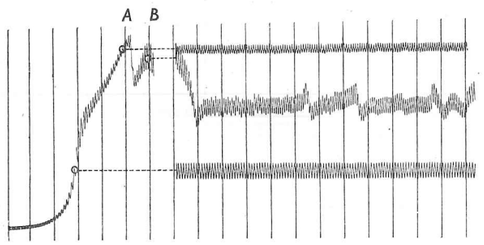

Fig. 6
Time Dependence of Current Registered at Denoted Constant Potentials
$3{\cdot}8 \,.\, 10^{-4}$M-$KAl(SO_4)_2$ in 0·1M-LiCl; distance of abscissae 31 s.

In 10^{-3}M solutions of aluminium salts in 0·1N supporting electrolyte the wave of aluminium ions is accompanied by evolution of small bubbles of gas on the electrode, as observed by means of a microscope. At potentials of the foot of the wave there appears a slow movement of the electrode surface.

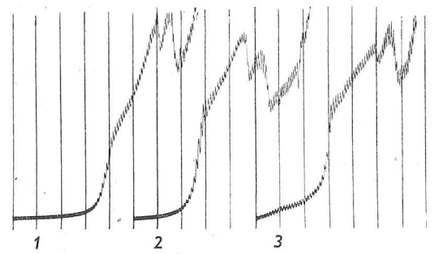

Fig. 7
Polarographic Curves of $4 \,.\, 10^{-4}$M *1* $BeCl_2$, *2* $AlCl_3$; *3* $SeCl_3$ in 0·1M-LiCl
From −1·3 V; 120 mV/absc., $S = 1 : 20$.

At more negative potential this movement becomes quicker, chaotic and jerky; on the surface there float small islets of a colourless crystalline substance which gradually get thicker and form a continuous white film. The intensity of the whirling motion of the surface becomes greatest at about 1/4 of the total height of the wave; when the white film covers the electrode, the motion becomes slower again. The solution surrounding the electrode remains during the motion of the surface entirely quiet. When the potential approaches the limiting current the electrode is covered by a thick white layer, in which crevices appear, resoldering and reappearing during the drop growth. At the potential of the fall of maximum the film is compact, it does not move nor burst any more. At potential of the second maximum the solution round the electrode becomes turbid and whirls slightly, whilst the electrode surface remains quiet. This whole process is accompanied by the formation of tiny bubbles of gaz collecting at the orifice of the capillary. In presence of alcohol, gelatin or complex forming anions in the solution the white film disappears and the motion of the surface ceases.

Quite analogous effects may be observed in solutions of beryllium and scandium at potentials of their reduction waves. White moving film and evolution of bubbles at the electrode surface appear even with thorium and lanthanum; the formed white layer does not appear so thick and voluminous as with aluminium, beryllium or scandium.

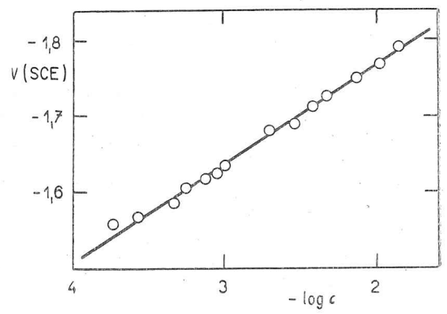

Fig. 8
Dependence of Half-wave Potential of the Aluminium Reduction Wave on Aluminium Ions Concentration in 0·1M-LiCl

With increasing concentration of aluminium ions the whole wave shifts towards negative potentials (Fig. 8); an analogous effect has the acidity of the solution (Fig. 9).

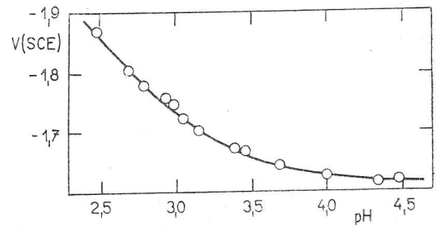

Fig. 9
Dependence of Half-wave Potential of the Aluminium Reduction Wave on pH
$1{\cdot}9 \cdot 10^{-4}$M-$KAl(SO_4)_2$ in 0·1N-LiCl; HCl added.

The temperature coefficient of the half-wave potential is 3·5 mV per degree at $1 \cdot 10^{-4}$M, 3·3 mV per degree at $3 \cdot 10^{-4}$M and 2·9 mV per degree at $7{\cdot}5 \cdot 10^{-4}$M-Al^{3+}. The temperature coefficient of the limiting current of the whole wave with the first maximum is constantly about 1·2% per degree; the relative height of the first maximum A decreases with increasing temperature. The second rounded maximum B has its temperature coefficient about 4·4% per degree.

With increasing concentration the wave first becomes steeper and then drawn out again. For $6 \cdot 10^{-5}$M-Al^{3+} the logarithmic analysis of the curve gives an approximately straight line with a slope of 94 mV. The approximate values of the slopes obtained for various concentrations are as follows: 48 mV for $2{\cdot}9 \cdot 10^{-4}$M-Al^{3+}; 45 mV for $4{\cdot}3 \cdot 10^{-4}$M-Al^{3+}, 42 mV for $7{\cdot}4 \cdot 10^{-4}$M-Al^{3+}. At still higher concentrations the steepness of the wave becomes less; the logarithmic analysis fits the linear relatioship better: 65 mV at $2 \cdot 10^{-3}$M-Al^{3+} and 84 mV at $4{\cdot}3 \cdot 10^{-3}$M-Al^{3+}. The autocatalytic nature of the current at the foot of the wave is maintained even at these concentrations. The dependence of the half-wave potential on the drop-time and on the rate of flow of mercury was measured at a concentration of $3{\cdot}8 \cdot 10^{-3}$M of aluminium, where the maximum is relatively small and the half-wave potential well defined. With increasing drop-time and with decreasing rate of flow of mercury the half-wave shifts towards positive potentials (by about 20 mV in the range of 1 to 5 s and by about 10 mV for $m = 2$ mg/s to $m = 1$ mg/s). This shift of the wave with lowering of the mercury reservoir occurs at all concentrations.

Addition of gelatin suppresses the autocatalytic nature of the current as well as the two maxima. In 10^{-4}M solutions of aluminium ions the addition of 0·01% of gelatin restores the usual monotonous shape of the i–t curves corresponding to the irreversible electrode reaction; at the same time the polarographic i–E curve loses its steepness.

The shift of the polarographic wave towards negative potentials is also caused by increasing concentration of the supporting electrolyte (with the exception of lithium salts, for which the shift occurs in opposite direction). The magnitude of the shift depends on the cation. In 0·1N solutions the half-wave potentials are practically the same, in 1N supporting electrolytes considerable differences appear. With $7 \cdot 10^{-4}$M-$AlCl_3$ the half-wave potential lies at −1·610 V in 0·1N solutions of chlorides at 20°C. In 1N solutions the half-

wave potentials are as follows: LiCl −1·575 V; NaCl −1·625 V; KCl −1·665 V; $N(CH_3)_4Cl$ −1·710 V; $MgCl_2$ −1·650 V; $CaCl_2$ −1·695 V; $BaCl_2$ −1·705 V.

A striking change in the complicated shape of the wave appears after addition of complex forming substances to the solution (Fig. 10). With sulphates we must increase the concentration over 0·1M, with fluorides, oxalates, tartarates (cf. [23]) and citrates it is sufficient to add amounts equivalent to the aluminium ion concentration to obtain the same effect. In all cases with successive additions of reagents the autocatalytic part of the wave as well as the maxima disappear; finally simple diffusion-controlled polarographic wave of a constant height ensues, which shifts to negative potentials, until it disappears in the current of the supporting electrolyte. A similar change in the curves may be observed when increasing the amount of enthanol in the solution: autocatalysis and the maximum disappear and a simple wave remains starting at slightly more positive potentials. In a 90% ethanolic solution there appears one more positive wave; both the waves are diffusion-controlled (Fig. 11).

On the other hand additions of alkaline hydroxides have a similar effect as when merely diluting the solution; we obtain a reversed sequence of curves as when the concentration of aluminium ions is increased.

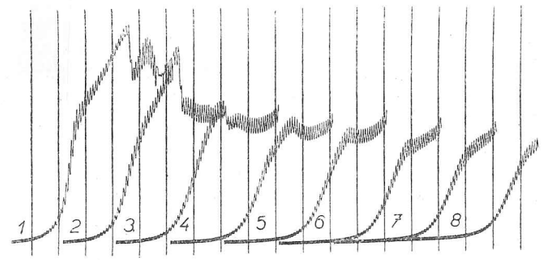

Fig. 10
Effect of Complex Forming Substances
1 5 ml of $3{\cdot}8 \cdot 10^{-4}$M-$KAl(SO_4)_2$ in 0·1M-LiCl; addition of 0·2 ml 10^{-2}M-KF: *2* 0·2 ml; *3* 0·4 ml; *4* 0·6 ml; *5* 0·8 ml; *6* 1·0 ml; *7* 1·2 ml; *8* 1·4 ml. From −1·3 V, 100 mV/absc.; $S = 1 : 20$.

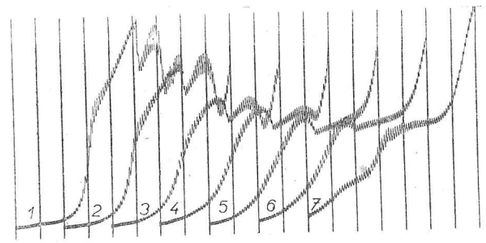

Fig. 11
Effect of Ethanol
$4 \cdot 10^{-4}$M-$KAl(SO_4)_2$; in 0·2 M-LiCl; concentration of ethanol: *1* 0; *2* 15%, *3* 30%; *4* 45%; *5* 60%; *6* 75%; *7* 90%. From −1·2 V; 100 mV/absc., $S = 1 : 20$.

Addition of aluminium salts into unbuffered solutions of substances polarographically reducible under consumption of protons causes an analogous effect as the addition of mineral acids[38]. Even a catalytic wave of hydrogen evolution due to some organic compounds occur in presence of aluminium ions similarly as in presence of hydrions[24,26]. Equal effects are obtained for solutions of corresponding concentrations, the pH values of which differ considerably: 10^{-3}M-$KAl(SO_4)_2$ (pH 4·12) influences the reduction of organic substances to the same extent as 10^{-3}M-H_2SO_4 (pH 2·8).*

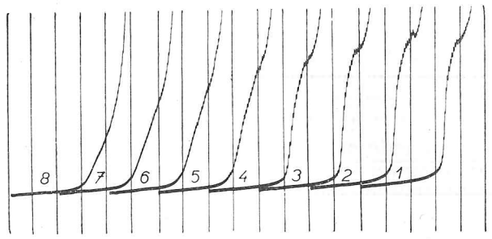

Fig. 12

Curves Registered with Commutator at Frequency 5 c/s; Influence of the Auxiliary Potential 2 . 10^{-3}M-$Al_2(SO_4)_3$ in 0·1M-KCl; Auxil. potential: *1* −1·4 V; *2* −1·5 V; *3* −1·6 V; *4* −1·65 V; *5* −1·7 V; *6* −1·75 V; *7* −1·8 V; *8* −1·85 V. From −1·0 V; 200 mV/absc., S = 1 : 100.

The curves of aluminium salt solutions registered with the commutator by Kalousek do not show any anodic wave even at the frequency of 32 c/s. If the auxiliary potential is shifted to the negative part of the wave, the wave diminishes, becomes drawn-out and indistinct. The foot of the wave shifts at the same time towards positive potentials (Fig. 12).

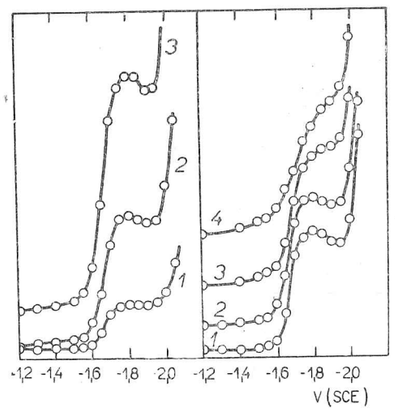

Fig. 13

A. C. Polarograms of 3·8 . 10^{-3}M-$KAl(SO_4)_2$ in 0·1M-LiCl

a Influence of the amplitude of alternating voltage component at frequency 50 c/s: *1* 5 mV; *2* 15 mV; *3* 30 mV; *b* influence of frequency of alternating voltage component at the amplitude 15 mV: *1* 20 c/s; *2* 50 c/s; *3* 100 c/s; *4* 200 c/s.

* The behaviour of chromic ions (at potentials more positive than the reduction wave of Cr^{3+}) was found to be analogous to Al^{3+} ions in this respect.

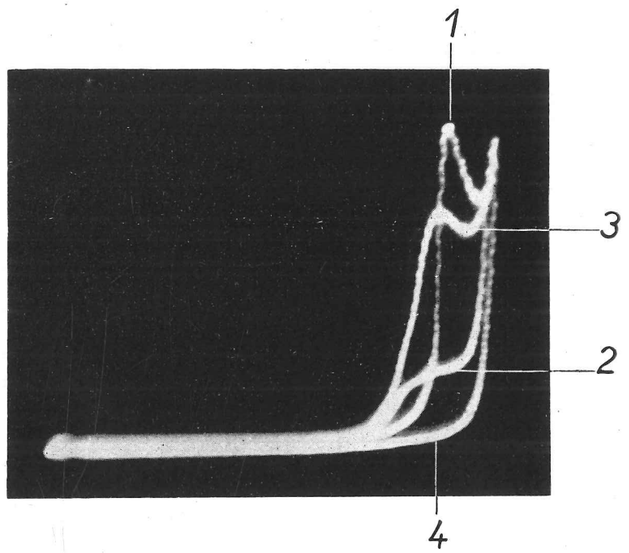

Fig. 16

Oscillographic *i*–*E* Curves with Triangular Voltage Impulses

3·8 . 10^{-3}M-$KAl(SO_4)_2$ in 1M-KCl. Electrode polarized by two successive triangular impulses from −0·1 to −1·95 V at the rate of 3·58 V/s. Current voltage curves corresponding to the increasing and decreasing phases of the impulses follow in the order *1,2,3,4*.

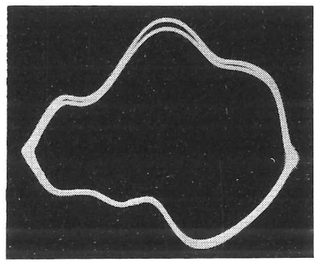

Fig. 18

Oscillographic $dE/dt = f(E)$ Curve of Aluminium Amalgam Dropping into 1M-KCl

A. C. polarographic curves of Al^{3+} ions registered with various frequencies and amplitudes of the alternating voltage component reveal peaks of an unusual shape, about 10times smaller than would correspond to a 3-electron reversible reduction (compared with Tl^{+}) (Fig. 13). The height of the peak is not a linear function of aluminium ions concentration but it reaches a limit. (Paralelly registered peaks due to hydrogen ion reduction from hydrochloric and acetic acids are strictly proportional to the concentration).

Ordinary current-voltage curve obtained with the streaming electrode looks like composed of two different waves: at the beginning the current increases only slowly with the applied voltage; then the wave attains a steep slope, steeper than a two-electron reversible reduction (Fig. 14).

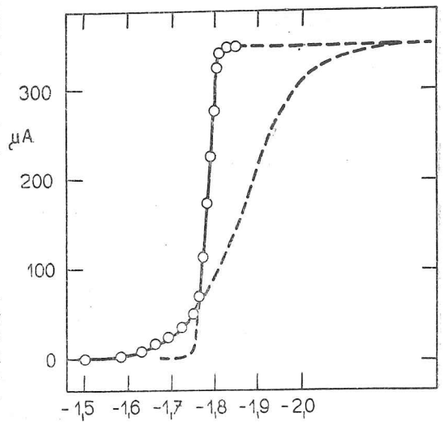

Fig. 14

Polarographic Curve of $1{\cdot}2 \cdot 10^{-3}$M-$KAl(SO_4)_2$ in 1M-LiCl on the Streaming Electrode (after correction for $i.R$ drop)

Dashed lines indicate the hypothetical curves of two separate processes, a 3-electron reaction and hydrogen-ion reduction.

With the hanging drop electrode aluminium ions give a current–voltage wave of a smaller slope than a reversible one-electron reduction, but steeper than the hydrogen wave. The position of the wave on the potential axis and its shape depend on the state of the electrode surface; with a fresh surface it

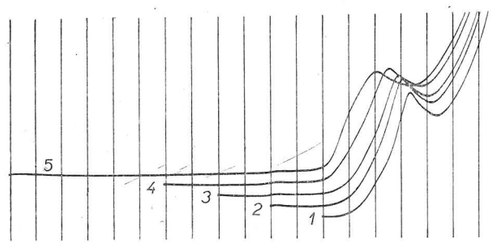

Fig. 15

Polarographic Curves on the Hanging Mercury Drop

$3{\cdot}8 \cdot 10^{-4}$M-$KAl(SO_4)_2$ in 0·1M-LiCl. Effect of time on peak potential: Curves registered from *1* −1·2 V; *2* −1·0 V; *3* −0·8 V; *4* −0·6 V; *5* 0 V; 100 mV/absc.; $S = 1 : 15$. Distance between abscissae 30 s.

depends on how long the electrode has been in contact with the solution before polarization (Fig. 15). The longer the drop hangs in the solution, either under an applied potential or not, the more positive is the wave. This shift has its limit at the potential of reduction of hydrogen ions from a strong acid beginning at −1·2 V, which is reached after about ten minutes of contact of the electrode with the solution prior to its polarization. In comparison with the curve registered immediately after dipping the electrode into the solution the curve registered after ten minutes is shifted to positive potentials by approximately 130 mV. This time effect does not occur in the presence of gelatin.

A similar, only less pronounced, influence of time of contact of the electrode with the solution on the shape and position of the wave may be observed for beryllium, scandium and lanthanum.

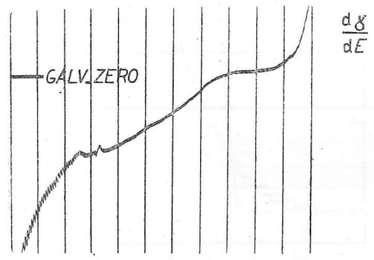

Fig. 17

Anodic Curve of Aluminium Amalgam Dissolution

0·1M-KCl; from 0 V; 200 mV/absc.; S = = 1 : 150.

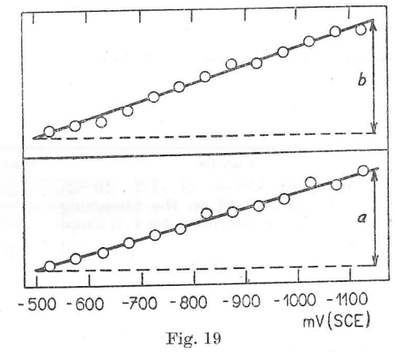

Fig. 19

Dependence of the Derivative of Surface Tension on Potential of Polarized Mercury Drops

a in 0·1M-LiCl; *b* in 10^{-3}M-$KAl(SO_4)_2$, 0·1M-LiCl.

Repeated cyclic polarization, both slow (by means of a polarograph) and rapid (oscillographic i–E curves), causes a marked decrease of the wave of aluminium ions. On all these curves there is no indication of any anodic process. At the ascending part of a rapid polarization pulse (from 3 V/s) the curve is steeper in the first polarization cycle and the foot of the wave is by 200 to 300 mV more negative than at the descending branch of the pulse and at all following cycles (Fig. 16*).

Oscillographic curves obtained by polarizing the dropping mercury electrode by alternating current or voltage at a frequency of 50 c/s do not show any depolarization due to aluminium ions. A slight difference from the curve for pure supporting electrolyte appears at negative potentials only during the first few moments of the formation of a new drop.

A specific effect appears with the cyclic polarization of the mercury electrode if besides aluminium ions also lithium ions are present in the solution. This special case has been dealt with by several authors[39–43,28,61]; it will not be discussed in this general treatment.

* See insert facing p. 3128.

Aluminium amalgam in aqueous solutions gives a drawn-out anodic wave beginning at −1·5 V (Fig. 17). Oscillographic alternating current and alternating voltage controlled curves show irreversible anodic dissolution of the amalgam (Fig. 18*). The electrocapillary curve in a 10^{-3}M solution of $KAl(SO_4)_2$ differs from the curve obtained for pure 0·1N-LiCl by steeper branches. This is clearly shown after differentiation of the electrocapillary curves. The resulting dependence of $d\gamma/dE$ on E gives two straight lines the slope of which has the physical meaning of the integral capacity of the electrode (Fig. 19). In our case on the negative part of the electrocapillary parabola the slope of the line increases in the presence of aluminium ions in the ratio 7 : 6.

Discussion

The existence of hexaquoaluminium ions in diluted aqueous solutions of aluminium salts is generally accepted in chemical literature[44]. Hydrolysis is due to the acidic properties of these ions. In polarography they act, similarly as the hexaquochromium ions (in a much narrower range of potentials), like proton donors in reduction reactions in which hydrogen ions are consumed. The reduction wave proper of aquo-aluminium ions has many properties of a reduction wave of hydrogen ions from weak acids. It is known that the potential of aluminium electrode becomes more positive with increasing acidity of the solution[45]; the polarographic wave, on the contrary, shifts to more negative values; this can be explained by the suppression of dissociation of the aquo-complex. This can account for the shift of the wave with increasing concentration as well; acetic acid gives qualitatively the same effect as was found by Tomeš[46].

The influence of cations of the supporting electrolyte on the reduction potential of a cation was observed in the case of the hydrogen wave[47] for which the sequence of action of alkali metals and alkaline earth cations is the same as with aluminium. The temperature coefficient of about + 3 mV per degree of the half-wave potential is unusually high; such a value is reported for the potential of a 45° tangent of the hydrogen wave[48]. The bubbles of gaz observable at the surface of the electrode can be ascribed to the hydrogen evolved. At stationary electrode the cathodic wave of aluminium ions is obtained more positive by about 200 mV than is the beginning of anodic dissolution of aluminium amalgam in the same solution. The total irreversibility of the electrode process was proved by experiments obtained with the stationary electrode, with the commutator of Kalousek as well as from the results of the method by Breyer and from oscillographic curves.

Since the height of the wave corresponds to a 3-electron reduction, it follows that the hexaquoaluminium ion acts as a tribasic acid. The single and continuous polarographic wave indicates that the values of all the three dissociation constants are nearly of the same magnitude; Brönsted and Volqvartz[49] found the value $1{\cdot}3 \cdot 10^{-5}$ for infinite dilution at 15°C. The potential of the wave is near to that of the wave of acetic acid with the dissociations constant[50] $1{\cdot}745 \cdot 10^{-5}$ (infinite dilution, 15°C). All these experimental facts confirm the proposed scheme of the electrode reaction:

$$Al(OH_2)_6^{3+} + 3\,e \rightarrow Al(OH)_3 + 3/2\,H_2 + 3\,H_2O$$

* See insert facing p. 3128.

At concentrations of aluminium ions of the order of 10^{-5}M, logarithmic analysis of the wave gives results similar to those obtained by Kůta[51] for the hydrogen wave in a large excess of the supporting electrolyte. From $5 . 10^{-5}$M-Al^{3+} upwards the wave begins to differ from that due to reduction of hydrogen ions. At this concentration the limiting diffusion current reaches the value of about $3{\cdot}5 . 10^{-7}$ A, when inside the diffusion layer of the thickness of $5 . 10^{-3}$ cm the solubility of aluminium hydroxide is exceeded within the drop time of 2·6 s and the precipitate remains adsorbed on the electrode surface. The appearance of a new phase at the electrode surface disturbs the surface tension of mercury what causes the motion of the surface*. Solid aluminium hydroxide is a strong adsorbent which is able, thanks to its amphoteric nature, to adsorb the acidic as well as the basic components of the solution[62]. The adsorbent influences the dissociation equilibria at the electrode surface and this fact appears to be the cause of differences between a simple reduction wave of hydrogen ions from weak acids and that of aluminium ions.

The kinetic character of the maximum and its sensitivity to pH of the solution lead to the conclusion that it is due to the reduction of hydrogen ions from water split off from it through the action of aluminium hydroxide. Similarly as in the case of water molecules the adsorbent reacts with other weak acids. The influence of stronger acids may be explained by occupation of free places on the surface of adsorbent by protons from the solution, which are then reduced at the maximum. This view is supported by the fact that the height of the maximum reaches a limit at high concentrations of H^+-ions.

Aluminium hydroxide as the reaction product acts catalytically, but on the other hand it occupies part of the electrode surface and thus slows down the reaction. Contrary to this the growth of the drop renews the surface. Further, the OH^--ions saturating the surface of the adsorbent as a result of the reaction may change new aluminium ions, coming to the electrode, directly into aluminium hydroxide which then contributes to the catalytic action. These contrary tendencies alternatingly prevailing in the electrode process may account for the formation of the irregular sharp cuts in the *i–t* curves at potentials of the polarographic maximum.

At the potential at which the maximum falls to the three electron height, the adsorbed layer changes probably its structure and loses the catalytic activity, analogously with the mechanism, assumed in usual cases of the catalytic hydrogen ion reduction[52]. Only above $2 . 10^{-4}$M-Al^{3+} a new catalytic wave appears after the fall of the first maximum. It is most probably due to catalytic reduction of hydrogen ions by a different mechanism. The decrease of current in the second maximum is caused by saturation of the vicinity of the electrode with reaction products, probably with aluminium hydroxide and hydroxyl ions, and by their transfer to the following drops.

Gelatin added to the solution occupies the electrode surface. It does not affect the reduction of hydrogen ions from the aquocomplex, but it hinders the formation of the precipitate and thus affects its catalytic activity, and the characteristic maximum is suppressed. An analogous influence of lanthanum ions can be explained by an inhibitory action on catalytic properties of aluminium hydroxide.

* A similar effect may be observed at positive potentials in solutions of chlorides when a film of calomel is formed at the electrode.

With the increasing concentration of aluminium ions the point on the polarographic curves, corresponding to the beginning of formation of solid aluminium hydroxide at the surface of the electrode, shifts gradually towards the foot of the wave. At about $2 . 10^{-4}$M-Al^{3+} the formation of solid hydroxide begins at about 1/10 of the total height of the wave, where the electrode reaction proceeds practically without concentration polarization. The autocatalytic character of *i–t* curves shows that aluminium hydroxide affects even the reduction of hydrions from the hexaquoaluminium complex. This property of the freshly precipitated aluminium hydroxide is also evident from the results with commutator and from oscillographic *i–E* curves; the hydroxide formed at the electrode surface shifts the beginning of the electrode reaction to more positive potentials. The catalytic activity can be observed only on freshly precipitated hydroxide, probably before bigger crystals are formed. Aluminium ions as such adsorbed at the negative interface, as evidenced from electrocapillary curves (see also[53]), do not show any catalytic effect on reduction of hydrogen ions from other acids. The same negative result gives aluminium hydroxide prepared separately and added into the solution.

The hindering effect of the layer of aluminium hydroxide on electrode reactions is evident from the results with alternating polarization of the electrode. Oscillographic curves indicate formation of the layer which after 6—10 cycles entirely suppresses the reaction proper of aluminium ions. On the curves obtained with the commutator the reduction wave decreases for the same reason with the shift of the auxiliary potential towards negative values at which the electrode is covered with hydroxide. Similarly the a. c. polarograms indicate that the electrode process is followed by adsorption of the reaction product preventing the linear increase of the peak with concentration.

In this way the autocatalytic nature of the reaction and its slackening by the reaction products together with the constant formation of the fresh electrode surface leads to a periodic electrochemical reaction. These principles are common for periodic chemical reactions in general[54]. Autocatalytic increase of current at the ascending part of the wave is the cause, why the aluminium wave is steeper than the hydrogen wave. Gelatin suppresses the action of aluminium hydroxide and reduces the steepness of the wave. At higher concentrations of aluminium ions the hindering effect of the adsorbed layer predominates and the increase of current in the ascending part is slowed down. The influence of the adsorbed layer of aluminium hydroxide on the electrode process explains the dependence of the half-wave potential on the rate of flow of mercury which has not been found in the case of the hydrogen wave.

At the surface of the stationary electrode there accumulates a species which makes the following reduction easier. As the time effect is the same whether or not potential is applied to the electrode the collecting particles must be electrically neutral. It is most probably again aluminium hydroxide, always present in minute quantities in aqueous solutions of aluminium ions, which is adsorbed at the electrode surface. There it may form small islets of solid phase, acting catalytically in the same way as observed in other experiments. Gelatin suppresses the catalytic effect by occupying the surface as a more adsorbable substance. The shift of the aluminium wave to positive potentials obtained with the hanging electrode has for a limit the reduction potential of hydrogen ions from strong acids. This shows that the catalytic action of

aluminium hydroxide does not consist in affecting the reduction proper of the proton, but probably in setting free the proton from its bond in the proton donor. Such a concept would agree with ideas about the influence of adsorption on chemical bonds.

At higher contents of alcohol in solution the catalytic maximum is suppressed, probably as a result of the suppression of dissociation of week acids in alcohol[55]. Since in alcoholic solutions there are great differences between the dissociation constants[56], the first wave in 90% ethanol belongs probably to the first hydrogen ion dissociated from the complex.

On addition of complex forming anions the aquocomplex is changed into different complexes which have no more hydrogen ions to be split off. This is the reason why the maximum and autocatalysis disappear. In the new wave the central aluminium ion is probably reduced directly to the metallic state. This would explain the shift of the new wave to negative potentials with further addition of anions. The addition of alkaline hydroxides, on the other hand, turns the aquoions directly into polarographically inactive particles of aluminium hydroxide.

At the streaming electrode the time of contact between the solution and the electrode surface is too short to let the reaction product affect the reaction process. The reduction curve of hydrion from a strong acid has the same slope at the streaming as at the dropping mercury electrode, but it shifted to negative potentials with the half-wave at $-1{\cdot}80$ V[31]. The foot of the aluminium wave seems to correspond to the reduction of hydrogen ion, but at more negative potentials the mechanism proceeds probably by direct reduction of the aluminium ion. The rate of this reaction increases more quickly with the potential and so it soon prevails over the hydrogen ion reduction. This allows us to suppose that even with the dropping mercury electrode, at sufficiently negative potentials, the direct reduction of aluminium cation takes part in the electrode process (cf.[27]). The abrupt fall of the polarographic maximum denotes probably the potential at which the reduction to the metallic state predominates. As the whole process is irreversible even at high frequencies of alternating polarization, the metallic aluminium must undergo a rapid inactivation with water to aluminium hydroxide and gazeous hydrogen. The crystalline structure of the aluminium hydroxide formed by this reaction differs probably from that formed in reduction of hydrogen ions; this would perhaps explain the different catalytic activity of the film at different potentials of the aluminium wave.

Between aluminium and other cations an analogy in polarographic behaviour may be found in various respects. Similarly to aluminium behave beryllium and scandium ions which indicates analogous forms of complexes in solution[57,58], as well as similar properties of hydroxides of these elements. The absence of autocatalytic phenomena at the foot of the thorium wave may be accounted for by the stepwise dissociation of the thorium aquocomplex[59]. Judging from the data given in literature (for a review see[60]) and from autocatalytic $i-t$ curves obtained for the reduction waves of rare earth elements it may be supposed that similar factors as described for aluminium play role in the respective electrode reactions.

References

1. Field S.: *The Principles of Electrodeposition*, 2. ed., p. 102. Pitman, London 1949.
2. Prajzler J.: This Journal *3*, 406 (1931).
3. Gokhstein J. P.: Zavodskaja lab. *5*, 28, 158 (1936).
4. Gull H. C.: J. Soc. Chem. Ind. *56*, 177 (1937).

5. Hövker G.: *Dissertation*. Hansische Universität, Hamburg 1938.
6. Heller B. A., Zanko A. M.: Zavodskaja lab. *8*, 1030 (1939).
7. Kozlova A. A., Portnov M. A.: Zavodskaja lab. *9*, 287 (1940).
8. Semerano G., Ronchi I.: Atti R. Ist. Veneto Sci., C II, 397 (1941).
9. De Almeida H.: Anais Inst. Vinho Porto, No. 7, 11 (1946).
10. Payne S. T.: Rept. No. 729, p. 17, Brit. Non-ferrous Metals Research Assoc., London 1947.
11. Ford C. L., Le Mar L.: Am. Soc. Test. Mater. Bull. *157*, 66 (1949).
12. Hodgson H. W., Glover J. H.: Analyst *76*, 706 (1951).
13. Ishibashi M., Fujinaga T.: J. Chem. Soc. Japan. *73*, 538 (1952).
14. Proszt J., Paulik J.: Magyar Kém. Folyóirat *58*, 113 (1952).
15. Hibino M., Hayashi Y., Shinagawa M.: Japan. Analyst *4*, 41 (1955).
16. Page J. A., Simpson D. H., Graham R. P.: Anal. Chim. Acta *16*, 194 (1957).
17. Perkins M., Reynolds G. F.: Anal. Chim. Acta *18*, 616 (1958).
18. Reynolds G. F., Webber T. J.: Anal. Chim. Acta *19*, 293, 406 (1958).
19. Stackelberg M. v.: *Polarographische Arbeitsmethoden*, p. 116. W. de Gruyter, Berlin 1950.
20. Ishibashi M., Fujinaga T.: *Proc. I. Internat. Polarogr. Congress*, Part I., p. 106. Published by Přírodovědecké vydavatelství, Prague 1951.
21. Heyrovský J.: *Polarographie*, p. 62. Springer, Wien 1941.
22. Jeřábek V.: *Thesis*. Charles University, Prague 1951.
23. Zuman P.: Chem. listy *46*, 326 (1952).
24. Heyrovský M.: *Thesis*. Charles University, Prague 1957.
25. Stradinš J. P., Liepina L. K.: Ž. fiz. chim. *32*, 196 (1958).
26. Heyrovský M.: Z. physik. Chem. (Leipzig), Sonderheft Juli *1958*, 97.
27. Stradinš J. P., Liepina L. K.: Izv. Akad. nauk Latvij. SSR *1958*, 97.
28. Heyrovský M.: *Proc. II. Internat. Polarogr. Congress*. Pergamon Press, London, in the press.
29. Heyrovský J.: J. Chem. Soc. *117*, 27 (1920).
30. Šerák L.: This Journal *18*, 439 (1953); Chem. listy *47*, 86 (1953).
31. Kůta J.: This Journal *23*, 383 (1958); Chem. listy *51*, 1274 (1957).
32. Kemula W., Kublik Z.: Anal. Chim. Acta *18*, 104 (1958).
33. Vogel J.: This Journal, in the press.
34. Valenta P.: Z. physik. Chem. (Leipzig), Sonderheft Juli *1958*, 46.
35. Kalousek M., Rálek M.: This Journal *19*, 1099 (1954); Chem. listy *48*, 808 (1954).
36. Němec L., Smoler I.: Chem. listy *51*, 1958 (1957).
37. Kalvoda R.: Chemie *10*, 529 (1958).
38. Ruetschi P., Trümpler G.: Helv. Chim. Acta *35*, 1021, 1486 , 1957 (1952).
39. Heyrovský J.: This Journal *18*, 749 (1953); Chem. listy *47*, 1762 (1953).
40. Kemula W., Kublik Z.: Roczniki Chem. *30*, 1005 (1956).
41. Kemula W., Kublik Z.: Roczniki Chem. *30*, 1259 (1956).
42. Heyrovský M.: Roczniki Chem. *31*, 1083 (1957).
43. Kemula W., Kublik Z.: Roczniki Chem. *31*, 1085 (1957).
44. Pokras L.: J. Chem. Educ. *33*, 152, 223, 283 (1956).
45. Smits A.: Z. Elektrochem. *30*, 423 (1924).
46. Tomeš J.: This Journal *9*, 150 (1937).
47. Herasymenko P., Šlendyk I.: Z. physik. Chem. *A 149*, 123 (1930).
48. Nejedlý V.: This Journal *1*, 319 (1929).
49. Brönsted I. N., Volqvartz K.: Z. physik. Chem. *134*, 97 (1928).
50. Conway E.: *Electrochemical Data*, p. 184. Elsevier 1952.
51. Kůta J.: *Thesis*. Charles University, Prague 1950.
52. Stackelberg M. v., Fassbender H.: Z. Elektrochem. *62*, 834 (1958).
53. Vorsina M., Frumkin A. N.: Ž. fiz. chim. *17*, 295 (1943).
54. Peard M. G., Cullis C. F.: Trans. Faraday Soc. *47*, 616 (1951).
55. Kůta J., Drábek J.: This Journal *20*, 902 (1955); Chem. listy *49*, 23 (1955).
56. Vlček A. A.: Nature *172*, 861 (1953).
57. Györbiró K.: Mag. Kém. Folyóirat *65*, 354 (1959).
58. Treindl L.: This Journal, in the press.
59. Mašek J.: This Journal *24*, 159 (1959); Chem. listy *52*, 7 (1958).
60. Treindl L.: This Journal *24*, 3389 (1959).
61. Treindl L.: This Journal *25*, 1427 (1960).
62. Pryor M. J.: Z. Elektrochem. *62*, 782 (1958).

Translated by the Author.

Резюме

Полярографическая волна алюминия

М. ГЕЙРОВСКИЙ
Полярографический институт, Чехословацкая Академия наук, Прага

Приведены экспериментальные данные для доказательства того, что полярографическая волна ионов алюминия на капельном электроде не соответствует восстановлению катиона до металлического состояния, но что здесь протекает восстановление трех протонов иона гексаквоалюминия. При помощи различных полярографических методов была обнаружена каталитическая активность продукта реакции, т. е. гидроокиси алюминия, при электролитическом выделении водорода и были объяснены все различия между волной алюминия и волнами обычных кислот.

Reprint from Nature 209, 708 /1966/
U.R.E. February 12, 1966 Vol. 209

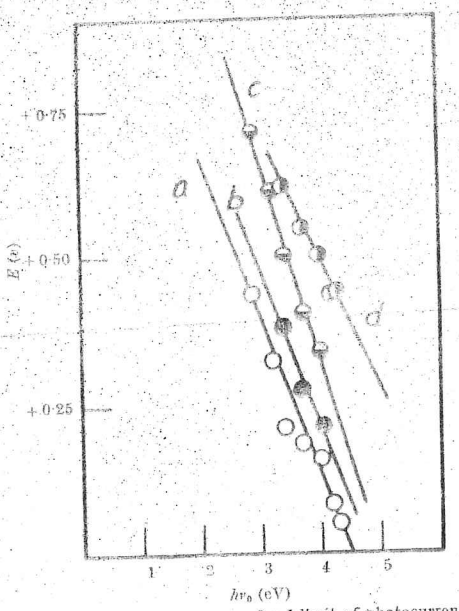

Fig. 1. Relation between the energy of red limit of photocurrent and the electrode potential in: (*a*) 0·1 M sodium tartrate in water; (*b*) 0·1 M oxalic acid in ethanol; (*c*) 1 M oxalic acid in water; (*d*) 0·1 M glycine in water. Potentials measured from the potential of zero charge

Anodic Photocurrent and the Primary Process in Electrochemical Photoeffect

ANODIC photocurrents are often produced when polarized metallic electrodes covered with oxide or other semiconducting material are illuminated in solutions[1]. The primary process is here the generation of a pair electron-hole, which results from the absorption of a light quantum in the surface layer.

A different kind of anodic photocurrent has been found in the case of a dropping mercury electrode illuminated by light not absorbed in the solution. This was observed in solutions of glyoxal, diacetyl, sodium oxalate, dimethyl oxalate, oxalic acid, pyruvic acid, glycine, Cl-acetic acid and a series of α-hydroxy acids. The condition of activity is apparently the presence of a $>C=O$ group in the molecule with a negative substituent on the neighbouring carbon atom. In solutions of compounds giving polarographic anodic currents due to formation of complexes with mercury, such as ethylenediamine tetraacetic acid or ethylenediamine, the anodic photocurrent does not appear.

In a similar fashion to cathodic photocurrents on the dropping mercury electrode[2,3], anodic photocurrents are directly proportional to the surface of the electrode and to the intensity of light; the relation between the energy of the red limit of photocurrent and the potential of the electrode is linear (Fig. 1). However, unlike their effect on cathodic photocurrents, aqueous and ethanolic solutions yield anodic photocurrents of the same order of magnitude.

Since the absorption of light in the bulk of the solution has been excluded in the present experiments and since the absorption by the metallic surface should lead to cathodic photoemission of electrons, there is only one possible explanation—that the light-absorbing species responsible for the anodic photocurrent is a complex between the adsorbed organic compound and the surface of the electrode.

The mechanism of photoexcitation of such a complex can be interpreted in terms of the charge-transfer-no-bond theory applied to adsorption[4]. The electrode plays the part of an electron acceptor, the organic molecules are electron donors, and the adsorption bond corresponds to the ground state of the complex. On absorption of light quantum the electron is transferred from the adsorbed substance to the electrode. If the electron returns to the ground state, no direct current can be observed. The occurrence of a photocurrent indicates, therefore, that the complex in its excited state has undergone some secondary irreversible change. In the example given here, this change is probably an electrolytic oxidation of the dative state of the donor.

In solutions of sodium oxalate, for example, judging from the photochemical behaviour of oxalate complexes of mercury[5], it can be assumed that from the oxalate anion in the dative state the oxalate radical-anion $C_2O_4^-$ is formed which, as a strong reducing agent[6,7], is readily oxidized on the electrode to carbon dioxide, thus yielding the anodic current.

The photoexcitation of a charge-transfer complex between the electrode and an adsorbed substance might also explain the primary processes in the cathodic photocurrent in cases where direct emission of electrons is not likely to occur, as it has been observed in aqueous solutions[2,3].

I thank Imperial Chemical Industries, Ltd., and the British Petroleum Co. for grants.

M. HEYROVSKÝ*

Department of Physical Chemistry,
University of Cambridge.

* Present address: The J. Heyrovský Polarographic Institute, Czechoslovak Academy of Sciences, Vlašská 9, Prague 1.

[1] Veselovskij, V. I., *Zh. fiz. Khim.*, **22**, 1427 (1948); *Trudy Soveshchaniya po Elektrokhimii*, 47 (Izdat. Akad. Nauk S.S.S.R., Moscow, 1953).
[2] Heyrovský, M., *Nature*, **206**, 1356 (1965).
[3] Heyrovský, M. (in preparation).
[4] Matsen, F. A., Makrides, A. C., and Hackerman, N., *J. Chem. Phys.*, **22**, 1800 (1954).
[5] Bisikalova, N. A., *Ukrain. Khim. Zh.*, **17**, 815 (1951).
[6] Saffir, P., and Taube, H., *J. Amer. Chem. Soc.*, **82**, 13 (1960).
[7] Abel, E., *Monatsh. Chem.*, **83**, 695 (1952).

3a. Vorsina M., and Frumkin A. N. *Zhur. fiz. Khim.* **17,** 295–309, 1943.
b. Heyrovský M. *Coll. Czech. Chem. Comm.* (To be published).
4. Brosset C., Biedermann G., and Sillen L. G. *Acta chem. scand.* **8,** 1917, 1954.
5. Heyrovský J. *Chem. Listy* **47,** 1762, 1953.
Kemula W., and Kublik Z. *Roczniki Chem.* **30,** 1005, 1956; **31,** 1085, 1957.

DISCUSSION

B. B. Bach: Has the work on the polarography of aluminium led to a method for determining it accurately?

M. Heyrovský: The height of the wave is proportional to concentration but interference may be experienced from the H wave. The use of Eriochrome or Solochrome dye methods would probably be preferable.

Reprint from
DVANCES IN POLAROGRAPHY
roceedings of the International Congress,
Cambridge, August 24-29th, 1959
ergamon Press, London 1960

POLAROGRAPHY OF ALUMINIUM

By M. Heyrovský

Polarographic Institute of the Czechoslovak Academy of Sciences, Prague

Aluminium ions exist in diluted aqueous solutions with co-ordinated six molecules of water, thus forming a hexaquoaluminium ion[1]. This ion behaves like a weak acid of pK about 4·9, capable of dissociation of altogether 3 protons, changing in this way into aluminium hydroxide. The acidic properties of the hydrated aluminium ion explain many strange points in its polarographic behaviour[2]. In solutions of neutral salts, which are slightly acidic because of hydrolysis, the aluminium ion gives a totally irreversible polarographic reduction wave, with the half-wave potential at about $-1{\cdot}7$ V (SCE), the shape and position of which depends on many factors. With increasing concentration or acidity the wave shifts towards more negative potentials, like the hydrogen wave of a weak acid, whereas from potentiometric measurements it is known that the potential of the aluminium electrode gets more positive with decreasing pH. Unlike the cases of metallic ion reduction, the temperature coefficient of the half-wave potential is positive and unusually high, at the concentration $7 \times 10^{-4}\,M$ being $+3$ mV/grade; the same value is known for the reduction wave of hydrogen ion.

When added to the solution of organic depolarisers, the aluminium ion has the same effect as hydrogen ion on their reduction waves—it causes a shift to more positive potentials and with some molecules containing nitrogen it gives a catalytic hydrogen wave. Also in the specific influence of the cations of the supporting electrolyte on the shift of the wave to negative potentials in the sequence Li < Na < K and Mg < Ca < Ba there is a close analogy between the aluminium and hydrogen wave. Moreover, by means of a microscope the evolution of small bubbles of hydrogen may be observed at the electrode surface from the beginning of the aluminium wave.

All these facts lead to the conclusion that the reduction of hydrogen ions from water molecules co-ordinated to the aluminium ion is the true electrode reaction giving this polarographic wave. The hexaquoaluminium ion loses successively $3H^+$-ions changing into the inactive aluminium hydroxide:

$$[Al(OH_2)_6]^{3+} \xrightarrow{3e} 3H + Al(OH)_3 + 3H_2O$$

However, a mere inspection of the shape of aluminium wave registered a

different concentrations shows that the whole electrode process is much more complicated than a simple hydrogen-ion reduction (Fig. 1).

At the concentration of about $6 \times 10^{-5}\,M$ there appears on the curve a maximum, the height of which depends linearly on the square root of the height of mercury reservoir. The maximum remains at all concentrations as

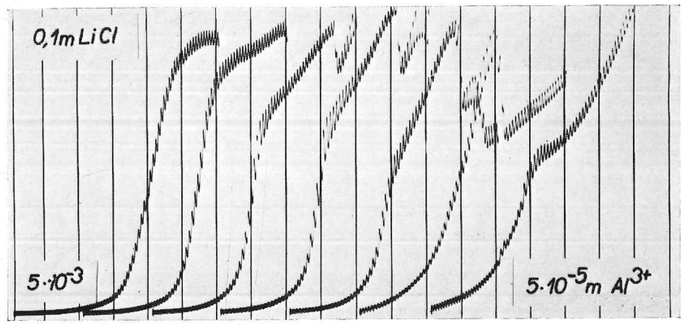

Fig. 1. Polarographic curves of Al^{3+} in 0·1 M LiCl at various concentrations. From right to left: 5×10^{-5}, 1×10^{-4}, 3×10^{-4}, 5×10^{-4}, 7×10^{-4}, 2×10^{-3}, $4 \times 10^{-3}\,M$ $KAl(SO_4)_2$; curves registered from $-1{\cdot}3$ V; 100 mV/absc.; anode—saturated calomel; sensitivity reduced stepwisely from 1/3 to 1/200; oxygen removed by N_2.

a characteristic mark of the aluminium wave; its height limits to a five-electron reduction at low concentrations, decreasing slowly to three as the concentration increases. After reaching a maximum the current falls rapidly down to a three-electron height. At potentials where the maximum exceeds three electrons, there appears a distortion of the i–t curves in form of acute indentations (Fig. 2). When the maximum falls off, the i–t curves indicate an adsorption of a permeable film taking place at the beginning of the

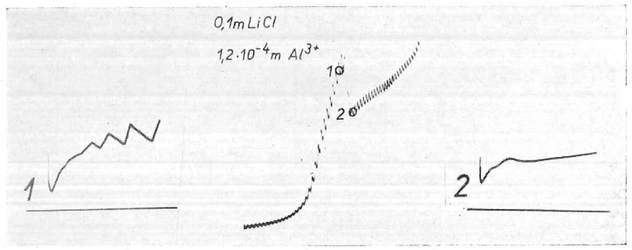

Fig. 2. Polarographic i–E curve of a $1{\cdot}2 \times 10^{-4}\,M$ solution of $KAl(SO_4)_2$ in 0·1 M LiCl and two i–t curves registered at denoted potentials; in absence of oxygen.

drop-time (Fig. 2). This phenomenon may be explained as follows: when at the surface of the electrode a stepwise reduction of hydrogen ions proceeds, a new reaction begins, the direct reduction of the aluminium-ion from the partly hydrolysed complex to the metallic state: one trivalent cation can in this way accept at most five electrons; two can be accepted by the two protons, dissociated without precipitation from the hydrated complex, and the remaining three are used up in the reduction of the ion itself. The reduction of the metallic ion from a partly hydrolysed aquocomplex is accompanied by the liberation of OH^--ions which cause precipitation of aluminium hydroxide at the electrode surface—hence the indentations in the i–t curves. Thus, in the middle part of the polarographic curve there are two electrode reactions, viz.:

$$[Al(OH_2)_6]^{3+} \xrightarrow{ne} nH + [Al(OH)_n(OH_2)_{6-n}]^{(3-n)+}$$

$$[Al(OH)_n(OH_2)_{6-n}]^{(3-n)+} \xrightarrow{3e} Al + nOH^- + (6-n)H_2O; \qquad n = 1 \text{ or } 2$$

Proceeding towards negative potentials the rate of the liberation of OH^--ions increases, the bonded water molecules are deprived of H^+-ions by the OH^--ions at the electrode surface, so that the Al^{3+} reduction becomes the only electrode reaction. As in aqueous solutions it is impossible to ascertain any following anodic dissolution of aluminium, the rate of inactivation, i.e. of the reaction between the freshly deposited aluminium atom and water leading to the formation of the hydrogen molecule and aluminium hydroxide, must be very rapid. Aluminium hydroxide is therefore the final product of the whole electrode process, which remains adsorbed at the surface as shown from i–t curves and from microscopic observations.

Another proof of the direct reduction of the aluminium ion is based on the effect of the substitution of water molecules for various anions in the co-ordination sphere of the aluminium ion (Fig. 3). The addition of chlorides,

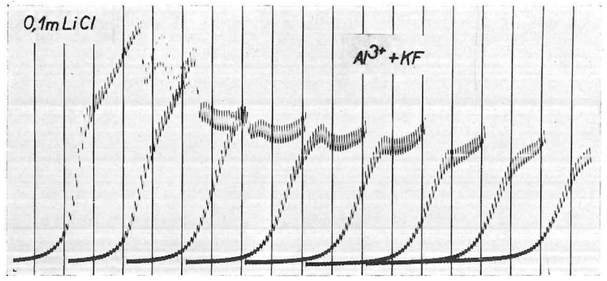

FIG. 3. $4 \times 10^{-4}\,M$ $KAl(SO_4)_2$ in $0{\cdot}1\,M$ LiCl; to 5 ml of solution $7 \times$ added $0{\cdot}2$ ml $10^{-2}\,M$ KF, curves registered from $-1{\cdot}3$ V; 100 mV/absc. anode—saturated calomel, sensitivity 1/20; oxygen removed by N_2.

bromides, sulphates in excess, or of fluorides, oxalates, tartrates, citrates in equivalent concentration causes generally a change of the characteristic shape of the wave of the aquo-ions, and a shift of the wave to negative potentials; the important thing is that the height of the transformed wave corresponds still to a three-electron reduction, which can be explained only by the deposition of the central aluminium ion from the corresponding complex.

At the concentration of about $1{\cdot}7 \times 10^{-4}\,M$ of Al^{3+} there appears at the beginning of the polarographic wave a steep increase of current of an autocatalytic nature (Fig. 4). With the aid of a stationary mercury drop electrode this was found to be due to catalysis of the liberation of hydrogen-ions caused

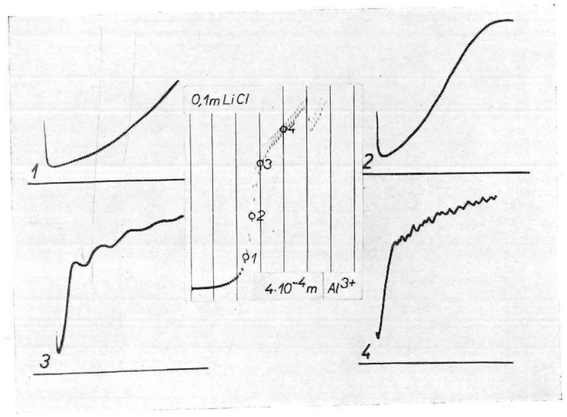

FIG. 4. Polarographic i–E curve of a $4 \times 10^{-4}\,M$ solution of $KAl(SO_4)_2$ in $0{\cdot}1\,M$ LiCl and four i–t curves registered at denoted potentials; in absence of oxygen.

by the adsorption of aquoaluminium ions at the electrode surface. This adsorption of aluminium ions on the mercury electrode is evident from electrocapillary measurements[3]. When the aluminium ion with the bonded water molecules is adsorbed at the negative electrode, the hydrogen ions become loose and their reduction takes place at more positive potentials. The current at constant potential rises according to the formula $i = kt^{1{\cdot}25}$, but at more negative potentials the reaction becomes slackened by the layer of the reduction product—aluminium hydroxide (Fig. 4). The new surface of the increasing drop permits new adsorption and catalysis, and so the succession of catalytic and slackening factors lead to periodic waves of the i–t curves (Fig. 4). The mercury drop is covered by a film of aluminium

hydroxide, bursting and restoring itself again, which causes irregular and rapid movements of the surface of the drop, similarly as when at positive potentials a calomel film is formed. This motion becomes still more vigorous when the reduction of aluminium begins and only after the fall off of the maximum does the movement cease immediately, the surface of the drop being totally covered by the adsorption layer of hydroxide from its very beginning.

At higher concentrations the maximum does not reach the height of five electrons, because the adsorbed aluminium hydroxide causes a hindrance of the electrode process, or a resistance in the polarographic circuit. This is clearly seen on the linear part of the curve which has the same slope at all concentrations.

After the first maximum there appears a second rounded one of catalytic nature (Fig. 5). It may be due to another catalytic effect of aluminium ions occluded in the layer of aluminium hydroxide.

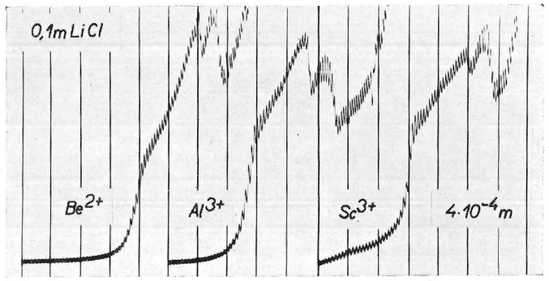

FIG. 5. Polarographic curves of $4 \times 10^{-4}\,M$ $BeCl_2$, $AlCl_3$, $SeCl_3$ in $0{\cdot}1\,M$ LiCl. All curves registered from $-1{\cdot}3$ V; 120 mV/absc., anode—saturated calomel, sensitivity 1/20; in absence of oxygen.

In solutions more concentrated than $10^{-3}\,M$ aluminium ions form polynuclear complexes through —OH bridges[4]; this is probably the cause of slowing down of the catalytic reaction and therefore of the decreasing slope of the polarographic wave.

This complicated reaction is in its main points of a more general character: beryllium and scandium ions, for instance, give polarographic waves of a very similar shape (Fig. 5); moreover, the sequence of i–t curves with autocatalysis and periodic structure may be obtained also with various rare-earth elements.

If we repeat polarisation curves several times with the same electrode surface—be it with a higher frequency at the dropping mercury surface, or slowly on a stationary electrode, the reaction product—aluminium hydroxide—covers the electrode and slackens further electrode reactions; after the forth or fifth cycle there is no sign of depolarisation. This is the reason why in the alternating current oscillography or with the multisweep voltage-scanning method aluminium ions give no effects.

The results are different when there are lithium ions present in the solution[5] (Fig. 6). Then after the first cathodic phase of polarisation there appears a sharp small peak at the anodic branch of the curve at about

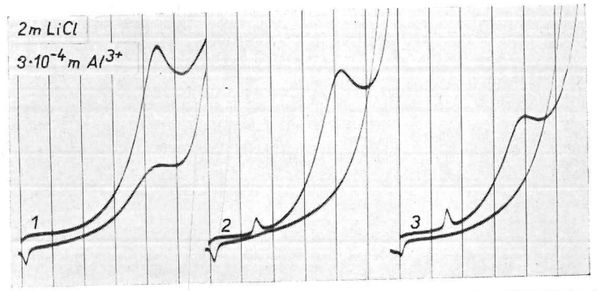

FIG. 6. Polarographic curves on one mercury drop; $3 \times 10^{-4}\,M$ $KAl(SO_4)_2$ in $2\,M$ LiCl; one stationary mercury drop polarised cyclically from $-1{\cdot}0$ to $-1{\cdot}6$ V (SCE) and back again in the sequence 1, 2, 3; 100 mV/absc.; sensitivity 1/10; in absence of oxygen.

$-1{\cdot}05$ V. In the following cycle there is already a cathodic analogue of the peak 150 mV more negative; with cyclically repeated polarisation the peaks grow to a constant height. The reaction causing this effect is a very mobile one, since the peaks appear on the polarising curves with the rate of potential variation 3 mV/sec as well as 6000 V/sec. A detailed study of this phenomenon leads to the conclusion that the peaks are caused by rapid changes of the capacity due to the adsorption and desorption of a surface film. Magnesium ion behaves similarly; here the substance adsorbed is magnesium hydroxide[3b]. It is probable that in the case of lithium and aluminium at negative potentials the insoluble lithium aluminate is formed and adsorbed on the electrode surface. In the anodic phase at a certain potential it is desorbed or some sudden change of its structure takes place, whereas this change proceeds in the reverse sense at the cathodic phase.

REFERENCES

1. POKRAS L. *J. Chem. Education* **33,** 152–161, 223–231, 282–289, 1956.
2. STRADIŅŠ J., and LIEPIN L. *Zhur. fiz. Khim.* **32,** 196–200, 1958; *Izv. Akad. Nauk Latv. SSR* **134,** 97–104, 1958.
HEYROVSKÝ M. *Z. physik. Chem.* (*Leipzig*), Sonderheft 97–107, 1958.

3a. Vorsina M., and Frumkin A. N. *Zhur. fiz. Khim.* **17,** 295–309, 1943.
b. Heyrovský M. *Coll. Czech. Chem. Comm.* (To be published).
4. Brosset C., Biedermann G., and Sillen L. G. *Acta chem. scand.* **8,** 1917, 1954.
5. Heyrovský J. *Chem. Listy* **47,** 1762, 1953.
Kemula W., and Kublik Z. *Roczniki Chem.* **30,** 1005, 1956; **31,** 1085, 1957.

DISCUSSION

B. B. Bach: Has the work on the polarography of aluminium led to a method for determining it accurately?

M. Heyrovský: The height of the wave is proportional to concentration but interference may be experienced from the H wave. The use of Eriochrome or Solochrome dye methods would probably be preferable.

Reprint from
ADVANCES IN POLAROGRAPHY
Proceedings of the International Congress, Cambridge, August 24-29th, 1959
Pergamon Press, London 1960